PhD degree in Systems Medicine (curriculum in Human Genetics)

European School of Molecular Medicine (SEMM),

University of Milan and University of Naples “Federico II”

Settore disciplinare: Bio/18, XXX cycle

ANALYSIS OF THE TRANSCRIPTIONAL REGULATION OF mTORC1 ACTIVITY BY MIT/TFE TRANSCRIPTION FACTORS

Diletta Siciliano

Tigem, Pozzuoli

Matricola n. R11146

Supervisor: Prof. Andrea Ballabio

Tigem, Pozzuoli

Internal Supervisor: Carmine Settembre

Tigem, Pozzuoli

External Supervisor: Prof. Mario Pende

Anno accademico 2017-2018

PUBLICATIONS

Di Malta C, **Siciliano D**, Calcagni A, Monfregola J, Punzi S, Pastore N, Eastes AN, Davis O, De Cegli R, Zampelli A, Di Giovannantonio LG, Nusco E, Platt N, Guida A, Ogmundsdottir MH, Lanfrancone L, Perera RM, Zoncu R, Pelicci PG, Settembre C, Ballabio A. *Transcriptional activation of RagD GTPase controls mTORC1 and promotes cancer growth.* Science. 2017 Jun 16;356(6343):1188-1192.

During my PhD, I was mainly involved in the project that was published on Science in 2017. I performed most of the *in vitro* experiments for the characterization of the MiT/TFE regulation of mTORC1, the characterization of the MiT/TFE-RagD-mTORC1 axis deregulation in cancers and some of the *in vivo* experiments.

TABLE OF CONTENTS

LIST OF FIGURES

LIST OF TABLES

LIST OF ABBREVIATIONS

4EBP	eIF4E Binding Protein
ARF1	ADP-ribosylation factor 1
ASPS	Alveolar Soft Part Sarcoma
bHLH	Basic helix-loop-helix domain
bHLH-LZ	Basic helix–loop–helix leucine zipper
CLEAR	Coordinated Lysosomal Expression and Regulation
DEPTOR	DEP domain containing-mTOR interacting protein
E-box	Enhancer box
EE	Early endosome
ER	Endoplasmic reticulum
ERK2	Extracellular signal-regulated kinase 2
FLCN	Folliculin
FKBP12	FK506-binding protein
GAP	GTPase activating protein
GEF	Guanine nucleotide exchanging factor
HIF1α	Hypoxia inducible factor 1α
IGF-1	insulin/insulin-like growth factor-1
Lamtor	Late endosomal/lysosomal adaptor, MAPK and MTOR activator
LE	Late endosome
LRS	Leucyl-tRNA Synthetase
LSDs	Lysosomal Storage Disorders
MALAT1	Metastasis associated lung adenocarcinoma transcript 1
MAPK1	Mitogen-activated protein kinase 1

MCLN1	Mucolipin 1
mLST8	Mammalian lethal with sec-13 protein 8
mSin	mammalian stress-activated map kinase-interactiprotein protein 1
mTOR	Mechanistic target of rapamycin
mTORC1	Mechanistic target of rapamycin Complex 1
mTORC2	Mechanistic target of rapamycin Complex 2
NLS	Nuclear Localization Signal
PIKK	PI3K-related kinase family
PKCβ	Protein Kinase C beta
PRAS40	Proline-rich Akt substrate 40 kDa
Rag	Ras-related GTP binding protein
Protor1/2	Protein observed with rictor 1 and 2
Rag	Ras-related GTP binding protein
Raptor	Regulatory-associated protein of mammalian target of rapamycin
RCC	Renal Cell Carcinoma
Rictor	Rapamycin-insensitive companion of mTOR
RPE	Rethinal Pigmented Epithelium
S6K1	p70S6 Kinase 1
SREBP1/2	sterol regulatory element-binding protein 1/2
TFE3	Transcription Factor E3
TFEB	Transcription Factor EB
TFEC	Transcription Factor EC
TSC	Tuberous Sclerosis Complex
TSS	Transcription Start Site
ULK1	Unc-51 like autophagy activating kinase 1

UPS Ubiquitin-proteasome system

v-ATPase Vacuolar H^+-ATPase

ABSTRACT

The mechanistic Target Of Rapamycin Complex 1 (mTORC1) regulates cellular biosynthetic pathways in response to variations in nutrient availability. Activation of mTORC1 is mediated by Rag GTPases, that act as heterodimers and promote mTORC1 recruitment to the lysosome. Many studies have clarified the post-translational control of mTORC1, but little is known about its transcriptional regulation. Our study demonstrates that TFEB, TFE3 and MITF, members of the MiT/TFE family of transcription factors and master regulators of lysosomal and melanosomal biogenesis and autophagy, are nutrient-sensitive transcriptional activators of mTORC1 signaling. During starvation they induce the expression of the *RagD* gene and this enhances mTORC1 recruitment to the lysosome and its reactivation when nutrients become available. Thus, in periods of nutrient deprivation, this mechanism allows the cell to rapidly reactivate anabolic pathways and turn off catabolism when nutrient levels are restored. Furthermore this mechanism plays an important role in cancer growth. Up-regulation of the *MiT/TFE* genes in renal cell carcinoma and melanoma is associated to RagD-induced mTORC1 activation, causing cell hyperproliferation and cancer progression.

INTRODUCTION

CHAPTER 1. MiT/TFE transcription factors

1.1 MiT/TFE transcription factors family.

Over the years, MiT/TFE factors have emerged as key players in several basic cellular processes. The family is composed of 4 members: TFEC, TFEB, TFE3 and MITF and it is considered a subgroup of basic Helix-Loop-Helix Leucine Zipper (b-HLH-LZ) transcription factors (Hemesath *et al.*, 1994). In mammals, most of the b-HLH-LZ factors are involved in cell proliferation and developmental processes and they usually bind to an hexameric sequence, CACGTG, called E-box. Moreover, the MiT/TFE factors are also able to bind to M-box (CATGTG) and to the non canonical E-box (TCATGTG or TCATGTGA) (Hemesath *et al.*, 1994; Aksan and Godin, 1998). These factors share three conserved domains: the DNA-binding region, that recognize specific target sequences, and the HLH and LZ regions, required for their protein-protein interactions (Steingrímsson *et al.,* 2004). Homo or hetero-dimerization is required for the binding to specific DNA sequences (Hemesath *et al.*, 1994) and MiT factors are able to dimerize only among themselves and not with other b-HLH-LZ factors (Hemesath *et al.*, 1994; Pogenberg et al., 2012). The functional relevance of these homo/hetero-dimerizations is still unknown.

TFEB, TFE3 and MITF also present a conserved activation domain, important for their role as transcriptional activators, which is missing in TFEC (Beckmann *et al.*, 1990; Sato *et al.*, 1997; Steingrímsson *et al.,* 2004). In fact, TFEC is reported to share less common features with the other members, in terms of sequence and also in functions (Zhao *et al.*, 1993) and its expression is restricted to

monocyte/macrophage lineage (Rehli et *al.,* 1999). A recent work shows its involvement in Hematopoietic Stem Cell expansion in zebrafish, but its role is still largely unknown (Mahony *et al.,* 2016). MITF factor is mostly expressed in melanocytes, but it is described to have prominent roles also in mast-cells, osteoclasts and in the retinal pigmented epithelium (RPE) (Steingrímsson *et al.,* 2004). Melanocytes, together with the RPE, are responsible for skin, hair and eye colour. In these cells, MITF is a master regulator of melanosomal differentiation, development and survival and play a crucial role in the generation of action potentials in the inner ear (Hodgkinson *et al*, 1993; Hemesath *et al.*, 1994). Mice lacking of a functional *MITF* gene show white coat, due to the absence of pigmentation, and eye developmental defects, as a consequence of MITF absence in the RPE (Steingrímsson *et al.,* 2004). In humans, *MITF* mutations are associated to the Waardenbrug Syndrome type 2, an inherited disorder associated with hearing loss and pigmentation defects (Tassabehji *et al*, 1994).

Less than a decade ago, TFEB was identified as a master regulator of lysosomal and autophagosomal genes (Sardiello *et al.*, 2009; Settembre *et al.*, 2011). Following studies demonstrated that also TFE3 and some isoforms of MITF were able to bind to the same consensus sequence named Coordinated Lysosomal Expression and Regulation (CLEAR) (Martina *et al.*, 2014). TFEB and TFE3 are ubiquitously expressed and studies in mice indicated that they share similar functions, such as involvement in humoral immunity (Huan *et al.,* 2006) and the cooperation in the regulation of glucose and lipid metabolism (Pastore *et al.,* 2017). These evidencies suggest that TFEB and TFE3 are reduntant factors, but their roles are not completely overlapping, since *Tcfeb* Knock-Out (KO) mice are not viable, due to defects in placental vascularization (Steingrímsson *et al.,* 1998),

while *Tfe3* KO mice showed no embryonic developmental defects (Steingrímsson *et al.,* 2002).

1.2. The lysosomes

Christian de Duve in the eary 50's discovered the lysosomes, intracellular vescicles that he named with a greek word meaning "digestive bodies" (de Duve, 2005). These cellular organelles are considered the "trash can" of the cells, since they degrade and recycle cellular waste. Since their discovery, several studies have revealed that the lysosome is much more than this, and it is a real cellular metabolic hub with multiple different roles as nutrient sensing, gene regulation, secretion, plasma membrane repair, metal ion homeostasis, cholesterol transport, and immune response (Safting and Klumperman, 2009; Lim and Zoncu, 2016; Perera and Zoncu, 2016). In particular, the main lysosomal functions can be grouped in degradation, secretion and signaling.

1.2.1 Lysosomal degradation

Lysosomes are primarly known as the cell's degradation center. They receive most of the extracellular material via endocytosis or phagocytosis, while intracellular material is mainly delivered by autophagy (Luzio *et al.*, 2007). Endocytosis or phagocytosis start from the plasma membrane with the formation of endocytic vescicles that subsequently pass through a maturation process: from Early Endosomes (EEs) they become Late Endosomes (LEs) and all the compartments formed during these maturation process differ in components and functions. The process ends when LEs finally fuse with lysosomes, forming endolysosomes, and, at this stage, all the materials trasported in this newly formed

compartment is degraded (Xu and Ren, 2015). On the contrary, during the autophagy process there are no vescicular maturation steps, but the materials are directly delivered to the lysosomes. Usually, the terms "autophagy" is referred to the so called "Macroautophagy": double-membrane vescicles, called autophagosomes, engulf damaged organelles, long lived proteins and pathogens, and they fuse directly with lysosomes, degrading all the cargos transported (Settembre *et al*., 2013b). The breakdown of all the molecules received (proteins, polysaccharids, complex lipids,..) into their building-blocks (amino acids, monosaccharids, free fatty acids,...) is accomplished by about 60 different hydrolases (lypases, proteases, glycosidases,...) that fill the lysosomal lumen (Xu and Ren, 2015). The presence, on the lysosomal membrane, of the vacuolar H^+-ATPases complex (v-ATPase), together with other ion channels, allow to constantly pump protons (H^+) into the lumen, adjusting the pH to ~4.5-5 (Lim and Zoncu, 2016). This acidification is required for lysosomal hydrolitic activities. The proton gradient is also the driving force that directs newly synthesized hydrolityc enzimes from Golgi to lysosomes and allows the recycling of the cargos back to the Golgi (Settembre *et al*., 2013b).

1.2.2 Lysosomal secretion

The lysosomal membrane is enriched in ion channels that transport ions like Na^+, K^+, Ca^{2+}, Cl^-. This ion movement across the lysosomal membrane generate a membrane potential that helps regulating the v-ATPase proton gradient and it is crucial for the process of lysosomal secretion, more often called "lysosomal exocytosis" (Perera and Zoncu, 2016). The lysosomes dock to the cell surface and the increasing levels of Ca^{2+} induce their fusion with the plasma membrane,

secreting their content into the extracellular compartment (Vernhage and Toonen, 2007). Despite the initial hypothesis of the exocytosis to occur only in some type of secretory cells, this process was then observed in all the cell types (Rodríguez *et al.,* 1997). Lysosomal exocytosis mediates several physiological processes, such as degranulation in cytotoxic T lymphocytes, bone resorption by osteoclasts, parasite defence by mast cells and eosinophils, melanocyte function in pigmentation, platelet function in coagulation and hydrolase release by spermatozoa during fertilization (Settembre *et al*., 2013b). Moreover, lysosomal exocytosis has also an important role in reparing plasma membrane damages, since these injuries recall lysosomes to the involved site which then fuse with the plasma membrane, repairing the disrupted sites (Reddy *et al*., 2001).

1.2.3 Lysosomal signaling

Over the years, it has become evident that the lysosomes are not simply the "trash can" of the cells, but they are involved in maintaining cellular metabolic homeostasis. Cells are able to adapt to nutrient changes and regulate accordingly cell growth and metabolism mainly thanks to mechanistic Target of Rapamycin Complex 1 (mTORC1) signaling pathway (Laplante and Sabatini, 2012; Saxton and Sabatini, 2017). Moreover, a crosstalk exists between the nutritional status of the cell, sensed by mTORC1, which function on the lysosomal surface, and TFEB, which transfers the information received to the nucleus (Settembre *et al.,* 2012).

1.3 Transcription Factor EB (TFEB): a master regulator of lysosomal function and autophagy

Originally, lysosomes were described as static organelles, involved only in degrading and recycling cellular waste, while further studies showed their involvement in the regulation of several processes important for the maintenence of cellular homeostasis (Lim and Zoncu, 2016; Settembre *et al.*, 2013b). In 2009 analysis of microarray data revealed that lysosomal genes are co-expressed in different cell types and conditions, suggesting the presence of one or more regulators (Sardiello *et al.*, 2009). Promoter analysis of lysosomal genes resulted in the identification of a palindromic sequence of 10 base-pairs (GTCACGTGAC) localized mainly within 200 base-pairs from the transcription start site (TSS), the CLEAR element, which contained the consensus E-box (CANNTG) that is typically recognized by bHLH-LZ transcription factors (Sardiello *et al*, 2009). TFEB directly binds to CLEAR elements and induce the expression of its target genes, such as several subunits of the v-ATPase, lysosomal hydrolases and lysosomal transmembrane proteins (Sardiello *et al*, 2009; Palmieri *et al.*, 2011). Furthermore, TFEB overexpression increases the number of lysosomes and the levels of lysosomal enzymes, boosting their catabolic function (Sardiello *et al*, 2009; Palmieri *et al.*, 2011). Subsequently, further studies revealed that TFEB regulates genes not only involved in lysosomal biogenesis and function, but also in autophagy and lysosomal exocytosis (Palmieri *et al.*, 2011). Specifically, TFEB binds to promoters of genes that regulates autophagosome biogenesis and autophagosome-lysosome fusion and can promote the degradation of autophagy substrates, like long-lived proteins (Settembre *et al.*, 2011). Moreover, TFEB induces the clearance of lipid droplets and damaged mithocondria (Settembre *et*

al., 2013a; Nezich *et al.,* 2015). TFEB has also been found to regulate lysosomal exocytosis, increasing the release of intracellular Ca^{2+} and the number of lysosomes ready to fuse with the plasma membrane (Medina *et al.*, 2011). Thus TFEB coordinates a complex transcriptional program that regulates the main degradative pathways and promotes cellular clearance. Moreover, it has been showed that TFEB overexpression can ameliorate the phenotype of mouse models with pathological conditions associated to lysosomal disfunction, such as Lysosomal Storage Disorders (LSDs), but also more common diseases like Parkinson's, Alzheimer's, Huntington's (Settembre *et al.*, 2013a; Ballabio, 2016).

1.4 TFEB regulation

The identification of TFEB as the "master regulator of lysosomes" supports the idea of these organelles as signaling platforms. TFEB regulation is dependent on post-translational modifications, subcellular localization and protein-protein interactions. In basal condition, when nutrients are present, TFEB is inactive into the cytosol, whereas, in starvation condition, when nutrients are no longer available, or in case of lysosomal stress, TFEB translocate into the nucleus and activates its target genes (Settembre *et al.*, 2011; Martina et *al.*, 2012; Roczniak-Ferguson *et al.*, 2012). TFEB subcellular localization is mostly regulated by the phosphorylation of two critical serine residues, Ser142 (Settembre *et al.*, 2011; 2012) and Ser211 (Martina et *al.*, 2012; Roczniak-Ferguson *et al.*, 2012; Settembre *et al.*, 2012): when these serines are phosphorilated TFEB is retained into the cytosol. ERK2 (or MAPK1) and mTORC1, both involved in the regulation of cellular growth, are the main kinases that phosphorylate TFEB respectively on Ser142 and on both Ser142 and Ser211. Mutations of these serines into alanines result in a constitutive nuclear TFEB, always active (Martina et *al.*, 2012;

Roczniak-Ferguson *et al.*, 2012; Settembre *et al.*, 2011, 2012). In osteoclasts, another kinase, protein kinase Cβ (PKCβ), phosphorylates TFEB on serine residues different from the previous ones: this event stabilizes the transcription factor, inducing lysosomal biogenesis and bone resorption in osteoclats (Ferron *et al.*, 2013). Despite all the residues phophorylated by these kinases, the phophorylation of Ser211 by mTORC1 results to be the key residue reponsible for TFEB cytosolic sequestration, since it promotes the binding of TFEB to the chaperone 14-3-3. Thus TFEB is inable to translocate into the nucleus, probably because the binding with this chaperone masks its Nuclear Localization Signal (NLS) (Martina *et al.,* 2012; Roczniak-Ferguson *et al.*, 2012). Furthermore, both mTORC1 and ERK2 exert their activity on the lysosomal surface (Sancak *et al.*, 2010; Nada *et al.*, 2009).

Once understood that TFEB cytosolic localization is mainly regulated by phosphorylation events, the following question was: what is the phopshatase involved in its dephosphorylation? Later studies demonstrated that nutrient deprivation induces the release of lysosomal Ca^{2+} through the Ca^{2+} channel mucolipin 1 (MCOLN1); this activates the phosphatase calcineurin, which in turn dephosphorylates TFEB and promotes its nuclear translocation (Medina *et al.*, 2015). MCOLN1 is crucial for lysosomal Ca^{2+} release and calcineurin activation, since depletion of MCOLN1 inhibits these processes, thus preventing TFEB activation (Medina *et al.*, 2015) (Fig.1)

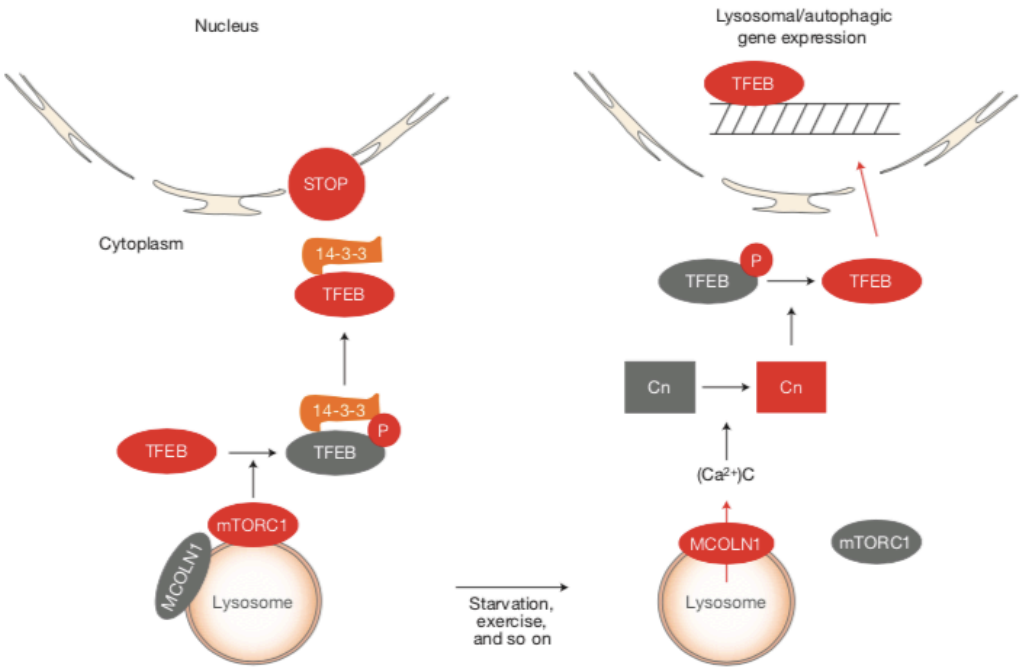

from Medina *et al.*, Nat Cell Biol 2015.

Fig.1. Model of TFEB regulation.

Under normal feeding conditions, TFEB is phosphorylated by mTORC1 on the lysosomal surface and is sequestered in the cytoplasm by the 14-3-3 proteins. During starvation, Ca^{2+} is released from the lysosome through MCOLN1 and this leads to local calcineurin (Cn) activation and TFEB dephosphorylation. Dephosphorylated TFEB is no longer able to bind 14-3-3 proteins and can translocate to the nucleus where it transcriptionally activates the lysosomal/autophagic pathway.

Interestingly, TFEB regulates the transcription of many genes important for its own regulation, such as *MCOLN1* and genes encoding for v-ATPase subunits and numerous lysosomal enzymes. This supports the idea that lysosomal adaptation to external stimuli is regulated by multiple feedback loops. In accordance with this, TFEB induces its own transcription, in a positive autoregulatory loop that is dependent on the presence of CLEAR elements located in its promoter (Settembre *et al.,* 2013a).

The same mechanisms of regulation are conserved for the other MiT/TFE factors. In particular, both TFE3 and some isoforms of MITF are phosphorylated by mTORC1 (Martina and Puertollano, 2013; Martina *et al.*, 2014).

1.5 MiT/TFE factors in cancer

MiT/TFE are known oncogenes deregulated in different cancer types (Haq and Fisher, 2011). Below their involvement in Renal Cell Carcinoma and Melanoma is described.

1.5.1 Renal Cell Carcinoma

Renal Cell Carcinoma (RCC) is the most common form of kidney cancer and includes different hystopathological subtypes (Linehan *et al.*, 2010). Approximately 5% of sporadic RCC tumors is part of a rare subgroup named translocation-RCC (t-RCC), most common in children and characterized by translocations and rearrangements involving *TFE3*, and less commonly *TFEB* genes (Kauffman *et al.*, 2014). T-RCC associated *TFE3* gene fusions can occur with several partners including *PRCC, ASPSCR1, SFPQ, NONO and CLTC* (Kauffman *et al.,* 2014; Linehan *et al.*, 2010). *ASPSCR1–TFE3* and *SFPQ–TFE3* fusions are not restricted to RCC, being originally identified in Alveolar Soft Part Sarcoma (ASPS) and in a subset of benign tumors, known as perivascular epithelioid cell neoplasms (Argani *et al.* 2001; Tanaka *et al.*, 2009). Regarding the fusion proteins obtained, rearrangements can involve different introns of the partner genes, that can vary in patients: this results in different mRNA isoforms, thus different fusion proteins in size. However, the fusion proteins always retain a 280 amino acid C-terminal

portion haboring the bHLH–LZ dimerization, DNA-binding domain and the putative NLS of TFE3 (Kauffman *et al.*, 2014). In the case of TFEB, a 6p21/11q13 translocation results in the fusion of the *TFEB* coding region with the regulatory region of the non-coding *MALAT1* gene (Davis *et al.*, 2003). Usually the *MALAT1-TFEB* breakpoints are located before the start codon in exon 3 of the *TFEB* coding sequence, thus resulting in the translation of the full lenght TFEB protein under the control of the strong *MALAT1* promoter (Inamura *et al*., 2012). TFEB-tRCCs patients usually have a better prognosis than TFE3-tRCC patients. More recently, a comprehensive genomic analysis of 161 primary papillary RCC led to identification of novel fusion partners for both *TFE3* and *TFEB*, including *RBM10* and *DVL2* for *TFE3* and *COL21A1* and *CADM2* for *TFEB* (Cancer Genome Atlas Research Network et al. 2016). The mechanisms explaining the oncogenic role of the TFE-fusion proteins in RCC are still unclear. Several hypothesis came out during the years, one is that these TFE-fusion proteins retain partially the functions of the partner genes, oftenly involved in promoting tumorigenesis (*NONO*, *SFPQ*, *PRCC* appear to have regulatory roles in mRNA splicing, whereas *PRCC*, *CLTC* are implicated in mitosis) (Kauffman *et al.*, 2014). Another hypothesis is that the fusion leads to upregulation of oncogenic activity already present in the wild-type protein: this is the case of *TFEB-MALAT1* gene (Kuiper *et al*., 2003), but also TFE3 fusion proteins show much higher expression levels than the wild-type TFE3 (Argani *et al.*, 2003; Clark *et al.*,1997; Weterman *et al.,* 1996; 2000). No MITF-fusion proteins have been associated to RCC.

1.5.3 Melanoma

Melanoma is an aggressive type of cancer involving the melanocytes. The most common type is the cutaneous melanoma, arising from the epidermal melanocytes

of the skin. Approximately 50% of melanoma are characterized by V600E activating mutation in the BRAF kinase, resulting in hyper-activation of the MAPK signaling pathway (Davies *et al.,* 2002; Hodis *et al.,* 2012). Amplification of the *MITF* gene was detected in 5-20% of melanoma and these tumors appear to have better prognosis (Genomic Classification of Cutaneous Melanoma 2015). MITF-associated tumors are usually caused by gene amplifications, but somatic mutations of *MITF* have also been reported. These mutations are generally located in the MITF transactivation domain, indicating a role of the transcriptional activity of MITF in driving tumorigenesis (Cronin *et al.*, 2009). Several studies claim that MITF levels influence different mechanisms and drive the response to therapies (Ennen et al. 2015; Hoek et al. 2008; Tirosh et al. 2016).

CHAPTER 2. The mechanistic Target of Rapamycin Complex 1 (mTORC1)

2.1 The mechanistic Target of Rapamycin (mTOR) complexes

Originally, the mechanistic Target of Rapamycin (mTOR) was identified as the target of Rapamycin in mammals, a compound that inhibits cell growth and proliferation (Sabatini *et al.*, 1994). mTOR is a serine/threonine kinase in the PI3K-related kinase family (PIKK), implicated in the catalytic activity of two different complexes: mTOR Complex 1 (mTORC1) and mTOR Complex 2 (mTORC2). The complexes differ in their subunits and in their function. As for their composition, both mTOR complexes are quite big, with mTORC1 having six and mTORC2 seven known protein components. They share the catalytic mTOR subunit, and also mammalian lethal with sec-13 protein 8 (mLST8, also known as GβL) (Jacinto et *al.*, 2004; Kim et *al.*, 2003), which interacts with the catalytic domain of mTOR and stabilize the kinase activation loop (Yang *et al.*, 2013), DEP domain containing mTOR-interacting protein (DEPTOR), an inhibitor subunit (Peterson et *al.*, 2009), and the Tti1/Tel2 complex, positive regulators of the complexes (Kaizuka et *al.*, 2010). However, two other subunits are specific for mTORC1: regulatory-associated protein of mammalian target of rapamycin (raptor), required for proper mTORC1 subcellular localization and substrates recruitment (Kim et *al.*, 2002) and proline-rich Akt substrate 40 kDa (PRAS40), an inhibitor subunit (Sancak et *al.*, 2007). On the contrary, mTORC2 is composed by three additional subunits: rapamycin-insensitive companion of mTOR (rictor), with analogous function of raptor (Sarbassov et *al.*, 2004), and the two regulatory subunits mammalian stress-activated map kinase-interacting protein 1 (mSin1) (Jacinto et *al.*, 2006) and

protein observed with rictor 1 and 2 (protor1/2) (Pearce et *al.*, 2007). The two complexes have different functions. mTORC1 responds to amino acids, stress, oxygen, energy, and growth factors, promoting cell growth and cell-cycle-progression and is acutely sensitive to rapamycin (Laplante and Sabatini, 2012). In fact, rapamycin forms a complex with the intracellular 12-kDa FK506-binding protein (FKBP12) (Sabatini et *al.*, 1994), masking mTOR catalytic domain and thus blocking the phosphorylation of its substrates (Yang *et al,* 2013). Rapamycin-FKBP12 complex directly interacts with and inhibits mTOR when it is part of mTORC1 but not mTORC2 (Yang *et al,* 2013). mTORC2 responds to growth factors and regulates cell survival and metabolism, as well as the cytoskeleton, and it is insensitive to acute rapamycin treatment (Laplante and Sabatini, 2012). Actually, prolonged exposure to this drug abolish mTORC2 signaling, probably due to the absence of unbound mTOR available to form new complexes (Sarbassov *et al.*, 2006).

2.2 Upstream regulators of mTORC1

Nutrient availability is a major determinant of survival and growth and most of the species have evolved mechanisms to efficiently switch between anabolic and catabolic states in order to deal with its fluctuation in the environment. mTORC1 is a main regulator of the metabolic adaptation to nutrient availability: it is activated in feeding conditions, to promote growth and energy storage, whereas the complex activity is inhibited in fasting conditions, to avoid the waste of insufficient nutrients (Laplante and Sabatini, 2012; Saxton and Sabatini, 2017).

Different stimuli can exert their effects on mTORC1 pathway, by modulating the activity of the components of this complex. Several growth factors, such as the insulin/insulin-like growth factor-1 (IGF-1) pathway (Inoki *et al.*, 2002), and

different mitogen-dependent signaling pathways, like the receptor tyrosine kinase-dependent Ras signaling (Roux *et* al, 2004), converge in the activation of mTORC1 signaling, through the inhibition of the Tuberous Sclerosis Complex (TSC), an heterotrimeric complex, composed by the subunits TSC1, TSC2 and TBC1D7 (Dibble *et al*, 2012). TSC is a crucial negative regulator of mTORC1, acting as a GTPase activating protein (GAP) for Rheb, a small GTPase, which resides at the lysosomal surface and activate mTORC1 when it is bound to GTP (Inoki *et al.*, 2003; Long *et al.*, 2005). TSC2 inhibition via Akt-dependent inhibitory phosphorylation, causes the dissociation of the TSC complex from the lysosomes hence removing Rheb inhibition and allowing mTORC1 activation (Inoki *et al.*, 2002; Roux *et al.*, 2004).

Other stimuli associated to cellular stress modulate mTORC1 activity, such as hypoxia, low ATP levels, glucose deprivation and DNA damage (Saxton and Sabatini, 2017). Most of these stimuli inhibit mTORC1 activity inducing the stress responsive metabolic regulator AMPK, which block mTORC1 signaling both indirectly, by TSC2 activating phosphorylation, and directly, phosphorylating raptor and causing an allosteric inhibition of mTORC1 (Gwin *et al.*, 2008).

2.2.1 Amino acid sensing by mTORC1

Amino acids levels are crucial for mTORC1 activity and this is one of the most conserved growth signal to mTORC1 pathway. After decades of studies, amino acid sensing by mTORC1 is still not fully understood. As example, it is still not completely clear if all the 20 amino acids have the same contribution to the signaling. Leucine and arginine are fundamental for mTORC1 activation but they are not sufficient if the other 18 amino acids are absent in the cell (Hara *et al.*, 1998). Amino acids directly regulate mTORC1 recruitment to the lysosome by

modulating the GTP/GDP bound state of the RagGTPases (Kim *et al.*, 2008; Sancak *et al.*, 2008). Mammals have four RagGTPases (Rags): RagA, RagB, RagC and RagD. They function as obligate heterodimers composed of RagA or RagB, together with RagC or RagD. When amino acids are available, the heterodimer is composed by the Rags in their active state: RagA/B-GTP bound and RagC/D-GDP bound, and it localizes to the lysosome. This GTP/GDP bound state is responsible for Rags interaction with raptor and thus mTORC1 lysosomal localization, where the complex can be activated by Rheb (Sancak *et al.,* 2008; Inoki *et al.*, 2003; Long *et al.*, 2005). Rags are anchored to the lysosomal surface through a pentameric complex, called Ragulator (Sancak *et al.*, 2010). Ragulator was identified as a Rag-interacting complex and its basic architecture consists of Lamtor1 (late endosomal/lysosomal adaptor, MAPK and MTOR activator 1) which represents a scaffold for two obligate heterodimers composed of Lamtor2–Lamtor3 and Lamtor4–Lamtor5 (Sancak *et al.*, 2010). Post-translational modifications, such as myristoylation and palmitoylation on the N terminus of Lamtor1, promote the localization of Ragulator and Rag GTPases to lipid rafts on lysosomal surface (Nada *et al.*, 2009). Moreover, initial studies indicated that Ragulator is a guanine nucleotide exchanging factor (GEF) for RagA/B which binds to RagA/B in their inactive state (GDP-bound), to promote the switch from GDP to GTP (Bar-Peled *et al.,* 2012). However, very recently new data have emerged indicating that even if Ragulator is implicated in RagA/B activation, their real GEF is the amino acid sensor SLC38A9 (Shen and Sabatini, 2018). However, the role of RagC/D is equally important, they have to be loaded with GDP to favour Rags' heterodimer interaction with Raptor, allowing translocation of mTORC1 to the lysosome (Tsun *et al.,* 2013). Folliculin (FLCN), together with its partner FNIP1/2, acts as GTPase Activating Protein (GAP) for RagC/D, promoting the

hydrolysis of GTP to GDP (Tsun *et al.*, 2013). In addition, GATOR complexes are key players of mTORC1 sensing machinery. GATOR is an octameric complex, composed by two subcomplexes called GATOR1 and GATOR2, respectively having 3 and 5 subunits: GATOR1 negatively regulates mTORC1 signaling, functioning as a GAP for RagA/B, whereas GATOR2 inhibits GATOR1 (Bar-Peled *et al.*, 2013).

MTORC1 can sense both intra-lysosomal and cytosolic amino acids through different mechanisms. Inside the lysosomal lumen, amino acids are able to regulate the nucleotide state of the Rags through the lysosomal v-ATPase, which, somehow, comunicates amino acids abundance to the activating complex for RagA/B composed by Ragulator and SLC38A9 (Zoncu *et al.*, 2011, Shen and Sabatini, 2018). SLC38A9 is a transmembrane protein, which also acts as sensor for arginine (Wang *et al.*, 2015). Some other amino acid sensors have also been recently found. Sestrin2 is a GATOR2 interacting protein, working as leucine sensor for mTORC1, that binds and inhibits GATOR2 in absence of leucine, or it dissociates from GATOR2 in presence of leucine, thus relieving GATOR1 inhibition of mTORC1 (Chantranupong *et al.*, 2014; Wolfson *et al.*, 2016). Cytosolic arginine is instead comunicated to mTORC1 signaling through a different sensor, CASTOR1, which associate or dissociate from GATOR2 in absence or in presence of arginine, respectively, resulting in mTORC1 activation only when arginine is available (Chantranupong *et al.*, 2016). Finally, glutamine, the most abundant free amino acid in the cell, seems to be able to promote mTORC1 lysosomal recruitment indipendently from Ragulator and Rags, via a mechanism that appears to involve the v-ATPase and ADP-ribosylation factor 1 (ARF1) (Jewell *et al.*, 2015).

Hence, amino acids represent a crucial stimuli that regulates mTORC1 activity, and further studies will be required to fully dissect all the components of this complex sensing machinery (Fig.2).

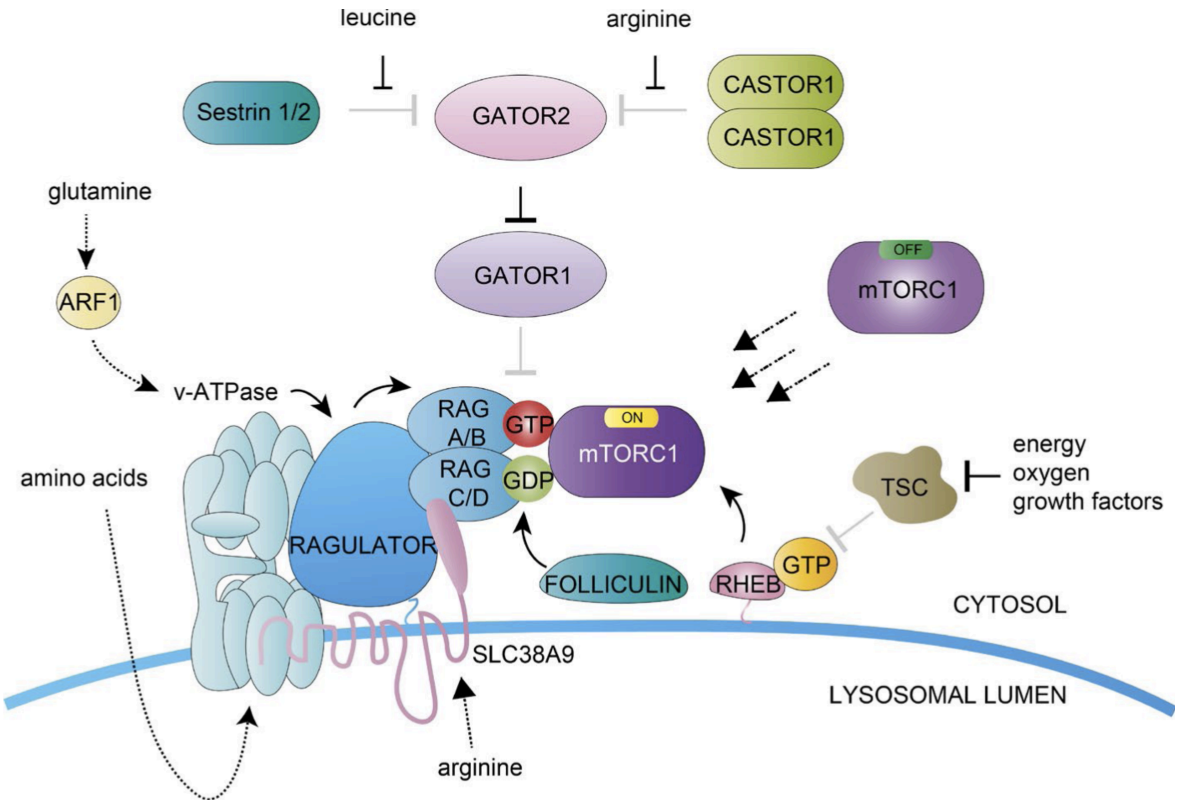

from Lim and Zoncu, J Cell Biol 2016.

Fig.2. The nutrient sensing pathway upstream of mammalian mTORC1.

Schematic model of the main components involved in amino acids regulation of mTORC1 activity.

2.3 Downstream of mTORC1

In order to promote cellular growth and proliferation, mTORC1 senses nutrients availability and controls the balance between anabolism and catabolism. Thus, mTORC1 activates protein, lipid and nucleotide synthesis when nutrients are available, while inhibiting catabolic processes, like autophagy and lysosome biogenesis (Laplante and Sabatini, 2012; Saxton and Sabatini, 2017).

2.3.1 Anabolic processes

MTORC1 promotes protein synthesis mainly through the phosphorylation of two key effectors, p70S6 Kinase 1 (S6K1) and eIF4E Binding Protein (4EBP). MTORC1 directly phosphorylates S6K1 at the Thr389, enabling its subsequent phosphorylation and activation by PDK1. As a consequence, S6K1 phosphorylates and activates several substrates that promote mRNA translation initiation, such as eIF4B, a positive regulator of the 5' cap binding eIF4F complex (Holz et *al.*, 2005). S6K1 also phosphorylates and promotes the degradation of PDCD4, an inhibitor of eIF4B (Dorrello et *al.*, 2006), and enhances the translation efficiency of spliced mRNAs through its interaction with SKAR, a component of exon-junction complexes (Ma et *al.*, 2008). Moreover, S6K1, together with its substrate ribosomal protein S6 (S6), was also thought to control the translation of an abundant subclass of mRNAs characterized by an oligo-pyrimidine tract at the 5' end (5' TOP mRNAs) and that encode most of the protein components of the translational machinery. Nevertheless, even if mTORC1 is a key regulator of the translation of these mRNAs, S6K1 and S6 are not involved in this process (Tang *et al.*, 2001). The substrate 4EBP is another mTORC1 direct substrate and inhibits translation by binding and sequestering eIF4E, blocking the assembly of the eIF4F complex. MTORC1 phosphorylates 4EBP at multiple sites, causing its dissociation from eIF4E, hence promoting the initiation of the cap-dependent translation (Gingras et *al.*, 1999).

In addition to the regulation of proteins production, mTORC1 also controls the synthesis of lipids necessary for proliferating cells to generate new membranes. This function is mainly executed through the regulation of the sterol regulatory element-binding protein 1/2 (SREBP1/2) transcription factors that control the expression of numerous genes involved in fatty acid and cholesterol synthesis.

The inactive SREBPs reside on the endoplasmic reticulum (ER) and they are activated in response to insulin or sterol depletion, translocating to the nucleus to activate transcription of lipogenic genes (Du¨vel *et al.*, 2010; Wang et *al.*, 2011). MTORC1 appears to regulate SREBP cellular localization (Wang et *al.*, 2011). Recent studies established that mTORC1 also promotes the synthesis of nucleotides required for DNA replication and ribosome biogenesis in growing and proliferating cells. In fact, mTORC1 increases the ATF4-dependent expression of MTHFD2, a key component of the mitochondrial tetrahydrofolate cycle involved in purine synthesis (Ben-Sahra et *al.*, 2016). Finally, mTORC1 positively regulates cellular metabolism and ATP production: it increases glycolytic flux by activating the transcription and the translation of hypoxia inducible factor 1α (HIF1α), a positive regulator of many glycolytic genes (Brugarolas *et al.*, 2003; Du¨vel et *al.*, 2010).

2.3.2 Catabolic processes

To promote cellular growth, in association with the induction of anabolic processes, mTORC1 inhibits autophagy, the main degradative process in the cell. An important early step in autophagy is the activation of ULK1, a kinase that forms a complex with ATG13, FIP2000, and ATG101 and drives autophagosome formation. In presence of nutrients, mTORC1 phosphorylates ULK1, thus preventing its activation by AMPK, a key autophagy activator (Kim *et al.*, 2011). In addition, mTORC1 inhibits autophagy through the phosphorylation of TFEB, which results in the downregulation of gene expression relative to its lysosomal and autophagy targets. (Martina et *al.*, 2012; Roczniak-Ferguson *et al.*, 2012; Settembre *et al.*, 2012).

In addition to autophagy, a major pathway responsible for protein turnover is the ubiquitin-proteasome system (UPS), through which proteins are tagged with ubiquitin and selectively targeted for degradation by the 20S proteasome. Two recent studies found that acute mTORC1 inhibition rapidly increases proteasome activity through a general increase in protein ubiquitylation (Zhao et *al.*, 2015) and an increase in the levels of proteasomal chaperones (Rousseau and Bertolotti, 2016). However, another study found that genetic hyperactivation of mTORC1 signaling also increases proteasome activity, through elevated expression of proteasome subunits downstream of Nrf1 (Zhang et *al.*, 2014). One possible explanation for this discrepancy is that while acute mTORC1 inhibition promotes proteolysis to restore free amino acid pools, prolonged mTORC1 activation could cause a compensatory increase in protein turnover to balance the higher rate of protein synthesis. Thus, how exactly mTORC1 regulates this process is not yet clarified.

2.4 Physiological roles of mTORC1

Accordingly with the *in vitro* studies, mTORC1 regulates whole-body metabolism in mice, maintaining the perfect balance between *in vivo* anabolic and catabolic processes in response to nutrients.

During fasting, circulating glucose and amino acids levels rapidly decrease and autophagy, gluconeogenesis and the release of peculiar energy sources, such as ketone bodies, are promptly induced in the liver. In fact, mTORC1 seems to have a crucial role in regulating the response of the liver to diet. For example, liver conditional KO mice for *tsc1*, that are characterized by mTORC1 hyperactivation, are not able to generate ketone bodies, due to mTORC1 repression of PPARα, a

transcription factor that activates genes involed in ketogenesis (Sengupta *et al*., 2010). Another example of the importance of mTORC1 inhibition in regulating liver response to fasting is the phenotype showed by $RagA^{GTP}$ mutant mice: constituive activation of mTORC1 is associated with perinatal death, due to the inability of the newborns to maintain blood glucose homestasis upon postnatal fasting (Efeyan *et al*., 2013). Indeed, mTORC1 plays an important role also in the regulation of glucose homeostasis: mice KO for *tsc2* only in pancreatic β cells show, first, an increase in β cells mass and insulin levels (probably an attempt to compensate for an increased glycemic load) while, at a later stage, these mice more rapidly develop reduced β cell mass, lower insulin levels, and hyperglycemia. Thus, high mTORC1 activity in the pancreas is initially beneficial for glucose tolerance but leads to a faster decline in β cell function over time (Mori *et al*., 2009).

The role of mTORC1 in promoting muscle growth is well known but the mechanisms involved in this effect are still not clear. In mice muscles, mechanical stimuli, through Raptor phosphorylation IGF-1 and leucine, can activate mTORC1 and induce hypertrophy (Anthony *et al.,* 2000; Rommel *et al.*, 2001; Frey *et al.,* 2014). Moreover, mice KO for *mTOR* and *Raptor* in muscle showed muscular atrophy and reduced body weight (Bodine *et al.*, 2001; Rommel *et al.*, 2001), suggesting a crucial role of mTORC1 in skeletal muscles. However, chronic mTORC1 hyperactivation in muscles results in severe muscle atrophy, low body mass, and early death, primarily due to an inability to induce autophagy in this tissue, where a normal turnover is fundamental to promote muscle growth.

Furthermore, many studies reveal a role for mTOR in promoting adipocyte formation and lipid synthesis in response to feeding and insulin. Nevertheless, mTORC1 inhibition in this tissue can have opposite effects, since adypocyte-specific *Raptor* KO mice showed lipodystrophy and hepatic steatosis (Lee et *al.*,

2016), but these mice are also resistant to diet-induced obesity due to reduced adipogenesis (Polak *et al.*, 2008).

In addition, the study of rapamycin properties has elucidated its immunosuppressive activity, due to the ability of this drug to block T cell proliferation. In fact, different signals present in the immune microenvironment, such as interleukin-2 (IL-2) or amino acids too, can activate mTORC1, thus promoting T cells activation and expansion (Powell *et al.,* 2012). MTORC1 inhibitors are currently used in immunosuppressive therapies but the mechanisms of action are very complex and still need to be addressed completely.

Finally, the phenotype of the hamartomatous syndrome tuberous sclerosis complex (TSC) patients has highlighted the role of mTORC1 hyperactivation in the brain. TSC is a genetic disease, caused by mutations of *TSC1* or *2*; patients exhibit a range of debilitating neurological disorders, including epilepsy, autism, and the presence of benign brain tumors. The strong correlation between mTORC1 hyperactivation and high occurence of epileptic seizures and autism traits in TSC patients suggest a more general involvement of mTORC1 in these phenotypes. The importance of mTORC1 in this tissue is associated in part to its role in promoting activity-dependent mRNA translation near synapses, a critical step in neuronal circuit formation (Lipton and Sahin, 2014). Furthermore, autophagy dysfunction is strongly implicated in the pathogenesis of neurodegenerative disorders, including Parkinson's disease and Alzheimer's disease (AD). Accordingly, inhibition of mTORC1 signaling has beneficial effects on mouse models of AD (Spilman et *al.*, 2010).

2.5 mTORC1 and cancer

As discussed above, mTORC1 represents the main node of a complex signaling network that controls cells, tissues and organismal growth. Since the activation of mTORC1 induces a cascade of anabolic processes associated to an high demand of nutrients and energy, this process is tightly regulated (Ilagan and Manning, 2016).

The first peculiar trait of cancer cells is the dysregulated growth caused by the loss of response to external stimuli, which, in physiological conditions, drive the activation/inactivation of mTORC1 (Ilagan and Manning, 2016). TSC1 and 2, known tumor suppressors and negative regulators of mTORC1 activity, represented the first link between mTORC1 hyperactivation and cancer (Crino *et al.*, 2006). Moreover, mTORC1 is the downstream effector of several mutated oncogenic pathways, such as the PI3K/Akt pathway and the Ras/Raf/Mek/ Erk (MAPK) pathway. Akt hyperactivation is a common oncogenic phenomenon that can result from *PTEN* deletion, *PIK3CA* activating mutations, the *BCR-ABL* translocation, and amplification of genes encoding HER-2, EGFR, or AKT itself (Guertin and Sabatini, 2005). For instance, Akt phosphorylates PRAS40, reducing its ability to inhibit mTORC1 (Sancak *et al.*, 2007), but aberrant Akt activation can also result in the increase of TSC2 phosphorylation, which in turn relieves mTORC1 inhibition (Inoki *et al.,* 2002). Other members of mTORC1 machinery have also been implicated in cancer progression: inactivating mutations in all the three subunits of *GATOR* have been found in glioblastomas (Bar-Peled *et al*., 2013); mutations in *RagC* were recently found, with an high frequency, in follicular lymphomas, causing its increased binding to Raptor, thus rendering mTORC1 signaling insensitive to amino acids deprivation (Okosun *et al.*, 2016). Furthermore, *FLCN* mutations are the causative lesions of the Birt-Hogg-Dube

hereditary cancer syndrome, with a phenotype similar to TSC features (Nickerson *et al.*, 2002), and *MTOR* mutations have been found in different cancer types (Grabiner *et al.*, 2014).

The first mTORC1 inhibitors used in cancer therapy were a class of compounds derived from rapamycin and called "Rapalogs". The rapalog temsirolimus (Pfizer) was first approved for treatment of advanced renal cell carcinoma in 2007, followed by everolimus (Novartis) in 2009. These compunds were really promising in pre-clinical studies but the efficacy was not the same in humans, since only few groups of patients responded to the treatment. Different explanations were suggested to justify this failure. Rapalogs are allosteric inhibitors of mTORC1, thus they block the phosphorylation of some substrates, not all of them, and the phosphorylation of 4EBP1 is highly insensitive to rapamycin (Choo *et al*., 2008). In addition, increased Akt signaling has been observed in biopsies of cancer patients treated with everolimus because inhibiting mTORC1 releases the negative feedback on insulin/PI3K/Akt signaling and therefore may paradoxically promote cell survival and prevent apoptosis in some contexts (Tabernero *et al*., 2008). Moreover, mTORC1 inhibition induces autophagy and macropinocytosis, which can be a source of nutrients for tumors, promoting cancer cell survival (Rabinowitz and White, 2010; Perera *et al*., 2015), thus a combined treatment of mTORC1 inhibitors with autophagy inhibitors could have good outcomes. Subsequently, a second generation of Rapalogs has been developed: they directly block the catalytic activity of mTOR, suppressing both mTORC1 and mTORC2, but the prolonged treatment was still causing Akt reactivation, thus resulting no more effective (Rodrik-Outmezguine *et al.*, 2011). Actually, for both first and second generation of mTOR inhibitors, the loss of efficacy is often associated to mutations in FKBP12–rapamycin-binding domain (FRB domain), causing reduced binding of

the first generation compounds, or mutations in mTOR kinase domain, resulting in inefficacy of the second generation inhibitors. Thus a third generation of mTOR inhibitors, called "RapaLinks", was developed in order to overcome the drug-resistence. These compounds are bivalent mTOR inhibitors consisting of a rapamycin–FRB-binding element appropriately linked to second-generation mTOR inhibitors. The exploitation of both the ATP- and the FRB-binding sites of mTOR allow the binding of the compound to one of the two binding domains, carrying the other half of the ligand in proximity to the second site, overcoming the reduced drug binding or the hyperactivity of the kinase, due to mutations in these domains (Rodrik-Outmezguine *et al.*, 2016).

MATERIALS AND METHODS

Materials

Reagents were obtained from the following sources: antibodies to human TFEB, phospho-T389 S6K1, S6K1, phospho-(Ser240/244) S6, S6, phospho-Ser757 ULK1, ULK1, phospho-(Ser 65) 4E-BP1, 4E-BP1, mTOR, RagA, RagB, RagC, RagD, FLCN, RAPTOR, ATG5, ATG7 and Histone H3 from Cell Signaling Technology; antibody to LAMP2 from Abcam; antibodies to TFE3, Actin and FLAG-BioM2 from Sigma Aldrich; antibody to murine TFEB from Bethyl laboratories; antibody to HA from Covance, antibody to LC3 from Novus Biologicals; antibody to P62 from Abnova; antibody to VAP-A was gently donated from De Matteis' laboratory. MEM, DMEM, McCoy's, RPMI, Fetal Bovine Serum (FBS) and Donkey Serum (DS) were from Euroclone; dialyzed FBS, Alexa 488 and 568-conjugated secondary antibodies, lipofectamine LTX and lipofectamine RNAimax were from Invitrogen; siRNAs were purchased as SMART pool from Dharmacon; torin 1, amino acids, MNase, polybrene were from Sigma Aldrich; puromycin was from Calbiochem; FuGENE 6, Complete Protease Cocktail and phosphatase inhibitors (Phospho Stop tablets) were from Roche; NeutrAvidin Agarose resin, SDS-OUT and D-biotin were from Pierce; amino acid-free RPMI from DBA; Mini-PROTEAN TGX Gels were from Biorad.

Cell culture and transfection

HeLa, HEK293T, HEPG2, U2OS, HK-2 cells were purchased from ATCC. *Atg5-/-*, *Atg7-/-* and *WT* MEFs cells were gently donated from Dr Maurizio Molinari. The

501Mel cells were a kind gift from Ruth Halaban (Halaban *et al*, 2000), and the A375P were from Colin Goding (Primot *et al.*, 2010). HCR-59 cells were gently provided by Dr. Malouf (Malouf *et al.*, 2014). Cells were cultured in the following media: HeLa in MEM; HEK293T and MEFs cells in DMEM high glucose; A375P, 501Mel and HEPG2 in RPMI; U2OS in McCoy's; HK-2 in DMEM-F12 supplemented with 1% ITS; HCR-59 in RPMI supplemented with MEM non-essential amino acids (1X), 1% ITS, Hydrocortisone 0,04ng/ml and EGF 0,01 ug/ml. All media were supplemented with 10% FBS. Primary kidney cells were obtained following the protocol described in Calcagni *et al.* (Calcagni *et al.,* 2016) and cultured in DMEM-F12 culture medium supplemented with 10% FCS, 1% ITS and 1% S1 hormone mixture. Plasmids were transfected with lipofectamine LTX and siRNA with lipofectamine RNAimax using a reverse transfection protocols and plated in 12 or 6-well dishes. After 48h of transfection with plasmids, cells were collected for RNA or protein analysis. Cells transfected with siRNAs (20nM) were collected after 72h since transfection.

Western blotting

Cells were lysed with ice-cold lysis buffer (TrisHcl 10mM pH 8.0-SDS 0.2% supplemented with protease and phosphatase inhibitors). Total lysate was briefly sonicated. Liver tissues were solubilized in homogenization buffer (25mM Tris-HCl pH 7.4, 10mM EDTA, 10mM EGTA, 1% NP40 supplemented with protease and phosphatase inhibitors). The soluble fractions from tissue lysates were isolated by centrifugation at 13,000 rpm for 10 minutes in a microfuge. From 10 to 30 micrograms of proteins were loaded on 10% or 4-15% Mini-PROTEAN TGX Gels transferred to PVDF membranes and analyzed by western blot using the ECL method (Pierce). Protein levels were quantified by using ImageJ software analysis.

Amino acid starvation/stimulation

Cells were rinsed with PBS and incubated in amino acid-free RPMI supplemented with 10% dialyzed FBS for 50 min, and then left untreated (0) or stimulated with increasing dosage of a mix of essential and non-essential amino acids for 15 min.

Organelle/cytosol fractionation

TFEB-CA HeLa cells were plated on 15cm plates and left untreated or treated with doxycycline. After 48h, they were rinsed with PBS and incubated in amino acid-free RPMI supplemented with 10% dialyzed FBS for 50 min, and then stimulated with a 3X amino acid mixture for 10min. Then, cells were rinsed with PBS and lysed using 10ml/dish of fractionation buffer (FB) (140mM KCl, 250mM Sucrose, 1mM DTT, 2mM EGTA, 2.5mM MgCl2, 25mM HEPES, pH 7.4) supplemented with 5mM glucose, protease inhibitor and 2.5mM ATP. After a brief centrifugation at 1700rpm for 10 minutes, pellet was resuspended in 750ul of FB and lysed by 23G needle; subsequently 750ul more of FB was added to the lysed and then it was centrifuged 10 min at 2700rpm in the 4C centrifuge. Post-nuclear supernatant (PNS) was transferred to a clean tube and centrifuged at 100K x g for 20min. The supernatant was the organelle-free cytosolic fraction. The pellet (organelles) was washed twice in buffer and eluted in SDS sample buffer. Equal fractions of pellets and supernatants were run on 4-15% Mini-PROTEAN TGX Gels for direct comparison.

Molecular biology

TFEB-WT and *TFEB-CA* TET-ON lentiviral plasmids were from Dr. Nick Platt; they carry the cDNAs for *TFEB-WT* or *TFEB-S142A, S211A* (*TFEB-CA*) *3X-FLAG*

tagged and cloned into KpnI and NotI sites of pLVX-Tight-Puro vector (Clontech). *EGFP-TFE3* plasmid was acquired from Addgene and used as template to amplify *TFE3* cDNA; this was subcloned into KpnI and NotI sites of pLVX-Tight-Puro vector. The cDNA for *TFE3* was mutagenized to convert the two serins 246 and 321 in alanines using the QuickChange XLII mutagenesis kit (Stratagene). Lentiviral plasmids for *TFEB* and *TFE3* were co-transfected with *Delta VPR* envelope and *CMV VSV-G* packaging plasmids into actively growing HEK-293T cells using FuGENE 6 transfection reagent. Virus-containing supernatants were collected 48h after transfection, diluted 1:2 and used to infect a 100mm dish (50% confluent) of HeLa Tet-ON cells (Clontech) in presence of polybrene (4ug/ml). 24 hours later, cells were selected with puromycin and analyzed 7 days after infection.

Stable HeLa TFEB-CA and TFE3-CA were treated, where indicated, with doxycycline (1ug/ml) for 48 hours. Retroviral plasmids encoding TFEB-3X-FLAG or GFP (as control) were previously described (Settembre *et al.*, 2012). They were co-transfected with *pCMV-gag/pol* and *CMV VSV-G* packaging plasmids into actively growing HEK-293T cells using FuGENE 6 transfection reagent. Virus-containing supernatants were collected 48h after transfection, diluted 1:2 and used to infect one six-well plate of MEFs in presence of 8ug/ml polybrene; then the plate was centrifuged at 2300 rpm RT for 90 min (spin infection). Cells were analyzed 3 days after infection.

The plasmid encoding human TFEB was previously described (Sardiello *et al.*, 2009); the plasmids for *HAGST-RagD* and *LAMP1-GFP* were purchased from Addgene.

Luciferase assay

The promoter region for *RagD* spanning from CLEAR 3 to CLEAR5 was amplified by PCR from HeLa genome and subcloned into pGL3-basic luciferase reporter plasmid. Consensus sequences for the three CLEARs were mutagenized by using the QuickChange XLII mutagenesis kit. Plasmids were co-transfected together with increasing amount of *TFEB* plasmid and luciferase assays were performed 48 h after transfection using Dual Luciferase Reporter Assay System (Promega) and normalized for transfection efficiency by cotransfected Renilla luciferase.

Chromatin Immunoprecipitation assay (ChIP)

HeLa TET-ON TFEB-CA cells were treated with doxycycline for 48h or left untreated (control) and then crosslinked in 1% formaldehyde for 10 min and lysed on ice for 20 min in ChIP-Lysis buffer (50 mM Tris–HCl, pH 7.5, 100 mM NaCl, 1% Triton X- 100, 1% Tween-20). After a 13 min MNAse digestion (2U, Sigma-Aldrich) at 37°C, the reaction was stopped by addition of sodium dodecyl sulfate (SDS) and ethylenediaminetetraacetic acid (EDTA) to a final concentration of 1% and 2 mM, respectively. The unbound SDS of the cleared lysate was precipitated using SDS-OUT (Pierce, Rockford, IL, USA) to avoid compromising the immunoprecipitation. The lysates were diluted 1:1 with ChIPdilution buffer (50 mM Tris–HCl, pH 7.5, 100 mM NaCl, 0.5% Triton X-100, 2 mM EDTA; all from Sigma-Aldrich) and preincubated with high capacity NeutrAvidin Agarose (Pierce). Protein-DNA complexes were immunoprecipitated for 4 h at 4°C with biotinylated FLAG antibody coupled to Neutravidin beads (2 mg ANTI-FLAG BioM2 from Sigma-Aldrich antibody with 50 ml Agarose slurry in ChIP-dilution buffer supplemented with 10 mg/ml BSA per sample). After three washings, the DNA

was eluted by addition of 8 mM biotin, 1% SDS in TE buffer. The DNA was precipitated after crosslink reversal using 200 mM NaCl at 65°C, overnight. One µl of DNA was used for each quantitative rtPCR reaction.

RNA extraction, reverse transcription and quantitative PCR

RNA samples from cells were obtained using the RNeasy kit (Qiagen) according to the manufacturer's instructions. RNA samples from mouse livers were extracted using TRIzol (Invitrogen) and re-purified with a RNeasy columns. cDNA was synthesized using QuantiTect Reverse Transcription kit (Qiagen).

Real-time quantitative RT-PCR on cDNAs was carried out with the LightCycler 480 SYBR Green I mix (Roche) using the Light Cycler 480 II detection system (Roche) with the following conditions: 95°C, 5 min; (95°C, 10 s; 60°C, 10 s; 72°C, 15 s) x 40. Fold change values were calculated using the DDCt method. Briefly, internal controls (*HPRT1* or *B2M* for cell samples and *Cyclophilin* or *S16* for mouse samples) were used as 'normalizer' genes to calculate the DCt value. Next, the DDCt value was calculated between the 'control' group and the 'experimental' group. Lastly, the fold change was calculated using 2(-DDCt). Biological replicates were grouped in the calculation of the fold change values.

Immunofluorescence assays

For detection of TFEB or TFE3, HeLa stable clones were grown on Lab-Tek chamber slides and treated with doxycycline for 48h. Cells were rinsed with PBS once and then: fixed for 15 min with 4% paraformaldehyde in PBS at RT, rinsed twice with PBS and then permeabilized with 0.2% Triton-X100 in PBS for 30min, and then incubated with blocking buffer (0.1% Triton-X100 plus 10% donkey

serum in PBS) for 1h. Subsequently, the slides were incubated with TFEB antibody (1:200) or TFE3 (1:500) in 0.1% Triton-X100 plus 5% donkey serum/PBS for 2h at RT, then rinsed three times with PBS and incubated with Alexa-Fluor conjugated secondary antibodies (Invitrogen) produced in donkey (diluted 1:700 in 0.1% Triton-X100 plus 5% donkey serum/PBS) for 1h at room temperature in the dark, washed four times with PBS. Slides were mounted on glass coverslips using Vectashield (Vector Laboratories) and imaged on a Leica SPE confocal microscope.

For detection of mTOR lysosomal localization: HeLa TFEB-CA cells were left untreated or treated with doxycycline for 48h; HeLa cells were transfected with scramble si-RNA or with siRNA for *TFEB* and then re-transfected with control plasmid and *LAMP1-GFP* plasmid, or with *HAGSTRagD* and *LAMP1-GFP* plasmid. Cells were grown on Lab-Tek chamber slides and the day of experiment they were rinsed with PBS and incubated in amino acid-free RPMI supplemented with 10% dialyzed FBS for 50 min, and then left untreated or stimulated with a 3X amino acid mixture for 10min. Then, slides were rinsed with PBS once and fixed for 15 min with 4% paraformaldehyde in PBS at RT. After fixation, slides were rinsed twice with PBS and cells were permeabilized with Saponine 0.1% in PBS for 10min. After rinsing twice with PBS, the slides were incubated with primary antibody (mTOR and LAMP2, both 1:200) in 5% normal donkey serum for 1 hr at room temperature, rinsed four times with PBS, and incubated with secondary antibodies produced in donkey (diluted 1:700 in 5% normal donkey serum) for 45 min at room temperature in the dark, washed four times with PBS. Slides were mounted on glass coverslips using Vectashield (Vector Laboratories) and imaged on LSM 800 confocal microscope. Co-localization analysis was performed using ZEN 2008 software and it is expressed as colocalization coefficient. For detection

of LC3 on the lysosome, cells were fixed with 100% methanol and then processed as described above. Analysis was performed using ZEN 2008 software and it is expressed as LC3 Mean Intensity versus LAMP2 Mean Intensity in the co-localization region.

Cell proliferation

For MTT assay, 5mg of MTT powder was solubilized in 1mL of PBS and filtered. 10µL of this solution was added to 100µl of cell culture medium without phenol red. At the end of the incubation time, cells were washed twice with PBS and incubated with MTT-media solution to form formazan crystals. After two-three hours, media was removed and 100µl/well of a solubilization solution was added to the cells (2 mL H_2O AMMONIA in 50 mL DMSO) for 10 minutes at 37°C to obtain a complete solubilization of the crystals. As readout, absorbance of the 96-well plate was measured recording the Optical Density (OD) at 540nm with a microplate spectrophotometer system.

Generation of *RagD*-promoter mutant HeLa cell line

HeLa (ATCC CCL-2) cells carrying a homozygous deletion of the CLEAR-binding sequence in the promoter of the *RagD* gene were generated by using the CRISPR/Cas9 system. We selected the DNA region with the protospacer adjacent motif (PAM) sites within the CLEAR-box sequence GACCACGTGAA (-284) of the *RagD* promoter. The gRNA sequence (CTGTGCGGGGACCACGTGA) with low off-target score has been selected using the http://crispr.mit.edu/ tool. An “ALL in One” vector expressing Cas9, the specific gRNA and GFP was obtained from SIGMA (CAS9GFPP). The CAS9GFPP was nucleofected in HeLa cells using the

Amaxa (Cat No VCA-1003) and transfected GFP-positive cells were FACS sorted into 96 well plates to obtain single-cell derived colonies carrying the INDEL mutations. Upon genomic DNA extraction and DNA Sanger sequencing, a cell clone carrying a 33bps deletion (-266_299del TGCGGGGACCACGTGAAGGAGAGGCGCGTGGGG) was selected and expanded.

Mouse models

All mice used were males and maintained in a C57BL/6 strain background. Mouse lines for conditional *Tcfeb-flox* was previously described (Settembre *et al.*, 2012); *Albumin (Alb)-Cre* mice were obtained from the Jackson laboratory; *Myosin light chain 1 (Mlc)-Cre* mice were previously described (Bothe *et al.*, 2000). The mouse line overexpressing Tcfeb in the kidney only was recently reported (Calcagnì *et al.*, 2016). The *HDAd-TFEB* virus was described previously (Settembre *et al.*, 2013a). Hepatic transduction was achieved by intravenous administration (retro-orbital) of $2x10^{13}$ viral particles/kg. Mice were analyzed one month after infection. The *RagD*-AAV vector was produced by the TIGEM AAV Vector Core Facility. Briefly, the human *HA-GST-RagD* coding sequence was cloned into the pAAV2.1-*CMV-GFP* plasmid by replacing the *GFP* sequence. The resulting pAAV2.1-*CMV-HA-GST-RagD* was then triple transfected in sub-confluent 293 cells along with the pAd-Helper and the pack 2/9 packaging plasmids. The recombinant AAV2/9 vectors were purified by two rounds of CsCl. Vector titers, expressed as genome copies (GC/mL), were assessed by both PCR quantification using TaqMan (Perkin-Elmer, Life and Analytical Sciences, Waltham, MA) and by dot blot analysis. As control virus, *GFP*-AAV vectors were used. Each mouse was retro-orbital injected with $1.25x10^{11}$ viral particles and sacrificed after 3 weeks. Experiments of

synchronization/fasting of mice were performed as previously reported (Ezaki *et al.,* 2011); 30 minutes before to be sacrificed, mice were injected intraperitoneally (IP) with puromycin (21,8mg/kg of mouse in 20 mM HEPES buffer pH 7.4). For exercise experiment, mice were let run for 1h at 25cm/sec on a treadmill, for one week. On the last day of training, mice received oral gavage administration of leucine (1,35g/kg of mouse in H2O); 30 minutes later they were injected IP with puromycin and after 30 minutes sacrificed for the analysis. Experiments were conducted in accordance with the guidelines of the Animal Care and Use Committee of Cardarelli Hospital in Naples and authorized by the Italian Ministry of Health.

Histology

Livers were dissected, post-fixed with buffered 4% paraformaldehyde overnight at 4°C, then they were dehydrated in a graded series of ethanol, cleared with xylene, and infiltrated with paraffin. Paraffin-embedded blocks were cut on a microtome in 6-µm sections. Immunohistochemistry was performed using the Vectastain ABC kit (Vector Labs) following the manufacturer's instructions. Signal was developed using 0.05% 3,3-diaminobenzidine tetrahydrochloride in 0.02% H_2O_2.

Xenograft experiments

Lentiviral particles (shLuc or shRagD) obtained from 293T transfection were added to 501Mel cells together with 4 µg/mL polybrene (Sigma) for 16 hours. After 48 hours, medium was replaced and 2µg/mL of puromycin was added for 72 hours before performing the experiment. 500,000 cells were resuspended in a 3:1 mix of cell medium and Matrigel Matrix (Corning 354248) and injected into the

subcutaneous abdominal space of NOD.Cg-Prkdcscid Il2rgtm1Wjl/SzJ mice (NSG) mice. Tumor formation was monitored weekly. Mice were sacrificed when tumors of the control group (shLuc) reached the volume of ~ 0.5 cm3. In vivo data are presented as mean ± s.d. (standard deviation) from three independent experiments. NSG mice were purchased from Charles River. Mice of both sexes, 6-12 weeks old, were used for experimental procedures. In vivo studies were performed according to fully authorized animal facility, notification of the experiments to the Ministry of Health (as required by the Italian Law)(IACUCs No 758/2015) and in accordance to EU directive 2010/63.

Statistics

Student t test was used when comparing two groups; Anova was used when comparing more than two groups.

RESULTS

1. TFEB regulates mTORC1 activity.

In presence of nutrients, mTORC1 negatively regulates the activity of the MiT/TFE transcription factors by phosphorylating critical serine residues, thus causing their cytoplasmic retention (Martina et *al.*, 2012; Roczniak-Ferguson *et al.*, 2012; Settembre *et al.*, 2011, 2012). Data from literature suggest that mTOR complexes may operate in the context of negative feedback loops to maintain various aspect of cellular homeostasis (Eltschinger *et al.,* 2016), thus we postulated the presence of a feedback loop by which MiT/TFE transcription factors, which are substrates of mTORC1, may in turn influence mTORC1 activity.

To test whether TFEB could influence mTORC1 activity, we analyzed mTORC1 pathway upon amino acids stimulation in a HeLa cell line overexpressing the wild-type form of TFEB (TFEB-WT) and the constitutive active form of TFEB (TFEB-CA) in a doxycycline inducible manner. These cell lines were obtained by infection of TET-inducible lentiviral vectors in HeLA cells stably expressing the reverse tetracycline-controlled TransActivator (rtTA). The Tetracycline-ON system (Tet-ON) is activated by doxycycline, which binds to the rtTA promoting the transcription of the DNA sequences cloned downstream the Tet Response Element (TRE) (Gossen *et al.*, 1995). We generated two TFEB-inducible HeLa cell lines, one expressing the WT form of TFEB and the other expressing the constitutive active form of TFEB (TFEB-CA), obtained mutating the serine residues 142 and 211 on TFEB coding sequence into alanines, thus relieving TFEB of mTORC1 inhibition (Martina et *al.*, 2012; Roczniak-Ferguson *et al.*, 2012; Settembre *et al.*, 2011, 2012) (Fig.3).

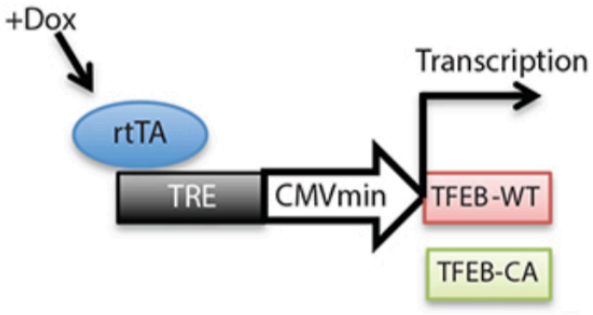

Fig.3. TetON system.

Scheme of doxycycline- inducible *TFEB*-WT and *TFEB*-CA constructs.

Upon doxycycline induction, the TFEB-WT cell line overexpressed the wild-type form of TFEB, showing a cytosolic localization in fed conditions and a nuclear localization in starved cells (Fig.4). Whereas the TFEB-CA cell line expressed a constitutively nuclear TFEB, in both fed and starved conditions (Fig.4). The two cell lines showed an increase in TFEB mRNA level of around 2 fold compared to non treated cells (Fig.5).

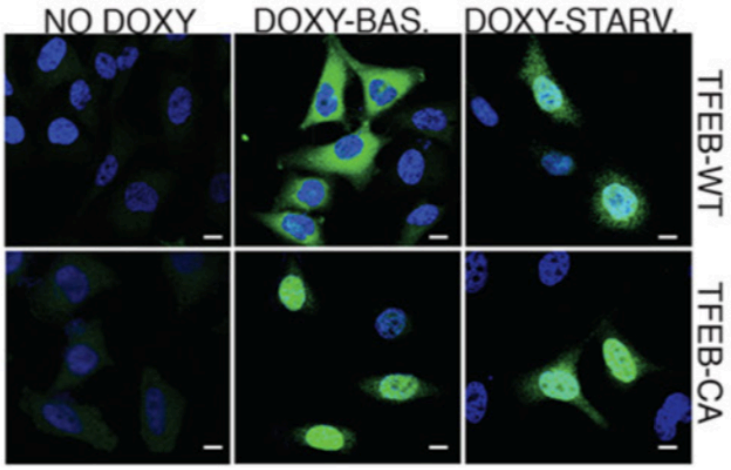

Fig. 4. TFEB subcellular localization in doxycycline-inducible Hela cell lines.

Representative immunofluorescence of TFEB in stable doxycycline-inducible cell lines, overexpressing the wild type form of TFEB (TFEB-WT) and TFEB-Constitutively Active (TFEB-CA).

Cells were untreated or treated with doxycycline (1mg/mL) for 48hours, in basal and in starved conditions. Scale bars 10 μm.

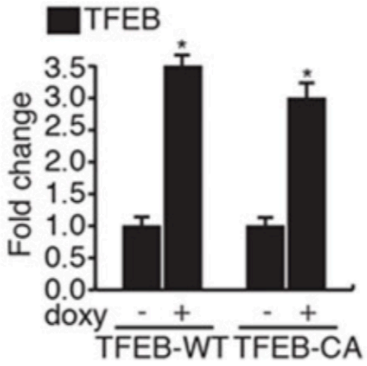

Fig. 5. TFEB expression levels in doxycycline-inducible Hela cell lines.

TFEB mRNA levels in TFEB-WT and TFEB-CA cells untreated or treated with doxycycline (1mg/mL) for 48hours. Gene expression was normalized relative to *HPRT1*. Values are mean ± SEM (*$p < 0.05$ Student t test).

We performed our studies preferentially in TFEB-CA cells, since this cell line represents a useful tool to escape mTORC1 regulation of TFEB. We observed that overexpression of TFEB-CA strongly affected mTORC1 activity in response to amino acids stimulation by looking at the phosphorylation of the main target proteins of mTORC1: direct targets, such as S6K1 and 4EBP1, and also indirect targets, like the ribosomal protein S6 (S6), phosphorylated by S6K1 (Fig.6).

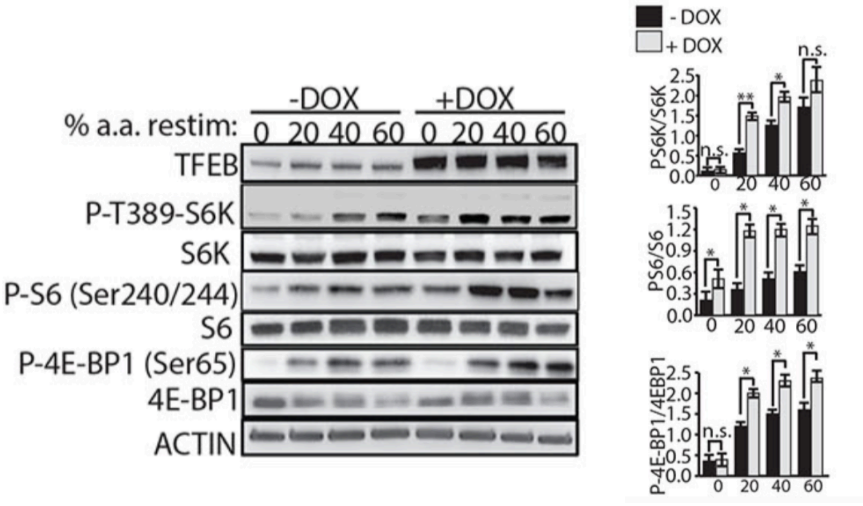

Fig. 6. Analysis of phosphorylation levels of mTORC1 substrates in TFEB-CA cell line.

TFEB-CA cells, treated or untreated with doxycycline (1mg/mL) for 48hours, were starved for amino acids (a.a.) for 50 min and then left untreated (0) or stimulated with increasing levels of amino acids (expressed as % of a.a concentration in RPMI medium). Cell lysates were analyzed for phosphorylation of S6K, S6 and 4E-BP1 proteins. The plots represent mean values of triplicate experiments expressed as ratio of phosphorylated S6K versus pan-S6K, phosphorylated S6 versus pan-S6 and phosphorylated 4E-BP1 versus 4E-BP1. Values are mean ± SEM (*$p < 0.05$, **$p<0.01$ Student t test).

Conversely, TFEB depletion in HeLa cells significantly decreased mTORC1 activity upon amino acids administration (Fig.7).

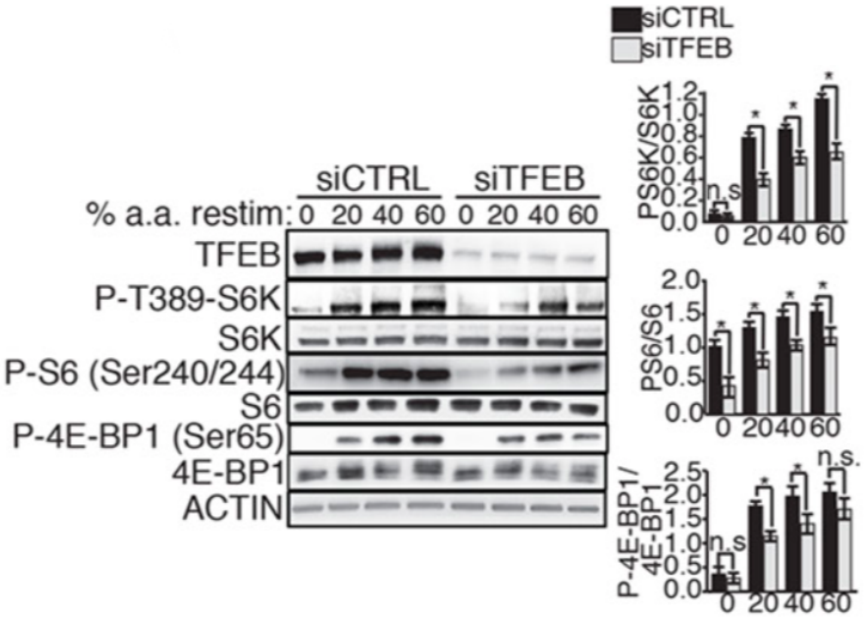

Fig. 7. Analysis of phosphorylation levels of mTORC1 substrates in TFEB silenced cells.

Immunoblot analysis of S6K, S6 and 4E-BP1 phosphorylation in HeLa cells transfected with scramble or TFEB siRNA. Cells were first starved for amino acids (a.a.) for 50 min and then left untreated (0) or stimulated with increasing levels of amino acids (expressed as % of a.a concentration in RPMI medium). The plots represent mean values of triplicate experiments expressed as ratio of phosphorylated S6K versus pan-S6K, phosphorylated S6 versus pan-S6 and phosphorylated 4E-BP1 versus 4E-BP1. Values are mean ± SEM (*p < 0.05, **p<0.01 Student t test).

To confirm that these evidencies were not strictly associated to the cell line analyzed, we evaluated the phosphorylation status of mTORC1 substrates, after amino acids stimulation, in different cell lines transfected with TFEB or with a control vector. We analyzed respectively HEK293-T cells (Fig.8), HEPG2 cells (Fig.9) and U2OS cells (Fig.10) and in all of them we observed a striking upregulation of mTORC1 signaling upon TFEB overexpression compared to control samples. These data indicate that TFEB regulate mTORC1 signaling in different cell lines.

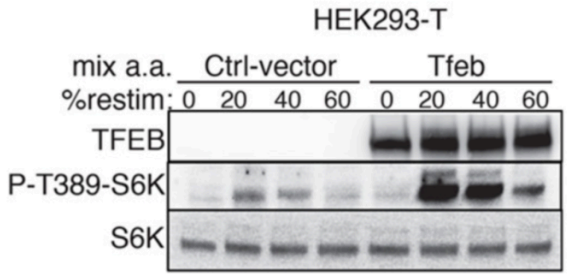

Fig.8. TFEB regulates mTORC1 activity in HEK293-T cells.

Immuno-blotting analysis of threonine 389-S6K phosphorylation in HEK293-T cells transfected with TFEB or with a control pCDNA plasmid vector. Cells were starved for amino acids (a.a.) for 50 min and then left untreated (0) or stimulated with increasing levels of a.a. for 20 min.

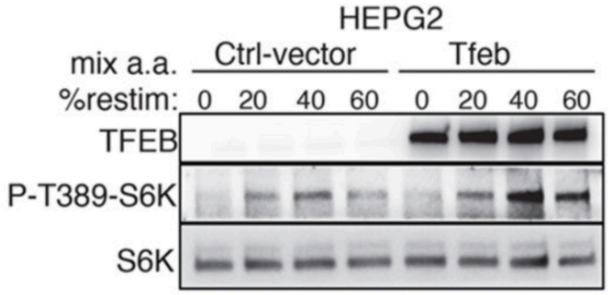

Fig.9. TFEB regulates mTORC1 activity in HEPG2 cells.

Immuno-blotting analysis of threonine 389-S6K phosphorylation in HEPG2 cells transfected with TFEB or with a control pCDNA plasmid vector. Cells were starved for amino acids (a.a.) for 50 min and then left untreated (0) or stimulated with increasing levels of a.a. for 20 min.

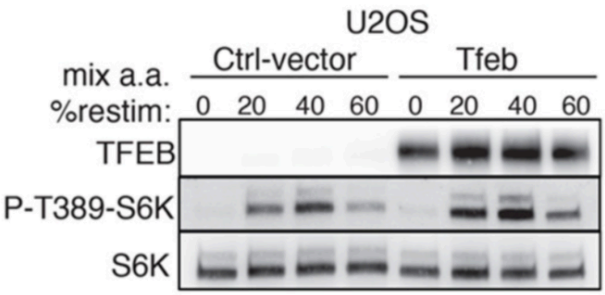

Fig.10. TFEB regulates mTORC1 activity in U2OS cells.

Immuno-blotting analysis of threonine 389-S6K phosphorylation in U20S cells transfected with TFEB or with a control pCDNA plasmid vector. Cells were starved for amino acids (a.a.) for 50 min and then left untreated (0) or stimulated with increasing levels of a.a. for 20 min.

Since cell growth is a well known redout of mTORC1 activation (Saxton and Sabatini, 2017), we analyzed cell size and proliferation upon TFEB overexpression, to assess if TFEB levels could modulate these parameters. In line with our hypothesis, TFEB overexpression caused an increase in both cell size (Fig.11) and cell proliferation rate (Fig.12), and these effects were lost upon treatment with an inhibitor of mTORC1, Torin 1, suggesting that these results were due to TFEB-dependent mTORC1 hyperactivation.

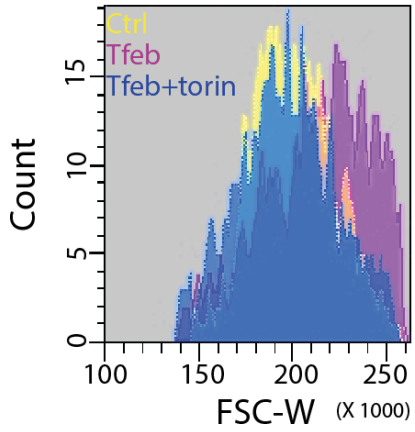

Fig.11. Analysis of cell size upon TFEB overexpression.

FACS analysis performed in HeLa cells transfected with TFEB compared to control. Torin 1 was added, where indicated, for 48h (100nM). Plot represents means of three independent experiments ± SEM; one-way ANOVA.

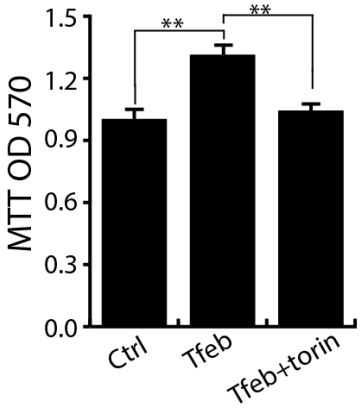

Fig.12. Analysis of cell proliferation rate upon TFEB overexpression.

MTT assay performed in HeLa cells transfected with TFEB compared to control. Torin was added, where indicated, for 48h (100nM). Plot represents means of three independent experiments ± SEM; one-way ANOVA.

These data, altogether, clearly indicate that TFEB regulates mTORC1 signaling pathway.

2. TFEB controls mTORC1 activity through RagD-GTPase.

Autophagy contributes to the pool of amino acids in the lysosomal lumen via lysosome-mediated proteolysis. Since TFEB belongs to the MiT/TFE family of transcription factors and it is an important regulator of autophagy (Sardiello *et al.* 2009, Settembre *et al.* 2011), we evaluated whether these factors regulate mTORC1 activity by modulating autophagy. Thus, we overexpressed TFEB in MEFs lacking the essential autophagy genes *Atg5* (Fig.13) or *Atg7* (Fig.14), and then we analyzed mTORC1 activity. TFEB overexpression in these autophagy-deficient cells still resulted in an enhanced mTORC1 activity, similar to the one observed in wild type MEFs, indicating that TFEB regulation of mTORC1 signaling is autophagy-indipendent (Fig.13, Fig.14).

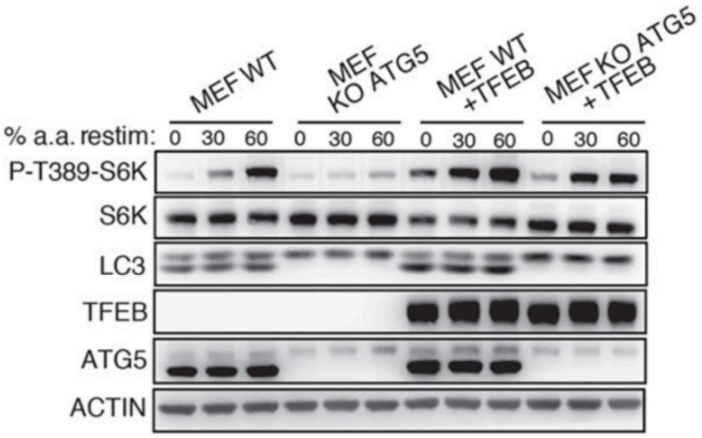

Fig.13. Analysis of mTORC1 activity in MEF Knock-Out for *Atg5*.

Mouse embryonic fibroblasts (MEFs) knock out for *Atg5* were retrovirally infected with a TFEB or control pCDNA plasmids. Cells were starved for a.a. for 50 min and then stimulated with increasing amount of a.a. for 20 min. Protein lysates were analyzed for the levels of threonine 389 S6K phosphorylation and the for the indicated proteins.

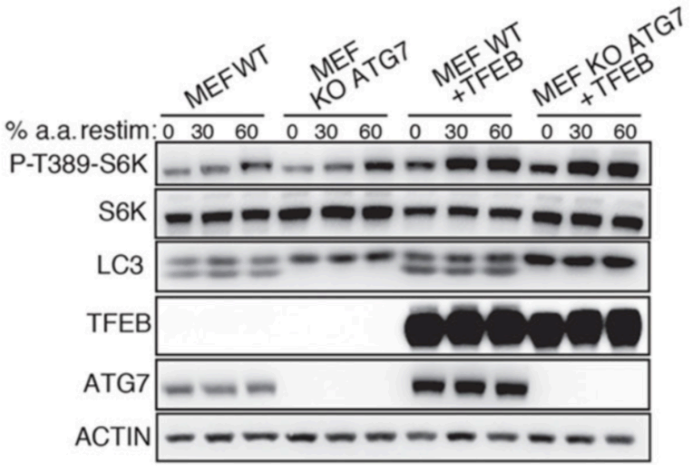

Fig.14. Analysis of mTORC1 activity in MEF Knock-Out for *Atg7*.

Mouse embryonic fibroblasts (MEFs) knock out for *Atg7* were retrovirally infected with a TFEB or control pCDNA plasmids. Cells were starved for a.a. for 50 min and then stimulated with increasing amount of a.a. for 20 min. Protein lysates were analyzed for the levels of threonine 389 S6K phosphorylation and the for the indicated proteins.

To identify the mechanism responsible for TFEB control of mTORC1 activity, we investigated whether TFEB was regulating mTORC1 activity through transcriptional regulation of one or more genes involved in this pathway. Starting from a selection of 50 genes involved in mTORC1 activation (Table 1), we performed a bioinformatic analysis to look for CLEAR elements in the promoters of these selected genes. From this analysis, we obtained 20 putative TFEB target genes (Table 2) and we validated them by real time PCR in HeLa cells depleted for TFEB (Fig.15). The transcript levels of RagD, one of the RagGTPases involved in mTORC1 recruitment on the lysosomes (Sancak *et al*. 2008), were the most significantly downregulated in cells silenced for TFEB (Fig.15). Conversely, *RagD* was strongly induced upon doxycycline treatment in TFEB-CA cells (Fig.16). Similar results were obtained by western blot, where we observed a strong increase of RagD protein levels (Fig.17). Also RagC and FLCN transcript and protein levels were increased upon TFEB overexpression, albeit at a lower extent compared to RagD (Fig.16, Fig.17).

Official Symbol	Official Full Name
AKT1S1	AKT1 substrate 1
ATP6V0A4	ATPase H+ transporting V0 subunit a4
ATP6V0B	ATPase H+ transporting V0 subunit b
ATP6V0D1	ATPase H+ transporting V0 subunit d1
ATP6V0D2	ATPase, H+ transporting, lysosomal V0 subunit D2
ATP6V0E1	ATPase H+ transporting V0 subunit e1
ATP6V1A	ATPase H+ transporting V1 subunit A
ATP6V1B1	ATPase H+ transporting V1 subunit B1
ATP6V1B2	ATPase H+ transporting V1 subunit B2
ATP6V1C1	ATPase H+ transporting V1 subunit C1
ATP6V1C2	ATPase H+ transporting V1 subunit C2
ATP6V1D	ATPase H+ transporting V1 subunit D
ATP6V1E1	ATPase H+ transporting V1 subunit E1
ATP6V1E2	ATPase H+ transporting V1 subunit E2
ATP6V1F	ATPase H+ transporting V1 subunit F
ATP6V1G1	ATPase H+ transporting V1 subunit G1
ATP6V1G2	ATPase H+ transporting V1 subunit G2
ATP6V1G3	ATPase H+ transporting V1 subunit G3
ATP6V1H	ATPase H+ transporting V1 subunit H
DEPDC5	DEP domain containing 5
DEPTOR	DEP domain containing MTOR-interacting protein
FLCN	folliculin
FNIP1	folliculin interacting protein 1
LAMTOR1	late endosomal/lysosomal adaptor, MAPK and MTOR activator 1
LAMTOR2	late endosomal/lysosomal adaptor, MAPK and MTOR activator 2
LAMTOR3	late endosomal/lysosomal adaptor, MAPK and MTOR activator 3
LAMTOR4	late endosomal/lysosomal adaptor, MAPK and MTOR activator 4
LAMTOR5	late endosomal/lysosomal adaptor, MAPK and MTOR activator 5
MIOS	meiosis regulator for oocyte development
MLST8	MTOR associated protein, LST8 homolog
MTOR	mechanistic target of rapamycin
NPRL2	NPR2-like, GATOR1 complex subunit
NPRL3	NPR3-like, GATOR1 complex subunit
RHEB	Ras homolog enriched in brain
RPTOR	regulatory associated protein of MTOR complex 1
RRAGA	Ras related GTP binding A
RRAGB	Ras related GTP binding B
RRAGC	Ras related GTP binding C
RRAGD	Ras related GTP binding D
SEC13	SEC13 homolog, nuclear pore and COPII coat complex component
SEH1L	SEH1 like nucleoporin
SESN1	sestrin 1
SESN2	sestrin 2
SESN3	sestrin 3
SLC36A1	solute carrier family 36 member 1
SLC38A9	solute carrier family 38 member 9
TSC1	tuberous sclerosis 1
TSC2	tuberous sclerosis 2
WDR24	WD repeat domain 24
WDR59	WD repeat domain 59

Table 1. List of mTORC1 related genes analyzed for the presence of CLEAR elements in their promoter regions

Gene Symbol	Score	Sequence	Chrom	Start	End	Strand	TSS Position
AKT1S1	0.8605206	CGGGCACGTGAGTG	chr19	49876596	49876609	-	-359
	0.8089129	GCACCACCTGGGGC	chr19	49877420	49877433	-	-45
	0.8463874	GAGTCGCCTGAGCC	chr19	49877933	49877946	-	-558
	0.8369624	GGGGCAGCTGAGCG	chr19	49876172	49876185	-	65
	0.9183985	GAGTCACGTGGCGC	chr19	49877526	49877539	-	-151
	0.8106931	GGCTCACGGGAGGG	chr19	49876509	49876522	-	-272
ATP6V0D1	0.9376113	GCGTCACCTGACGC	chr16	67481187	67481200	-	-13
	0.8840902	GCGTCAGCTGACCT	chr16	67481149	67481162	-	25
	0.9353275	TGGTCACGTGAGGC	chr16	67481207	67481220	-	-33
	0.8262983	GCGTCAAGTGCAGC	chr16	67481399	67481412	-	-225
ATP6V0E1	0.8605773	ACCTCAAGTGATCC	chr5	172983372	172983385	+	-387
	0.8003814	TGGTCACGCGGTCA	chr5	172983779	172983792	+	20
	0.9040944	GGGTCACGTGGGGG	chr5	172983740	172983753	+	-19
ATP6V1A	0.8714547	AGATCACGTGATTG	chr3	113746694	113746707	+	-324
	0.8131261	CCAGCAGGTGAGCG	chr3	113747107	113747120	+	89
	0.8398537	ACGTCATGTGACTG	chr3	113746987	113747000	+	-31
ATP6V1C1	0.8637182	CGGTCAGCTGACTG	chr8	103021050	103021063	+	31
	0.8245659	CTGGCACGTGACTT	chr8	103021069	103021082	+	50
ATP6V1G1	0.9052289	CGGTCACGTGACAA	chr9	114587707	114587720	+	-6
	0.8713504	CGGTCAGCTGATGC	chr9	114587684	114587697	+	-29
	0.8859463	GTGTCAGCTGACCC	chr9	114587769	114587782	+	56
	0.8087201	TCCTCACCTGAAGT	chr9	114586875	114586888	+	-838
ATP6V1H	0.8736252	ACCTCAGGTGATCC	chr8	53844034	53844047	-	-735
	0.8228824	GGTTCAAGTGATTT	chr8	53844169	53844182	-	-870
	0.8345218	AGGTCAGGCGACTC	chr8	53842979	53842992	-	51
	0.9348623	CGATCACGTGACCG	chr8	53843282	53843295	-	17
	0.9348623	CGATCACGTGACCG	chr8	53843282	53843295	-	-252
	0.8007044	TGGTCAGCTGGTCT	chr8	53844058	53844071	-	-759
	0.8748247	CAGTCACGTGCCTC	chr8	53843296	53843309	-	3
	0.8748247	CAGTCACGTGCCTC	chr8	53843296	53843309	-	-266
DEPDC5	0.8294047	TTCTCAGGTGAGCG	chr22	31753990	31754003	+	40
	0.8115772	AGGCCACATGAGTC	chr22	31753628	31753641	+	-394
	0.8294047	TTCTCAGGTGAGCG	chr22	31753990	31754003	+	-32
	0.8399601	GAGTCACTTGGCAC	chr22	31754742	31754755	+	-119
	0.8115772	AGGCCACATGAGTC	chr22	31753628	31753641	+	-322
	0.8294047	TTCTCAGGTGAGCG	chr22	31753990	31754003	+	-871
FLCN	0.8028213	GAGTCACGCGCCTG	chr17	17237175	17237188	-	1
	0.8736252	GGATCACCTGAGGT	chr17	17238053	17238066	-	-877
	0.95246	GCGTCACGTGACGG	chr17	17237679	17237692	-	-503
FNIP1	0.8858526	CCGCCACGTGATGC	chr5	131797102	131797115	-	-51
	0.8602704	CTGCCACGTGACGG	chr5	131797183	131797196	-	-132
LAMTOR1	0.8374083	GCATCACGTGCTTG	chr11	72103453	72103466	-	-78
	0.9121162	GGGTCATGTGACCG	chr11	72103289	72103302	-	86
	0.8487087	AAGTCATGTGATCC	chr11	72103483	72103496	-	-108
LAMTOR4	0.8560043	CAAGCACGTGACCG	chr7	100148900	100148913	+	-77
	0.8560043	CAAGCACGTGACCG	chr7	100148900	100148913	+	2
RRAGB	0.8824455	TGCCCACGTGATCC	chrX	55717752	55717765	+	76
	0.8894155	CAGTCACGTGACAG	chrX	55717720	55717733	+	44
	0.8568544	AGGCCACGTGATGA	chrX	55717630	55717643	+	-46
	0.8928861	GCCTCAAGTGATCC	chrX	55717134	55717147	+	-542
RRAGC	0.8797411	CCGGCACGTGACGG	chr1	38859875	38859888	-	-64
	0.8876463	GAGTCAGGTGATTC	chr1	38859888	38859901	-	-77
RRAGD	0.8946558	GTGTCAGGTGACTC	chr6	89412283	89412296	-	-19
	0.8539427	GGACCACGTGAAGG	chr6	89412548	89412561	-	-284
	0.8224805	GAGTCATGTGATTT	chr6	89412914	89412927	-	-650
SEC13	0.8736252	ACCTCAGGTGATCC	chr3	10321463	10321476	-	-434
	0.8736252	ACCTCAGGTGATCC	chr3	10321463	10321476	-	-287
SESN3	0.8090171	GCATCAAGCGACCT	chr11	95233038	95233051	-	-509
	0.8111394	GGGGCAGCTGCCGC	chr11	95231044	95231057	-	26
SLC36A1	0.9058515	GGATCACGTGATGA	chr5	151447591	151447604	+	-4
	0.8901018	GGAGCACGTGACCT	chr5	151447556	151447569	+	-39
SLC38A9	0.8007021	CGCCCACCTGGGCG	chr5	55712503	55712516	-	-180
	0.8309181	TTCTCACGTGGCCT	chr5	55712625	55712638	-	-302
	0.8250914	GCCTCAAATGATCC	chr5	55713299	55713312	-	-976
	0.8666579	GCCTCAAGTGATTC	chr5	55713162	55713175	-	-839
TSC2	0.8239222	GGGGCAAGTGGCGG	chr16	2048084	2048097	+	-117
	0.9275004	CCGTCACGTGATGC	chr16	2047867	2047880	+	-27
	0.9275004	CCGTCACGTGATGC	chr16	2047867	2047880	+	-334

Table 2. Distribution of CLEAR elements in the promoters of the selected mTORC1 related genes.

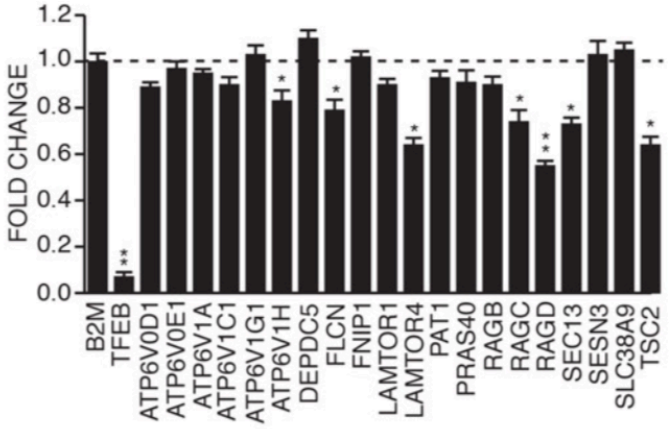

Fig.15. Expression levels of mTORC1 related genes in TFEB depleted cells.

mRNA levels of mTORC1-related genes in HeLa cells depleted for TFEB. *B2M* mRNA levels were measured as control gene. mRNA levels were normalized using *HPRT1* and expressed as relative to cells transfected with scramble siRNA. *B2M* mRNA levels were measured as control gene. Values are normalized relative to *HPRT1* and expressed as fold change relative to untreated cells. Bar graphs represent mean ± SEM of 3 independent experiments (*p < 0.05, **p < 0.01, Student t test).

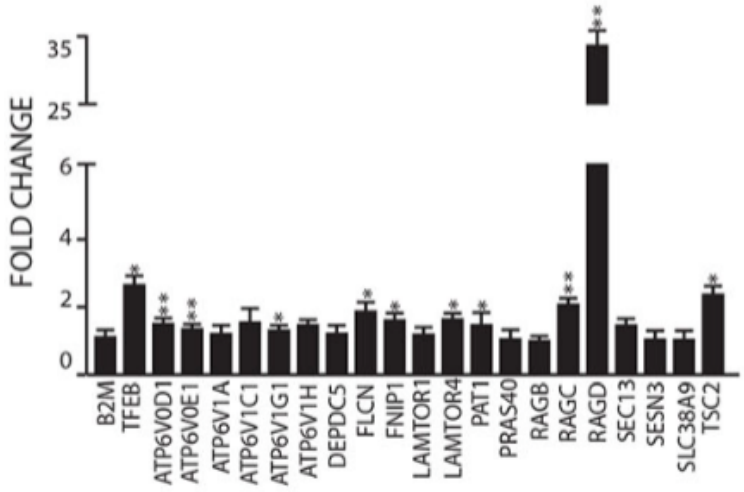

Fig.16. Expression levels of mTORC1 related genes in TFEB-CA cells.

mRNA levels of mTORC1-related genes in TFEB-CA HeLa cells treated with doxycycline (1mg/mL) for 48h. *B2M* mRNA levels were measured as control gene. Values are normalized relative to *HPRT1* and expressed as fold change relative to untreated cells. Bar graphs represent mean ± SEM of 3 independent experiments (*p < 0.05, **p < 0.01, Student t test).

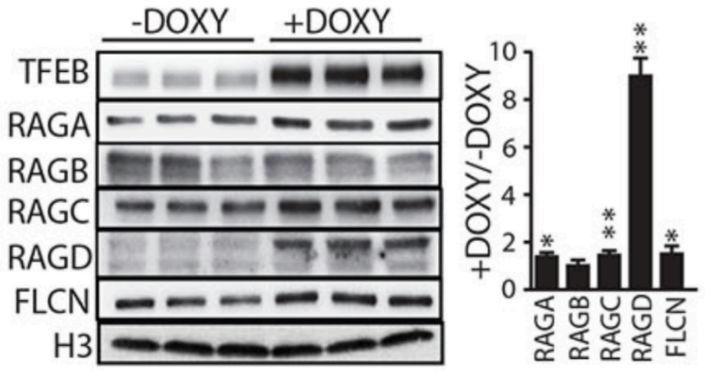

Fig.17. Protein levels of some of the mTORC1-related genes in TFEB-CA cells.

Immuno-blotting analysis of the indicated proteins in TFEB-CA HeLa cells treated with doxycycline (1mg/mL) for 48h compared to control. The plot represents average values of triplicates normalized to histone H3 (*p < 0.05, **p < 0.01 Student t test).

RagD was strongly induced upon TFEB overexpression, both at transcript and at protein level, in different cell lines (HEK293-T, HEPG2, U20S)(Fig.18, Fig.19).

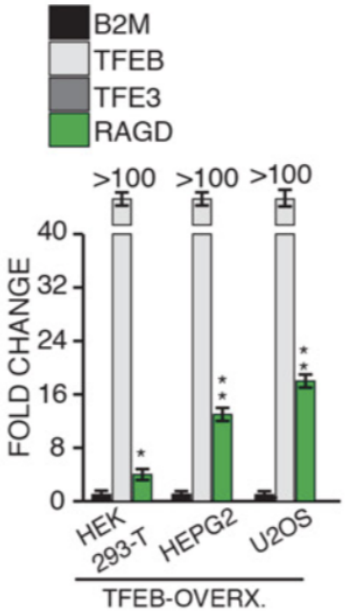

Fig.18. Expression analysis of *RagD* gene in HEK293-T, HEPG2 and U2OS cells transiently transfected with TFEB plasmids.

Bars refer to fold changes of mRNA levels in TFEB-transfected cells versus cells transfected with control pCDNA plasmid. *B2M* levels were measured as control gene. Bar graphs represent mean ± SEM of 3 independent experiments (*p < 0.05, **p <0.01 Student t test).

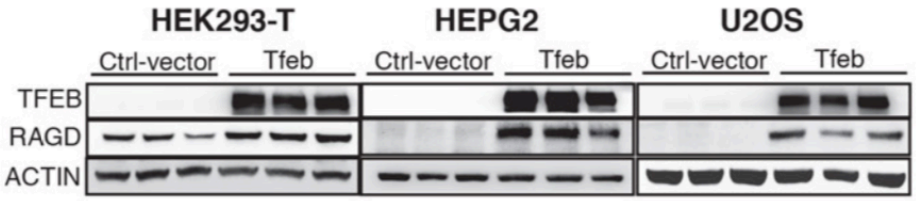

Fig.19. Analysis of RagD protein levels in HEK293-T, HEPG2 and U2OS cells transiently transfected with TFEB plasmids.

Immuno-blotting analysis of RagD protein in lysates from HEK293-T, HEPG2 and U2OS cells transfected with TFEB or TFE3 compared to samples transfected with a control vector.

These data, altogether, support the hypothesis of RagD as the putative direct target of TFEB responsible for upregulation of mTORC1 signaling.

To confirm whether RagD was a direct target of TFEB, we performed chromatin immunoprecipitation (ChIP) experiments in our TFEB-CA cells. After the immunoprecipitation of the protein-DNA complexes, we performed a real time PCR using oligos amplifying the three CLEAR sites present in *RagD* promoter and we observed that TFEB binds to all three of them (Fig.20).

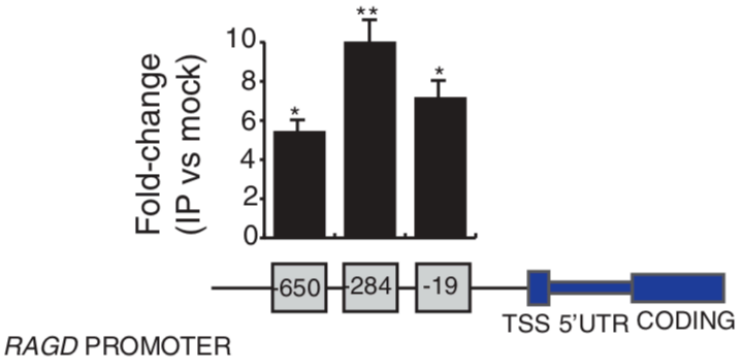

Fig.20. TFEB directly binds to *RAGD* promoter.

ChIP analysis of TFEB binding to *RAGD* promoter in doxycycline-treated HeLa TFEB-CA cells. Cells were treated with doxycycline (1mg/mL) for 48h. Squares represent CLEAR sites in *RAGD* promoter and numbers refer to their distance [in base pairs (bp)] from the transcriptional start site (TSS). Immunoprecipitated DNA was normalized to the input and plotted as relative enrichment over a mock control.

Next, we performed luciferase assays amplifying by PCR in HeLa genome *RAGD* promoter from CLEAR 3 to CLEAR 5 and cloning it into a luciferase reporter plasmid. As negative control, we generated a construct carrying point mutations in the CLEAR sites, by using the QuickChange XLII mutagenesis kit, in order to limit TFEB binding to *RAGD* promoter. We observed a progressive increase in the luciferase activity of WT RagD-luciferase reporter vector upon transfection of increasing amounts of TFEB, while luciferase activity relative to the mutated vector was strongly blunted (Fig.21).

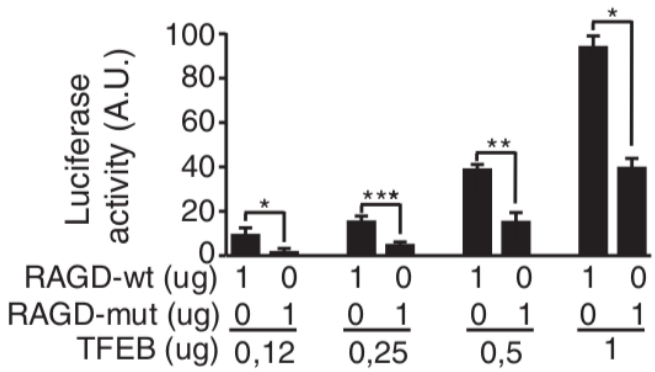

Fig.21. Analysis of TFEB binding to RagD promoter.

Luciferase assay after transfection of increasing amounts of TFEB construct was performed in HeLa cells cotransfected with wild-type (RAGD-wt) or mutated (RAGD-mut) RagD-promoter luciferase reporter plasmids. Plots represent mean ± SEM of three independent experiments (*p < 0.05; **p < 0.01; ***p < 0.001 Student's t test).

As an additional evidence of the role of RagD in TFEB modulation of mTORC1 activity, we used a clustered regularly interspaced short palindromic repeats–Cas9 (CRISPR-Cas9) approach to remove the most responsive CLEAR element in RagD proximal promoter region in HeLa cells (HeLa-RagD^{promedit}) (Fig.22).

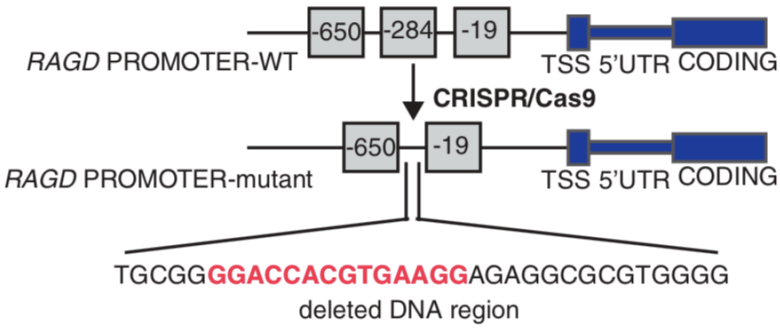

Fig.22. A CRISPR-Cas9 approach to edit *RAGD* promoter.

Scheme of CRISPR-Cas9–mediated mutation in the endogenous *RAGD* promoter of HeLa cells. A region of 33 bp containing the CLEAR site at position –284 (in red) was ablated.

This cell line showed reduced levels of RagD, both at mRNA (Fig.23) and protein levels (Fig.24), whereas the levels of the other RagGTPases were not affected. We observed no significant changes also for the mRNA and protein levels of FLCN (Fig.23, Fig.24).

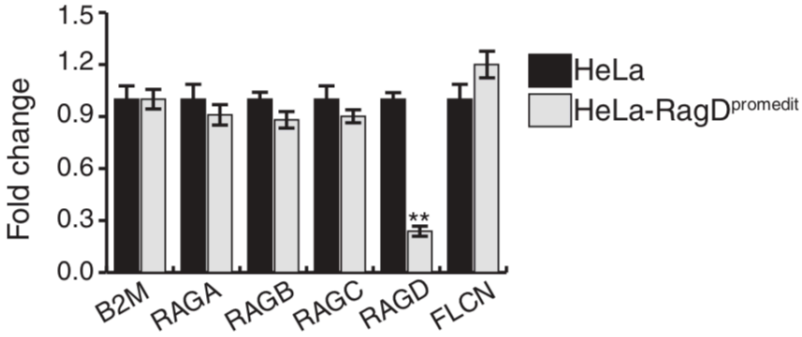

Fig.23. RagGTPases and Folliculin (FLCN) mRNA levels in HeLa-RagD^{promedit} cells.

Transcript levels of Rags and *FLCN* genes were analyzed in the mutated HeLa cell line (HeLa-RagD^{promedit}) versus control HeLa and normalized relative to *HPRT1* gene. Plots represent mean ± SEM of three independent experiments (**p < 0.01 Student's t test).

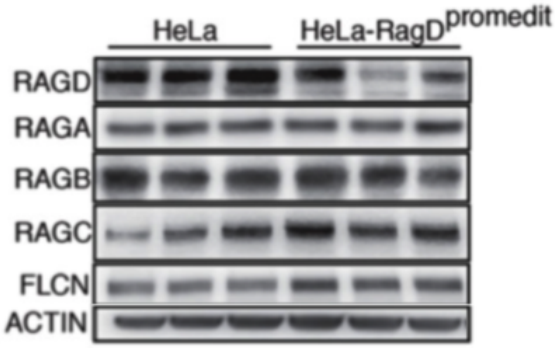

Fig.24. Western blot analysis of RagGTPases and FLCN levels in HeLa-RagD^{promedit} cells.

Immuno-blotting analysis of RagGTPases and mTORC1-related proteins in three different samples of HeLa-RagD^{promedit} cells compared to control HeLa.

These data suggest that TFEB plays an important role in the regulation of *RagD* gene.

Furthermore, to understand if the reduced binding of TFEB to RagD promoter could affect mTORC1 activity in HeLa-RagD^{promedit} cells, we analyzed the phosphorylation levels of mTORC1 canonical substrates in this cell line. We observed a significant reduction in mTORC1 signaling in stimulated HeLa-RagD^{promedit} cells compared to control HeLa cells (Fig.25).

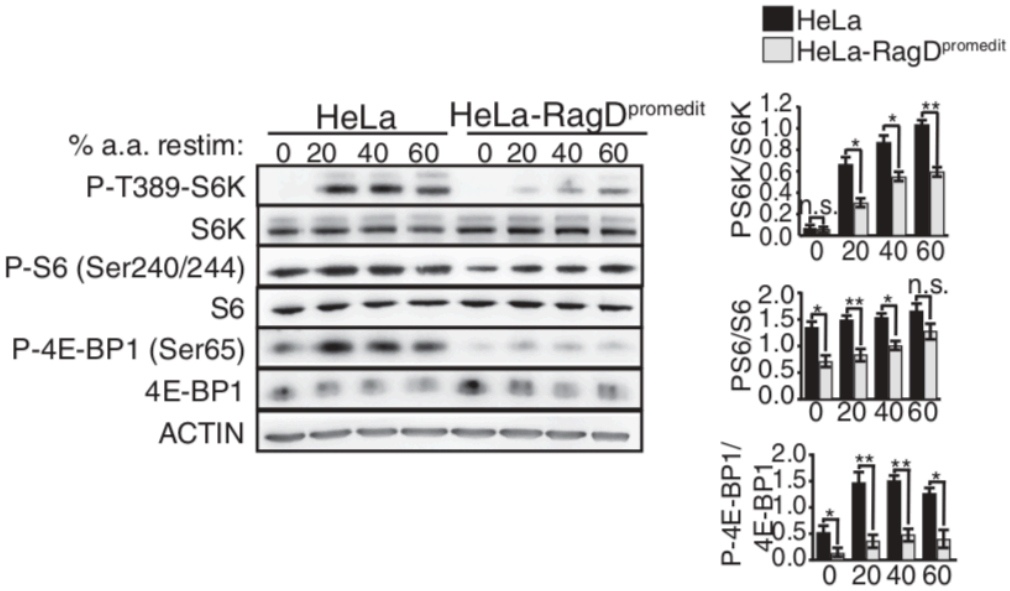

Fig.25. Analysis of mTORC1 signaling in HeLa-RagD^{promedit} cells.

Immuno-blots of mTORC1 signaling in HeLa-RagD^{promedit} cells compared with control HeLa. Cells were starved for amino acids (a.a.) for 50 min and then left untreated (0) or stimulated with increasing levels of amino acids (expressed as % of a.a concentration in RPMI medium). Cell lysates were analyzed for phosphorylation of S6K, S6 and 4E-BP1 proteins. The plots represent mean values of triplicate experiments expressed as ratio of phosphorylated S6K versus pan-S6K, phosphorylated S6 versus pan-S6 and phosphorylated 4E-BP1 versus 4E-BP1. Values are mean ± SEM (*$p < 0.05$, **$p<0.01$ Student t test).

The impairment of mTORC1 activity was then rescued upon overexpression of a plasmid carrying the wild type form of RagD (Fig.26).

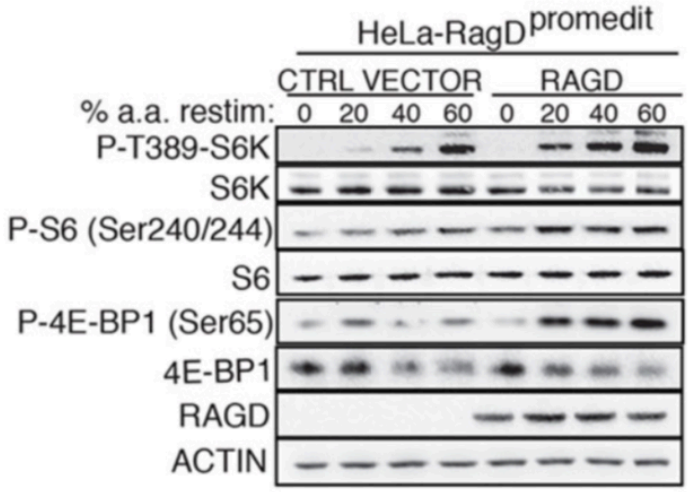

Fig.26. Analysis of mTORC1 signaling in HeLa-RagD^{promedit} cells transfected with RagD plasmid or with a control vector.

Immuno-blots of mTORC1 signaling in HeLa-RagD^{promedit} cells transfected with RagD plasmid or with a control vector. Cells were starved for amino acids (a.a.) for 50 min and then left untreated (0) or stimulated with increasing levels of amino acids (expressed as % of a.a concentration in RPMI medium). Cell lysates were analyzed for phosphorylation of S6K, S6 and 4E-BP1 proteins.

As a redout of mTORC1 decreased activity, we also analyzed the autophagy process in HeLa-RagD^{promedit} cells. Since mTORC1 inhibits autophagy (Ganley *et al*. 2009, Hosokawa *et al.* 2009), we expected to have increased autophagy levels in this cell line, due to the reduction of mTORC1 activity. We measured the protein levels of LC3 and P62, the commonly used markers of autophagy (He and Klionsky 2009), in HeLa-RagD^{promedit} cells and we observed increased LC3-II protein levels and reduced P62 levels, suggesting an increase in the autophagy process (Fig.27).

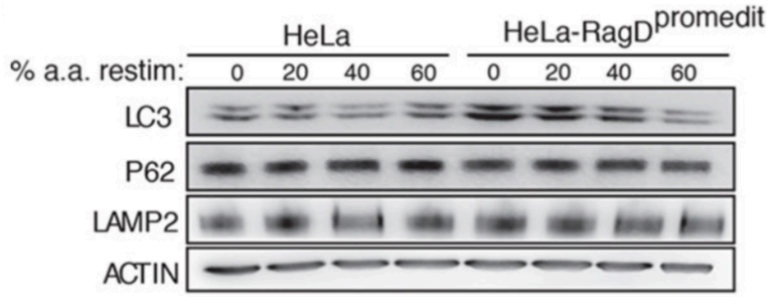

Fig.27. Analysis of autophagy markers in HeLa-RagD promedit cells.

Western blot analysis of the indicated proteins in HeLa-RagD promedit cells relative to control cells. Cells were starved for amino acids (a.a.) for 50 min and then left untreated (0) or stimulated with increasing levels of amino acids for 20 min.

Furthermore, we performed LC3 co-staining together with LAMP2, a lysosomal membrane protein, to look at autophagosomes. Immunofluorescence images showed an increase of LC3-LAMP2 colocalization in HeLa-RagD^{promedit} cells in starved conditions compared to HeLa control cells, indicating the presence of more autophagosome in HeLa-RagD^{promedit} cells (Fig.28). This colocalization coefficient still remained higher than the one in the control cells and almost similar to the values observed in starved conditions in HeLa-RagD^{promedit} cells, after refeeding with amino acids, supporting the inabilty of mTORC1 to shut down autophagy in these cells (Fig.28).

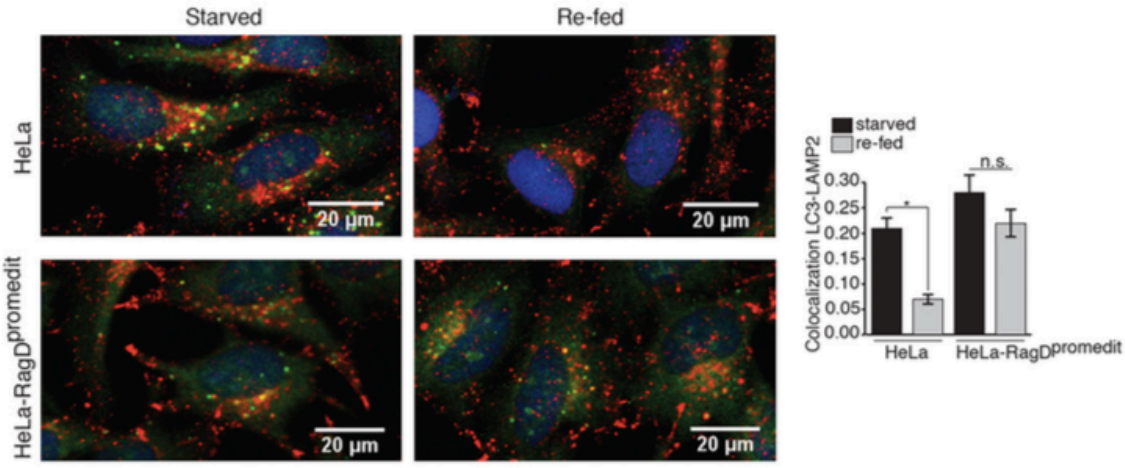

Fig.28. LC3-LAMP2 staining in HeLa- RagD^{promedit} and control HeLa cells.

Representative immunofluorescence images of LC3 (green) and LAMP2 (red) in HeLa-RagD^{promedit} and control HeLa cells starved or starved and then re-fed for 2 hour with nutrient rich media. The plot shows LC3-LAMP2 co-localization values. n= 20 cells/condition from three independent experiments (mean ± SEM, *p <0.05 Student t- test). Scale bars 20 µm.

Hence, these data altogether clearly indicate that TFEB transcriptionally regulate *RagD* gene, supporting a prominent role of this RagGTPase in TFEB regulation of mTORC1.

3. TFEB promotes mTORC1 recruitment to the lysosome.

RagGTPases are involved in mTORC1 recruitment on the lysosomal membrane, interacting with the subunit Raptor of the mTORC1 complex (Sancak *et al.,* 2008; Kim *et al.,* 2008). Thus, we decided to evaluate if TFEB levels could affect mTORC1 lysosomal localization.

Immunofluorescence analysis, performed in TFEB-CA cells, showed an increase colocalization coefficient of mTOR and the lysosomal marker LAMP2, upon amino acids stimulation, compared to control cells (Fig.29).

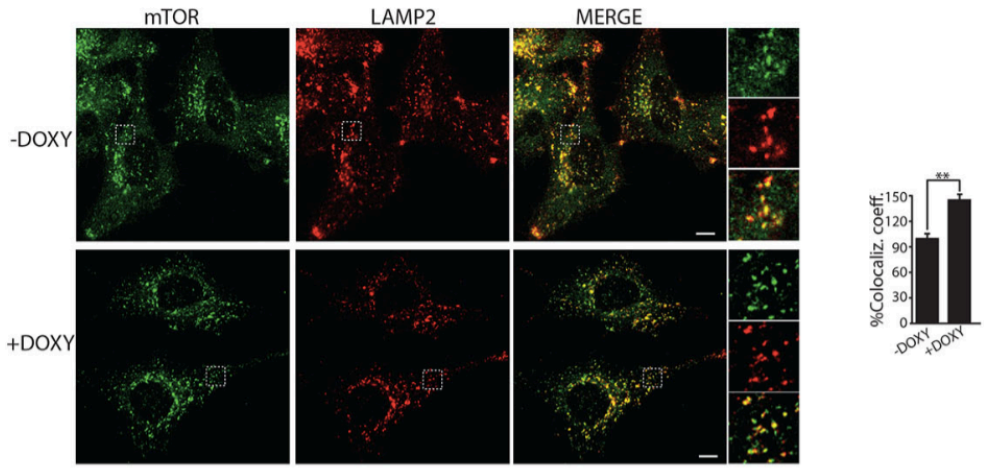

Fig.29. mTOR localization in TFEB-CA cells.

Representative immunofluorescence images of mTOR and LAMP2 in TFEB-CA HeLa cells left untreated or treated with doxycycline (DOXY, 1mg/mL for 48h). Cells were amino acids deprived for 50 minutes and then stimulated with amino acids for 15 minutes. The plot represents quantification of the data from 15 cells per condition from three independent experiments. Results are shown as means of co-localization coefficient of mTOR and LAMP2 ± SEM (**p <0.01, Student t test). Scale bars 10 μm.

To support the immunofluorescence data obtained, we performed organelle/cytosol fractionation experiments in TFEB-CA overexpressing cells compared to control. This biochemical assay showed an enrichment of mTORC1 components in the organelle fraction after TFEB overexpression, indicating an increased presence of mTORC1 in the pool containing also the lysosomes (Fig.30).

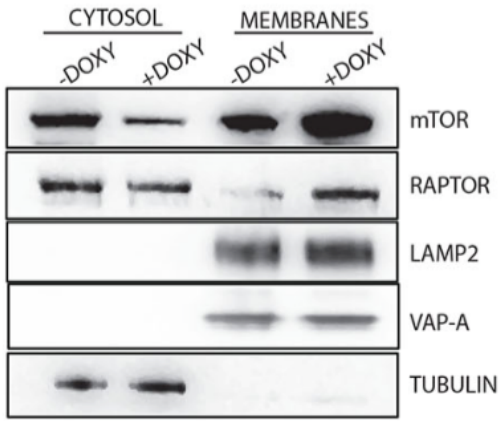

Fig.30. Organelle/cytosolic fractionation in TFEB-CA cells.

Western blot analysis of the indicated proteins in membranes and cytosolic fractions isolated from TFEB-CA HeLa cells left untreated or treated with doxycycline (1mg/mL) for 48h. LAMP2 and VAP-A were used as loading control for membrane fractions, tubulin for cytosolic fractions.

Conversely, we observed a reduction in mTORC1 recruitment on the lysosomes in cells depleted for TFEB after amino acids stimulation (Fig.31). This phenotype was rescued by the overexpression of a RagD-HA plasmid in these cells: relocalization of mTOR on the lysosomal membrane was visible only in cells silenced for TFEB but positive for the HA tag (Fig.31).

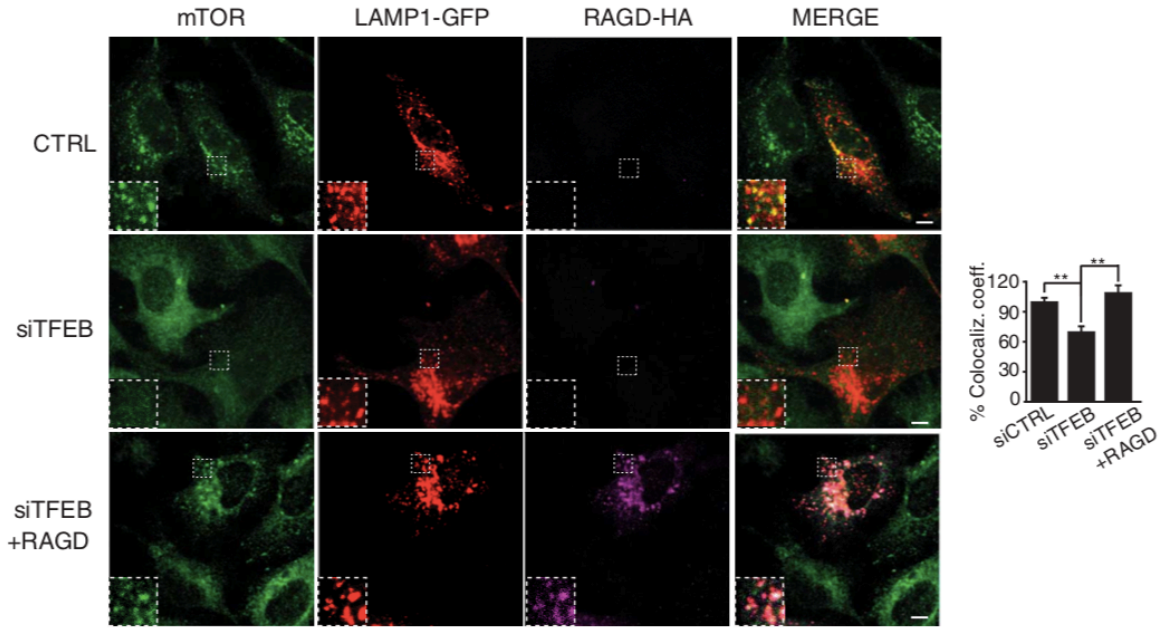

Fig.31. mTOR localization in cells depleted for TFEB, transfected with control vectors or with RagD-HA plasmid.

Representative immunofluorescence images of endogenous mTOR, LAMP1-GFP (visualized as red) and RAGD-HA (in purple) in HeLa cells. Cells were transfected with scramble (CTRL) or with TFEB siRNA (siTFEB) and after 48 hours with LAMP1-GFP and with RagD-HA plasmids for an additional 24 hours. Cells were deprived of amino acids for 50 min and then stimulated with amino acids for 15 min. Plots represent quantification of the data from 15 cells per condition from three independent experiments. Results are shown as means of colocalization coefficient of mTOR and LAMP2 ± SEM (**p < 0.01 Student's t test). Scale bars, 10 mm.

Finally, we analyzed mTOR lysosomal localization in HeLa-RagD^{promedit} cells and found a significant reduction in mTOR recruitment to the lysosome relative to control HeLa cells upon amino acid stimulation (Fig.32).

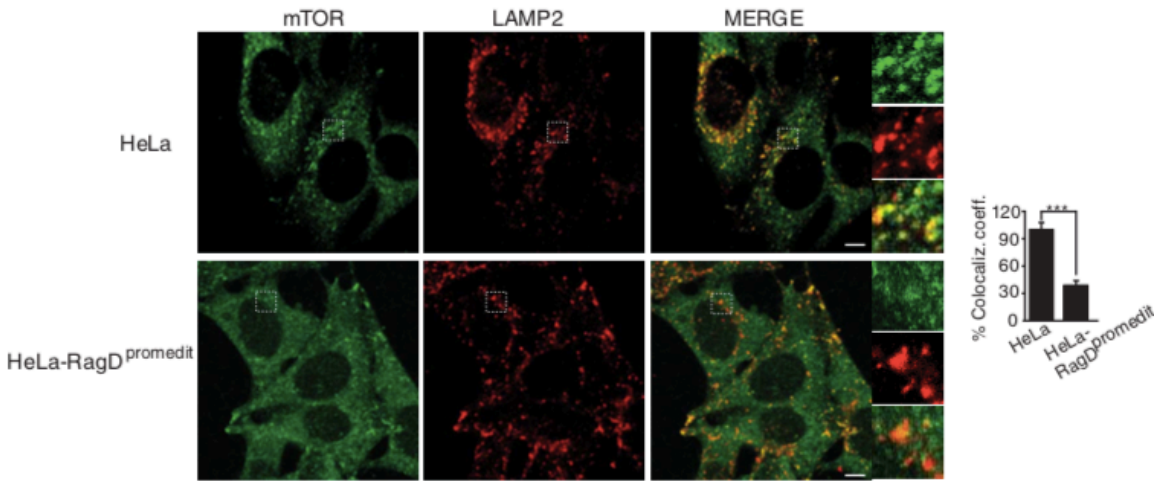

Fig.32. mTOR localization in HeLa-RagD^{promedit} cells.

Representative immunofluorescence images of mTOR and LAMP2 in HeLa-RagD^{promedit} and in control HeLa cells. Cells were deprived of amino acids for 50 min and then stimulated with amino acids for 15 min. Plots represent quantification of the data from 15 cells per condition from three independent experiments. Results are shown as means of colocalization coefficient of mTOR and LAMP2 ± SEM (***p< 0.001 Student's t test). Scale bars, 10 mm.

These data clearly indicate that TFEB-mediated transcriptional regulation of RagD promotes an efficient recruitment of mTORC1 complex to the lysosome upon nutrient stimulation.

4. Nutrient-induced mTOR reactivation after starvation and exercise is mediated by TFEB

TFEB is a nutrient-sensing transcription factor: in starvation conditions, it translocates into the nucleus and activates its target genes involved in catabolic processes (Settembre *et al.,* 2011). To understand if RagD could participate to the starvation response, we analyzed RagD expression levels in cells deprived for amino acids and we observed an increase in RagD mRNA levels, around 2 fold compared to control, that was blunted in cells depleted for TFEB (Fig.33).

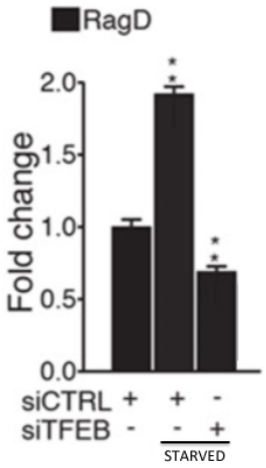

Fig.33. RagD expression levels in starvation.

mRNA levels of RagD in HeLa cells transfected with scramble (CTRL), TFEB siRNAs and kept in basal medium or starved for amino acids (a.a.) for 4 hours. Bars represent RagD mRNA levels in the indicated cells/conditions expressed as fold changes relative to cells transfected with scramble siRNA kept in basal medium. The plot represents mean ± SEM of 3 independent experiments (**p < 0.01 Student t test).

Similarly, RagD protein levels were increased after 4 hours of amino acids starvation, and this increase was lost in cells silenced for TFEB (Fig.34). There were no significant changes in the levels of the other RagGTPases and of FLCN (Fig.34).

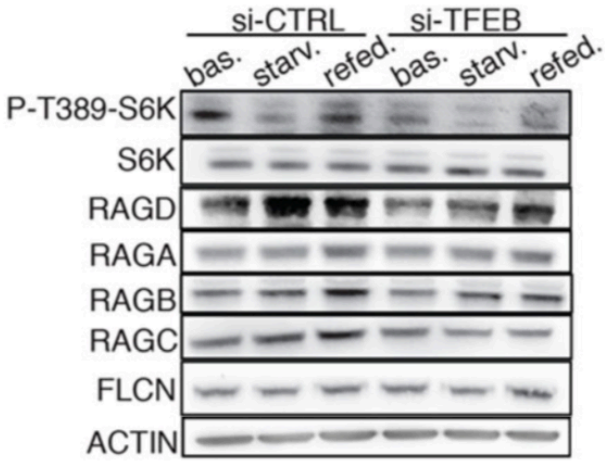

Fig.34. Analysis of mTORC1 activity and mTORC1-related protein levels in relation to nutrients availability and to TFEB levels.

Immunoblot analysis of S6K phosphorylation and of mTORC1-related proteins in HeLa cells transfected with CTRL (scramble) or TFEB siRNA, kept in basal medium (bas.), starved for 4 hours (starv.) or starved and then refed (refed) for 6 hours.

Furthermore, we followed TFEB localization in TFEB-WT and in TFEB-CA inducible cells in response to nutrients availability (Fig.35) and *RagD* gene expression levels in the same conditions (Fig.36). In TFEB-WT cells, TFEB localization responds to nutrient conditions: it resides into the cytoplasm when nutrients are available, while it translocates into the nucleus upon amino acid starvation. Instead, in TFEB-CA cells, TFEB is always localized into the nucleus (Fig.35). Importantly, we found that RagD expression levels correlated with TFEB cellular localization (Fig.36).

These data suggest that TFEB is driving RagD upregulation in starvation conditions.

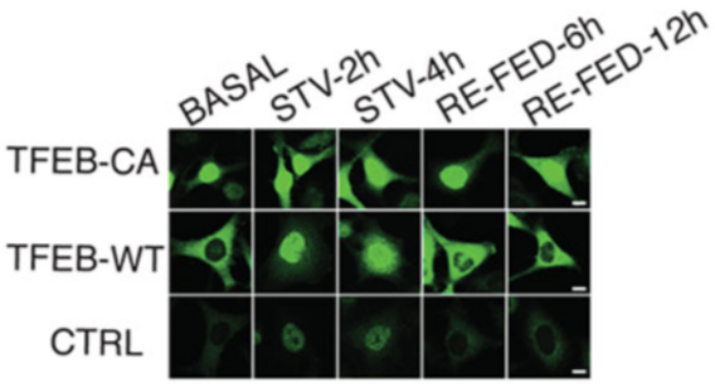

Fig.35. TFEB subcellular localization in TFEB-WT and TFEB-CA cells.

Immunofluorescence analysis of TFEB localization in TFEB-CA, TFEB-WT and control (CTRL) HeLa cells kept in basal condition (basal), starved for amino acids for 2 and 4 hours (STV-2h, STV-4h), or starved for 4 hours and stimulated with complete medium for 6 (RE-FED-6h) and 12 hours (RE-FED-12h). Cells were treated with doxycycline (1mg/mL) for 48h. Scale bars 10 μm.

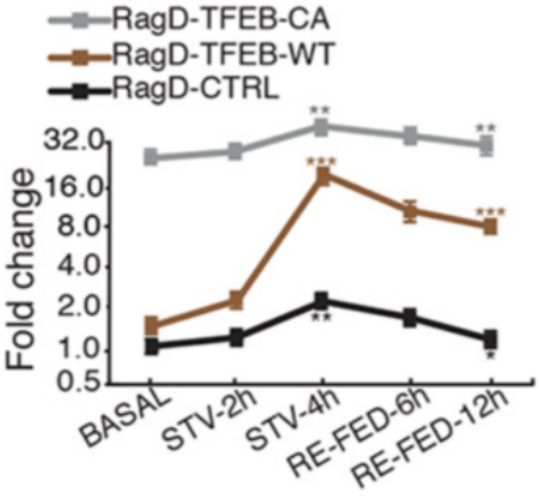

Fig.36. RagD expression levels in response to nutrient availability in TFEB-WT and TFEB-CA cells.

mRNA levels of RagD in TFEB-CA (grey lines), TFEB-WT (brown lines) and in control (black lines) HeLa cells in response to nutrient starvation/stimulation at the indicated times. The plot represents

mean ± SEM of 3 independent experiments. Values were normalized to *HPRT1* and expressed as relative to basal conditions. (*p < 0.05, **p < 0.01, ***p < 0.001 Anova (two-way)). Scale bar is logarithmic. Cells were treated with doxycycline (1mg/mL) for 48h.

To unravel the physiological relevance of TFEB-mediated transcriptional regulation of RagD we move *in vivo*. We first analyzed RagD mRNA levels in the liver of wild type mice that were fasted for different timepoints. Similarly to what observed in cell cultures, fasting in mice induced upregulation of RagD expression in the liver (Fig.37).

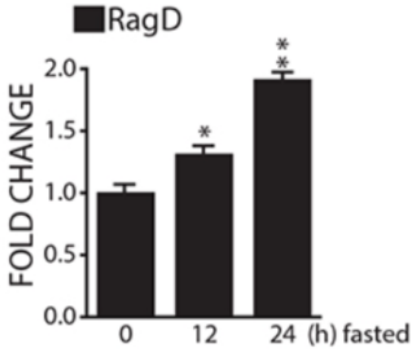

Fig.37. Upregulation of RagD expression in the liver of WT mice fasted.

mRNA levels of RagD in C57BL6 WT mice fasted for the indicated times. Bar graph shows values (means ± SEM for n=3 mice) expressed as fold increase compared to fed mice (*=p < 0.05, **p < 0.01 Student t test).

Moreover, we injected C57BL6 WT mice with an Helper-Dependent-Adenovirus (HD-Ad) expressing human TFEB under the control of a liver-specific promoter (PEPCK) or with control virus. One month after injection, mice were fasted for 24 hours or nutritionally synchronized by fasting them for 22 hours and then giving the food back for 2 hours, and later on they were sacrificed. Liver samples from the different murine groups were analyzed by RT-PCR and we found a strong

increase in RagD transcript levels upon TFEB injection, which was even stronger in fasted mice (Fig.38).

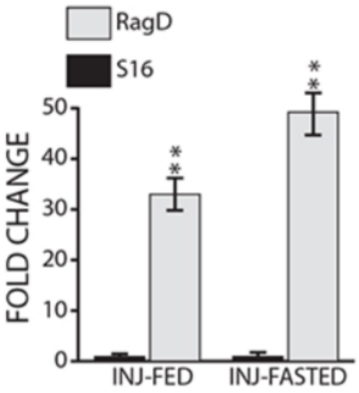

Fig.38. RagD mRNA levels in TFEB-injected mice.

C57BL6 mice injected with a Helper-Dependent Adenovirus that expresses human *TFEB* (HDAd-*TFEB*) under the control of a liver-specific promoter (PEPCK), or with saline PBS (control) were starved for 22h, then reefed for 2h (FED), or starved for additional 12 h (FASTED) prior to sacrifice. Liver tissues were analyzed for mRNA levels of *RagD*. Bar graph shows values (means ± SEM for n=5 mice) expressed as fold increase compared to control mice (**=$p < 0.01$ Student t test).

Accordingly, western blot analysis of liver samples from the same groups of mice showed increased mTORC1 signaling activation in TFEB-Injected mice upon nutrient synchronization (Fig.39). This was confirmed by immunohistochemistry analysis of S6-phosphorylation in TFEB-injected versus control mice tissues (Fig.40). Notably, signal for S6-phosphorylation correlated with the one for TFEB in transduced hepatocytes (Fig. 40 insets).

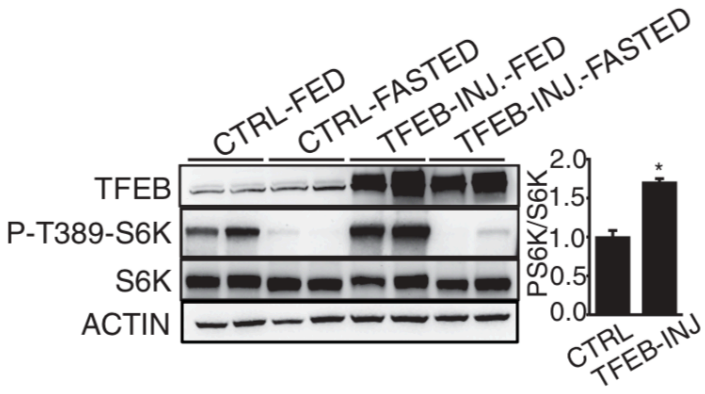

Fig.39. Analysis of mTORC1 substrates in TFEB-Injected mice.

C57BL6 mice injected with HDAd expressing human TFEB under the control of a liver-specific promoter (TFEB-INJ) or with phosphate-buffered saline (PBS) (CTRL) were starved for 22 hours and then refed for 2 hours (FED), or starved for additional 12 hours (FASTED). Liver lysates were analyzed for levels of indicated proteins. Actin was used as loading control. Plot shows ratio of phosphorylated S6K/pan-S6K (mean of three independent experiments).

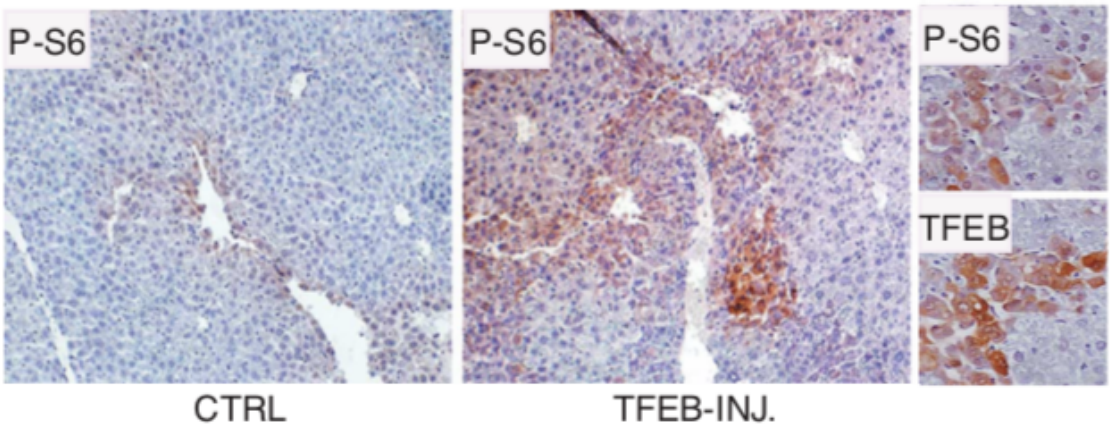

Fig.40. Analysis of mTORC1 signaling by immunohistochemistry in TFEB-Injected mice.

Immunohistochemistry of liver sections from mice injected with saline PBS (CTRL) or HDAd-TFEB (TFEB-INJ). Tissues were stained for serine 240/244 phosphorylated-S6 (P-S6). Insets show overlapping P-S6 and TFEB immunostainings in two consecutive 5-mm liver sections isolated from HDad- TFEB–injected mice.

Next, we analyzed the consequences of TFEB depletion on mTORC1 signaling *in vivo,* taking advantage of murine models already available in the lab. Due to the embrional lethality of *Tcfeb* KO mice (Steingrímsson *et al.,* 1998), several tissue-specific conditional *Tcfeb* KO models were generated. We chose to study *Tcfeb* liver-specific conditional knockout (KO) mice (*Tcfeb*$^{flox/flox}$; *Alb-CRE*$^{+}$; hereafter *Tcfeb*-LiKO) and *Tcfeb* muscle-specific KO mice (*Tcfeb*$^{flox/flox}$; *Mlc-CRE*$^{+}$; hereafter *Tcfeb*-MuKO), since mTORC1 has a prominent role in regulating liver and muscle metabolism. *Tcfeb-flox* mice were described in Settembre *et al.* 2012 and muscle specific Cre mice (*Mlc-Cre* mic*e)* were described in Bothe *et al.* 2000, whereas liver specific Cre mice (*Alb-Cre* mice) were obtained from the Jackson laboratory. Accordingly to what we observed previously, we could detect an increase in RagD expression levels upon fasting, but this effect was blunted in *Tcfeb*-LiKO mice (Fig.41).

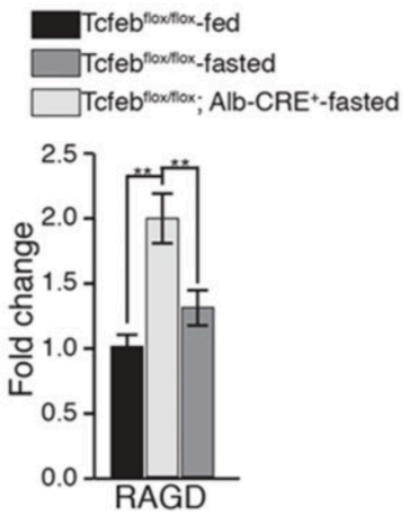

Fig.41. RagD mRNA levels are reduced in *Tcfeb*-LiKO fasted mice.

Transcript levels of RagD in liver tissues isolated from mice with indicated genotypes fasted for 24hours. Values were normalized to *Cyclophilin* gene and expressed as fold change relative to control fed mice. Bars represent means ± SEM (n=5 mice/ group; **=p < 0.01 Anova (one-way) followed by Tukey's test).

Furthermore, we observed a reduction in mTORC1 activity in *Tcfeb*-LiKO mice compared to controls (*Tcfeb*$^{flox/flox}$ mice), as shown by the decrease in the phosphorylation of S6K(Thr389) in these mice relative to control mice (Fig.42). Additionally, we followed protein synthesis, a well known redout of mTORC1 activity. Mice were nutritionally synchronized and injected with puromycin 30 minutes prior to sacrifice. Puromycin gets incorporated in the nascent polypeptides, thus allowing to follow protein synthesis by western blot analysis using an antibody against puromycin. We observed a strong decrease in puromycin signal in samples from *Tcfeb*-LiKO mice, compared to control, indicating a reduced protein synthesis (Fig.42). Both the decresed phosphorylation of S6K(Thr389) and the impairment of protein synthesis, observed in *Tcfeb*-LiKO mice, were rescued by viral-mediated delivery of human *RagD* gene, by using an Adeno-Associated Virus serotype 2/9 (AAV-2/9) (Fig.42).

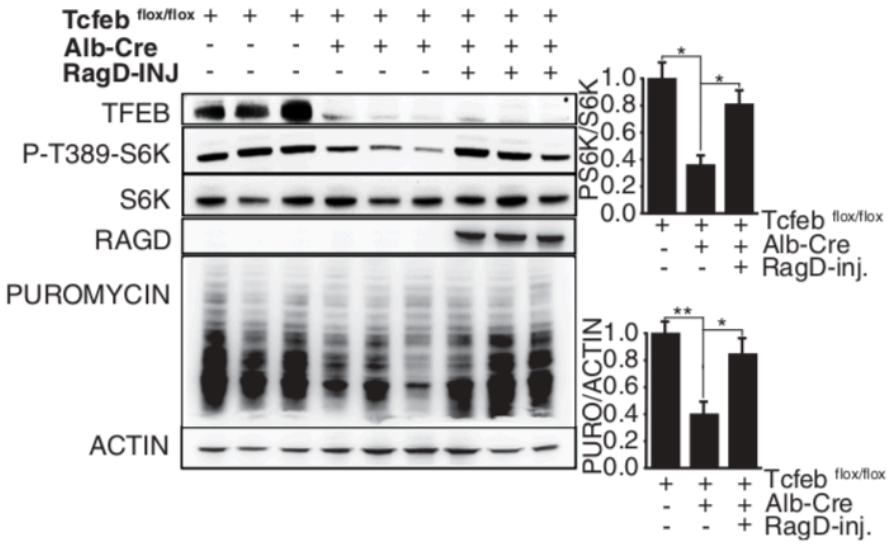

Fig.42. mTORC1 activity is reduced in *Tcfeb*-LiKO mice.

Mice with indicated genotypes were nutritionally synchronized and injected with puromycin 30 min before sacrifice. Where indicated, *Tcfeb*$^{flox/flox}$*;Alb-Cre*$^{+}$ mice were injected with an adeno-associated virus vector carrying human RagD cDNA. Liver lysates were analyzed for

phosphorylation of S6K and levels of puromycin incorporation. Phosphorylation of S6K and levels of puromycin incorporation analysis in muscle samples from mice with indicated genotypes after oral gavage of leucine. Mice were exercised where indicated. Plots show ratios of phosphorylated S6K/pan-S6K and puromycin/actin. Plots represent means ± SEM; N = 3/condition; one-way analysis of variance (ANOVA) followed by Tukey's test. (*$p < 0.05$; **$p < 0.01$)

Subsequently we analyzed the *Tcfeb*-MuKO mice. It is reported that a protein-rich-meal after exercise increases the rate of muscle protein synthesis via activation of mTORC1 signaling, even if the signaling pathways underlying this mechanism are not yet fully understood (Watson and Baar, 2014). Moreover, exercise is known to promote TFEB nuclear translocation in muscle via calcineurin-mediated dephosphorylation (Medina et *al.*, 2015). *Tcfeb*-MuKO mice and control mice (*Tcfeb*$^{flox/flox}$) were subjected to physical exercise or kept in resting condition. For exercise experiments, mice were let run for 1h at 25cm/sec on a treadmill, for one week. On the last day of training, mice received oral gavage administration of leucine (1,35g/kg of mouse in H2O); 30 minutes later they were injected intraperitoneally (IP) with puromycin and after 30 minutes sacrificed. Analysis of muscles samples from the different murine groups revealed that physical exercise induced RagD expression in control mice, but this response was blunted in *Tcfeb*-MuKO mice (Fig.43).

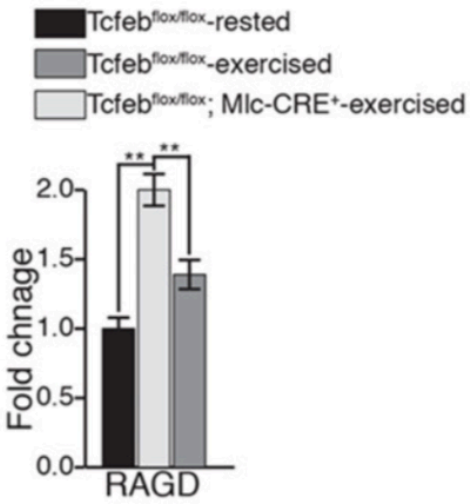

Fig.43. RagD upregulation induced by the exercise is reduced in *Tcfeb*-MuKO mice.

mRNA levels of RagD in exercised mice with indicated genotypes. Values were normalized to *cyclophilin* gene. Bars represent means ± SEM for n=4 mice and are expressed as fold change relative to control rested mice (**=$p < 0.01$; Anova (one-way) followed by Tukey's test).

Moreover, we observed an impairement in mTORC1 activation and in the protein synthesis in response to the protein meal after exercise in *Tcfeb*-MuKO mice compared to controls, represented respectively in the reduction of the phosphorylation levels of S6K (Thr389) and in the decreased puromycin signal detected (Fig.44).

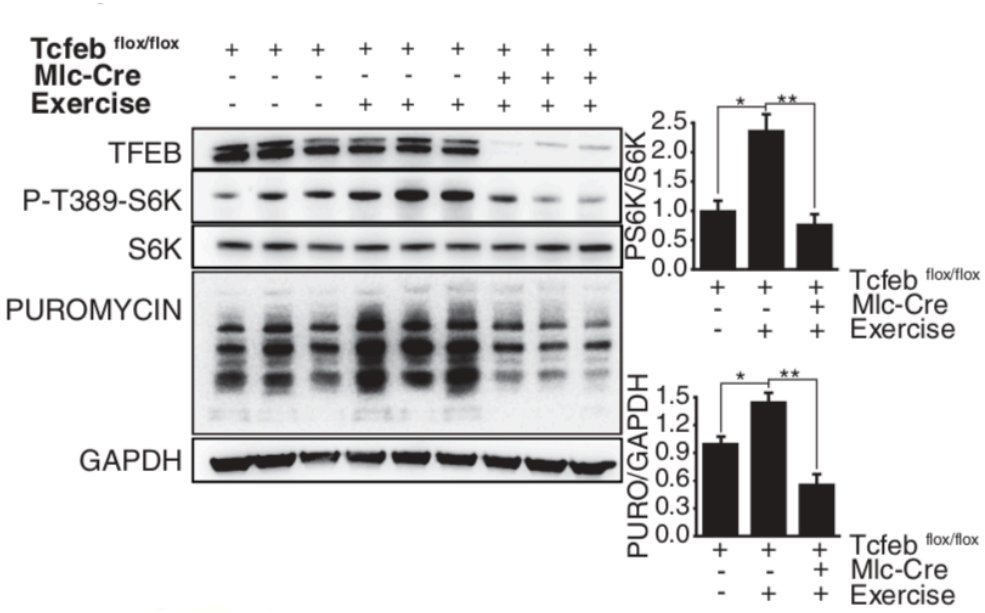

Fig.44. mTORC1 activity, induced by physical exercise, is impaired in *Tcfeb*-MuKO mice. Phosphorylation of S6K and levels of puromycin incorporation analysis in muscle samples from mice with indicated genotypes after oral gavage of leucine. Mice were exercised where indicated. Plots show ratios of phosphorylated S6K/pan-S6K and puromycin/glyceraldehyde phosphate dehydrogenase (GAPDH). Plots in represent means ± SEM; N = 3/condition; one-way analysis of variance (ANOVA) followed by Tukey's test. *p < 0.05; **p < 0.01.

Together these results suggest that amino acid-induced mTORC1 signaling after starvation and exercise is strongly influenced by TFEB via the transcriptional regulation of RagD.

5. MiT/TFE family factors, and not only TFEB, regulate mTORC1 activity through RagD-GTPase.

MiT/TFE transcription factors family members, TFEB, TFE3 and MITF, recognize the same E-box sites in the proximal promoter regions and therefore they can regulate the same target genes (Steingrıḿsson *et al*., 2004; Sardiello *et al*., 2009).

To test whether, not only TFEB, but also TFE3 and MITF, could control mTORC1 activity, we repeated some of the experiments performed for the characterization of TFEB role in mTORC1 signaling, in the same conditions, but pointing the attention to the other two factors.

Regarding TFE3, as we did it for TFEB, we generated a doxycycline-inducible cell line overexpressing the wild-type form of TFE3 (TFE3-WT) and its constitutively active form (TFE3-CA), where we mutated the serine residues 246 and 321, phosphorylated by mTORC1 (Martina *et al.*, 2014), into alanines. Upon doxycycline induction, the TFE3-WT cell line overexpressed the wild-type for of TFE3 with a subcellular localization in line with the nutrient availability, whereas the TFE3-CA cell line expressed a constitutively nuclear TFE3 (Fig.45). Both cell lines showed an increase in TFE3 mRNA levels of around 2 fold compared to un-treated cells (Fig.46).

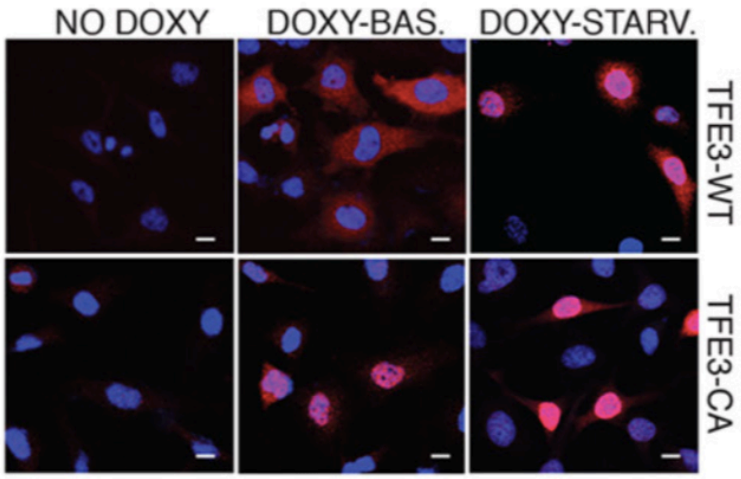

Fig.45. TFE3 subcellular localization in doxycycline-inducible Hela cell lines.

Representative immunofluorescence of TFE3 in stable doxycycline-inducible cell lines, overexpressing the wild type form of TFE3 (TFE3-WT) and TFE3-Constitutively Active (TFE3-CA). Cells were untreated or treated with doxycycline (1mg/mL) for 48hours, in basal and in starved conditions. Scale bars 10 μm.

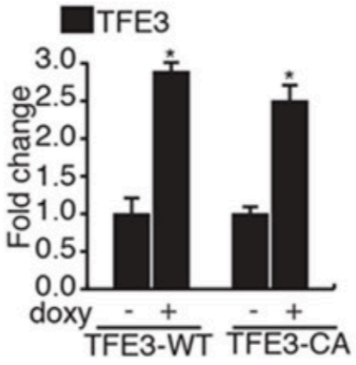

Fig.46. TFE3 expression levels in doxycycline-inducible Hela cell lines.

TFE3 mRNA levels in TFE3-WT and TFE3-CA cells untreated or treated with doxycycline (1mg/mL) for 48hours. Gene expression was normalized relative to *HPRT1*. Values are mean ± SEM (*p < 0.05 Student t test).

Subsequently, we analyzed mTORC1 signaling, upon amino acids administration, in TFE3-CA cells, and we observed an increased phosphorylation of all mTORC1 canonical substrates, as observed in TFEB-CA cells (Fig.47).

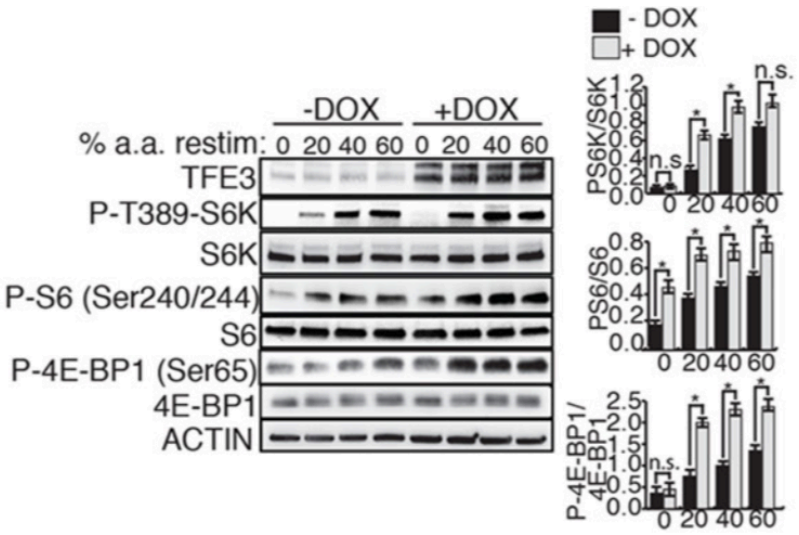

Fig.47. Analysis of phosphorylation levels of mTORC1 substrates in TFE3-CA cell line.

TFE3-CA cells, treated or untreated with doxycycline (1mg/mL) for 48hours, were starved for amino acids (a.a.) for 50 min and then left untreated (0) or stimulated with increasing levels of amino acids (expressed as % of a.a concentration in RPMI medium). Cell lysates were analyzed

for phosphorylation of S6K, S6 and 4E-BP1 proteins. The plots represent mean values of triplicate experiments expressed as ratio of phosphorylated S6K versus pan-S6K, phosphorylated S6 versus pan-S6 and phosphorylated 4E-BP1 versus 4E-BP1. Values are mean ± SEM (*p < 0.05 Student t test).

Conversely, we detected a reduction in mTORC1 signaling, upon amino acids stimulation, in cells depleted for TFE3 (Fig.48), indicating that also TFE3 is involved in mTORC1 regulation.

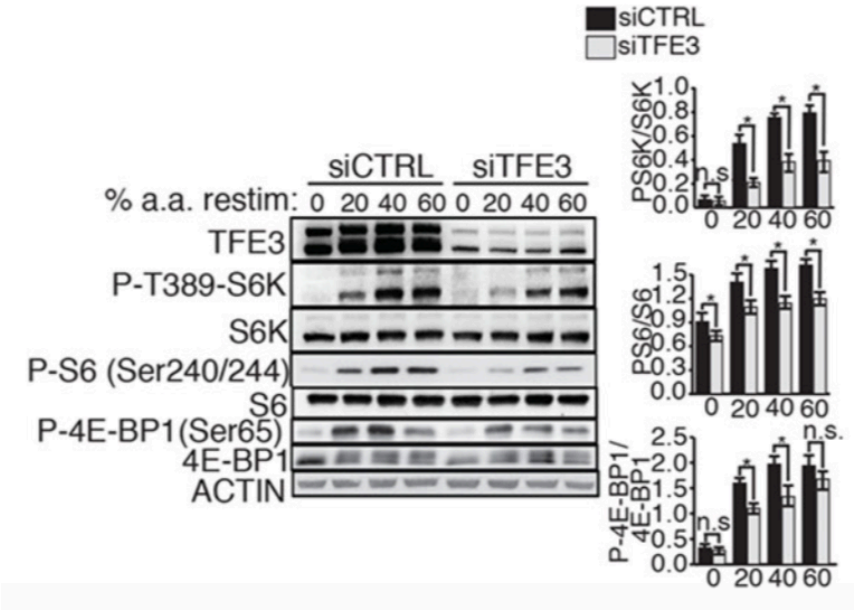

Fig.48. Analysis of phosphorylation levels of mTORC1 substrates in TFE3 silenced cells.

Immunoblot analysis of S6K, S6 and 4E-BP1 phosphorylation in HeLa cells transfected with scramble or TFE3 siRNA. Cells were first starved for amino acids (a.a.) for 50 min and then left untreated (0) or stimulated with increasing levels of amino acids (expressed as % of a.a concentration in RPMI medium). The plots represent mean values of triplicate experiments expressed as ratio of phosphorylated S6K versus pan-S6K, phosphorylated S6 versus pan-S6 and phosphorylated 4E-BP1 versus 4E-BP1. Values are mean ± SEM (*p < 0.05 Student t test).

Moreover, RagD was the most significantly down-regulated gene in cells depleted for TFE3 (Fig.49), suggesting that, similarly to TFEB, TFE3 regulates mTORC1 activity through RagD.

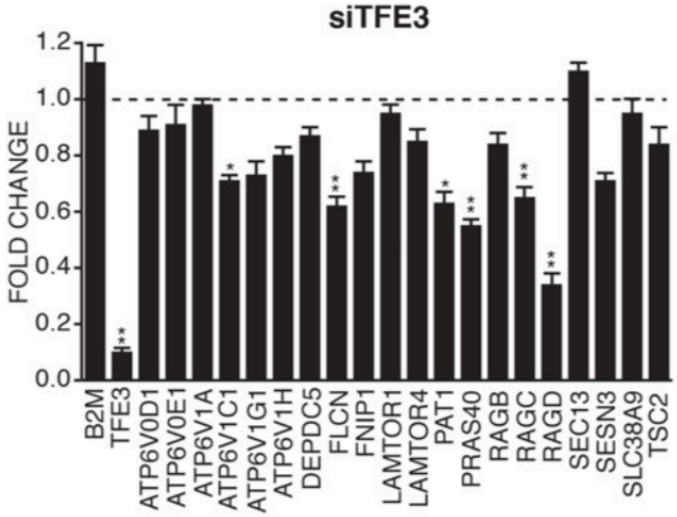

Fig.49. RagD mediates TFE3 regulation of mTORC1 activity.

Expression analysis of mTORC1-related genes in HeLa cells depleted for TFE3. *B2M* mRNA levels were measured as control gene. mRNA levels were normalized using *HPRT1* and expressed as relative to cells transfected with scramble siRNA. Bar graphs represent mean ± SEM of 3 independent experiments (*p < 0.05, **p < 0.01 Student t test).

Then, we transiently overexpressed MITF in HeLa cells and we evaluated mTORC1 activity, upon amino acids stimulation, (Fig.50), and RagD mRNA levels (Fig.51), and we found that both were strongly induced in MITF overexpressing cells relative to control cells (Fig.50, Fig.51).

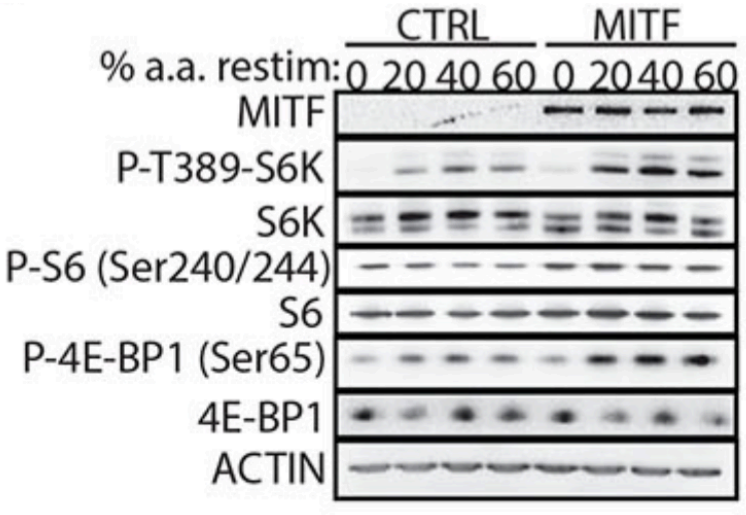

Fig.50. mTORC1 activity is increased in MITF overexpressing cells.

HeLa cells, transfected with a vector encoding MITF or with an empty vector, were starved for amino acids (a.a.) for 50 min and then left untreated (0) or stimulated with increasing levels of amino acids (expressed as % of a.a concentration in RPMI medium). Cell lysates were analyzed for phosphorylation of S6K, S6 and 4E-BP1 proteins.

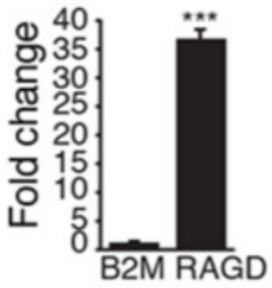

Fig.51. RagD transcription is upregulated in MITF overexpressing cells.

HeLa cells were transfected with a vector encoding MITF or with an empty vector and analyzed for RagD mRNA levels. Bar graphs in represent fold change of mRNA levels in MITF-transfected cells relative to cells transfected with control vector. Values represent means ± SEM, N=3 (***$p < 0.001$ Student t test).

In conclusion, these results support our hypothesis that MiT/TFE factors share the ability to control mTORC1 via RagD transcriptional regulation.

6. Deregulation of the MiT/TFE-RagD-mTORC1 regulatory axis supports cancer growth.

MiT/TFE factors are known oncogenes, overexpressed in a variety of tumors such as renal cell carcinoma (RCC), melanoma, sarcoma, and pancreatic ductal adenocarcinoma (Haq and Fisher, 2011; Kaufmann *et al.*, 2014; Perera *et al.*, 2015). Furthermore, mTOR pathway is highly implicated in cancer pathogenesis (Laplante and Sabatini, 2012). Due to these evidences, we decided to characterize MiT/TFE-RagD-mTORC1 regulatory axis in tumors overexpressing the MiT/TFE factors.

It was already available in our lab a *Tcfeb* kidney-specific conditional overexpressing transgenic mouse model that displayed a phenotype similar to human RCC (Calcagnì *et al.,* 2016). We thus analyzed mTORC1 signaling both in kidney tissues and primary kidney cells obtained from these mice, relative to control mice. We found hyperactivation of mTORC1 signaling in terms of increased signal of P-S6 staining, by immohistochemistry, in transgenic mice compared to controls (Fig.52), and primary kidney cells derived from transgenic mice displayed an increased phosphorylation of mTORC1 substrates upon amino acids stimulation (Fig.53).

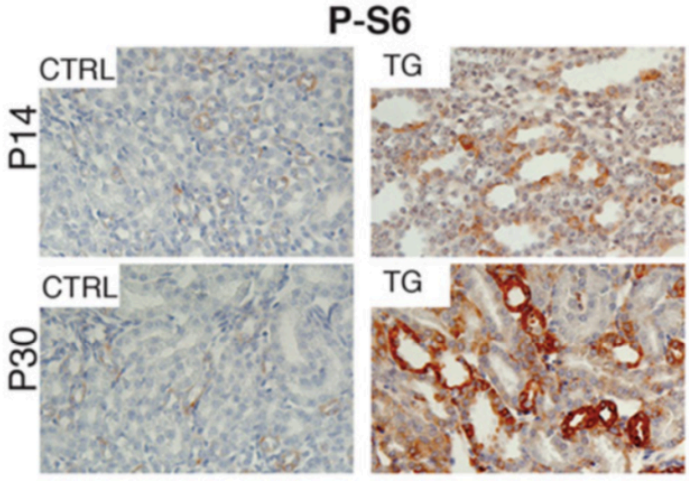

Fig.52. mTORC1 hyperactivity in kidney tissues from TFEB kidney-specific conditional overexpressor mice.

Representative images of kidney sections from controls (CTRL, Cond-tg*Tcfeb*$^{+/-}$) and TFEB kidney-specific conditional overexpressor mice (*KSPcdh16*$^{+/-}$;Cond-tg*Tcfeb*$^{+/-}$ indicated as TG) stained for serine 240/244 phosphorylated-S6 (P-S6) ribosomal protein at post-natal days 14 (P14) and P30 .

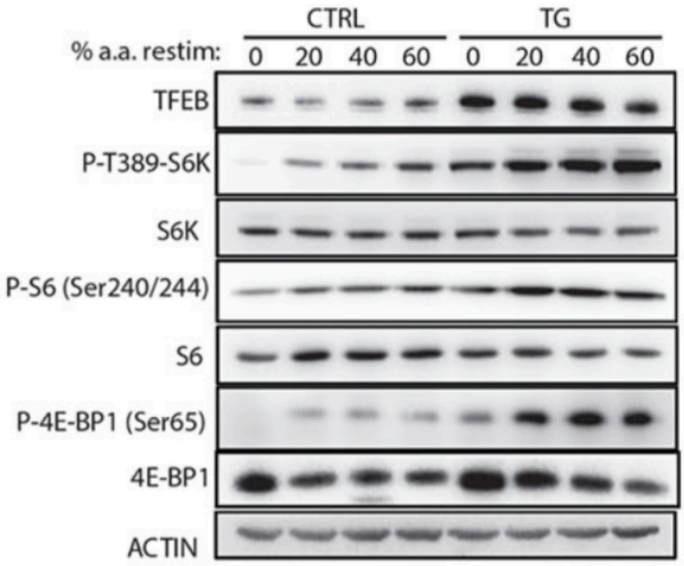

Fig.53. Increased phosphorylation of mTORC1 substrates in primary kidney cells from TFEB kidney-specific conditional overexpressor mice.

Representative immuno-blotting analysis of phosphorylation levels of the indicated mTORC1 substrates in control and in TFEB-overexpressing primary kidney cells. Actin was used as loading control.

We then evaluated RagD expression levels in primary kidney cells obtained from these mice. As expected, we found increased RagD transcript levels in TFEB-overexpressing primary kidney cells compared to control cells (Fig.54).

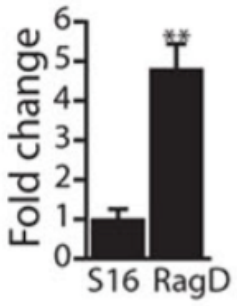

Fig.54. RagD transcription is increased in TFEB-overexpressing kidney primary cells.

RagD mRNA levels in primary kidney cells isolated from TFEB kidney-specific conditional overexpressor mice expressed as fold change relative to control mice. Gene expression was normalized relative to *Cyclophilin*; *S16* expression was shown as control unrelated gene. Bar graph shows mean ± SEM of 3 independent experiments (**p < 0.01 Student t test).

Furthermore, primary kindney cells from transgenic mice presented an hyperproliferative phenotype, revertable by Torin 1 treatment (Fig.55), indicating that this phenotype was associated to mTORC1 hyperactivation.

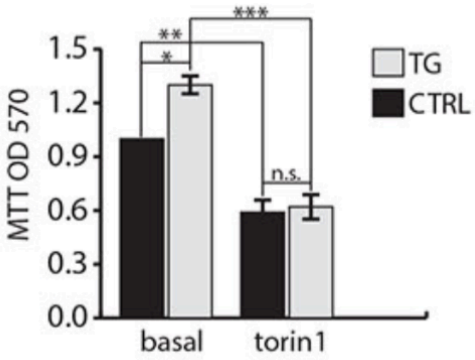

Fig.55. TFEB-overexpressing primary kidney cells hyperproliferation is mTORC1 dependent.

MTT assay was used to measure cell proliferation of TFEB-overexpressing primary kidney cells (TG) compared to control cells (CTRL). Torin 1 was added, where indicated, for 48h (100nM). The plot represents means of three independent experiments (*p < 0.05, **p < 0.01, ***p < 0.001 Student t test).

Successively, we analyzed kidney cells derived from a RCC-patient carrying a chromosomal translocation that involves the TFE3 gene (HCR-59 cell line) (Malouf *et al.,* 2014). HCR-59 cells showed increased RagD transcript (Fig.56) and protein levels (Fig.57) and enhanced mTORC1 signaling relative to HK2 kidney cell line (Fig.57).

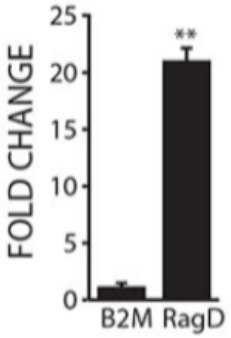

Fig.56. RagD transcription is increased in HCR-59 cells.

mRNA levels of RagD in a cell line from a patient with RCC (HCR-59) relative to control kidney cells (HK-2). *B2M* expression shown as control unrelated gene. Gene expression was normalized relative to *HPRT1*. Plot represents means of three independent experiments ± SEM (**p< 0.01 Student's t test).

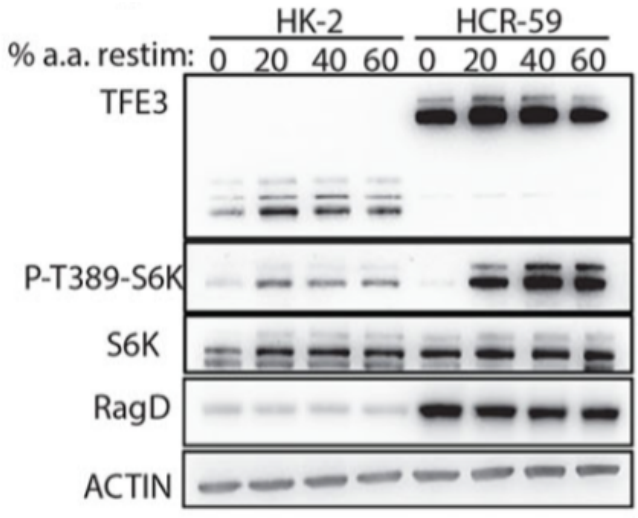

Fig.57. mTORC1 signaling and RagD protein levels are increased in HCR-59 cells.

Analysis of S6K phosphorylation at threonine 389 in HK-2 and HCR-59 cells 50 min starved for amino acids (0) and then stimulated with increasing levels of amino acids for 20 min.

Silencing of both TFE3 (Fig.58) or RagD (Fig.59) reduced the increased phosphorylation of mTORC1 substrates, upon amino acids administration in HCR-59 cells, indicating that both TFE3 and RagD are implicated in mTORC1 hyperactivity.

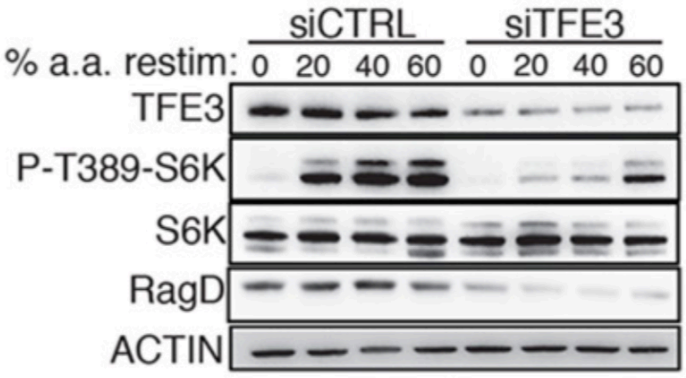

Fig.58. mTORC1 hyperactivation is reduced in HCR-59 depleted for TFE3.

HCR-59 cells were transfected with scramble (siCTRL) or TFE3 siRNA and then analyzed for the indicated proteins upon stimulation with increasing % of amino acids.

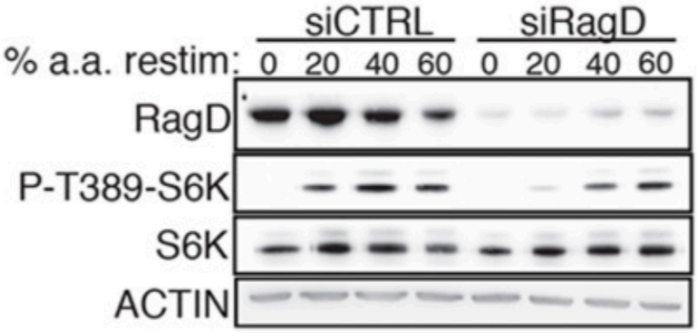

Fig.59. mTORC1 hyperactivation is reduced in HCR-59 depleted for RagD.

HCR-59 cells were transfected with scramble (siCTRL) or RagD siRNA and then analyzed for

phosphorylation levels of S6K upon stimulation with increasing % of amino acids.

Moreover, HCR-59 cells, silenced for TFE3 or RagD, showed also reduced proliferation rate (Fig.60), indicating that the MiT/TFE-RagD-mTORC1 axis deregulation is responsible for the tumor cell proliferation in RCC.

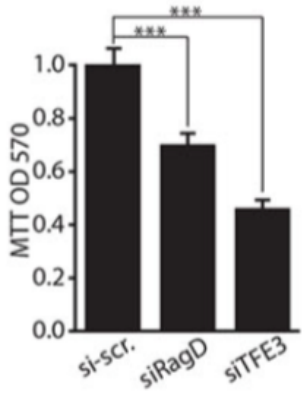

Fig.60. Hyperproliferation of HCR-59 cells is reduce upon depletion of TFE3 or RagD.

Proliferation levels of HCR-59 cells transfected with scramble (SCR), RagD, or TFE3 siRNAs. Plot represents means of three independent experiments ± SEM; one-way ANOVA. (***p < 0.001, Student's t test).

MITF, the MiT/TFE family member involved in melanosomal biogenesis (Hodgkinson *et al.*, 1993), has an oncogenic role well established in melanoma (Tsao *et al.,* 2012). To understand if the MiT/TFE-RagD-mTORC1 axis deregulation could be involved in melanoma pathogenesis, we analyzed a melanoma cell line derived from a patient (501Mel) presenting MITF overexpression. 501Mel cells showed increased RagD mRNA (Fig.61) and protein levels (Fig.62) and upregulation of mTORC1 signaling upon amino acids stimulation, compared to control melanoma cells non-overexpressing MITF (A375P) (Fig.62). Thus, also in MITF-related-melanomas we observed a strong

increase of mTORC1 signaling pathways, correlating with a strong upregulation of RagD trascript levels.

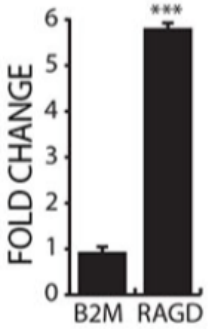

Fig.61. RagD transcription is increased in 501Mel cells.

MITF-dependent melanoma patient–derived cells (501Mel) were analyzed for mRNA levels of *RagD* (*B2M* expression was shown as control unrelated gene). Values expressed as relative to control melanoma cells (A375P). Gene expression was normalized relative to *HPRT1*. Plot represents means of three independent experiments ± SEM (***p < 0.001, Student's t test).

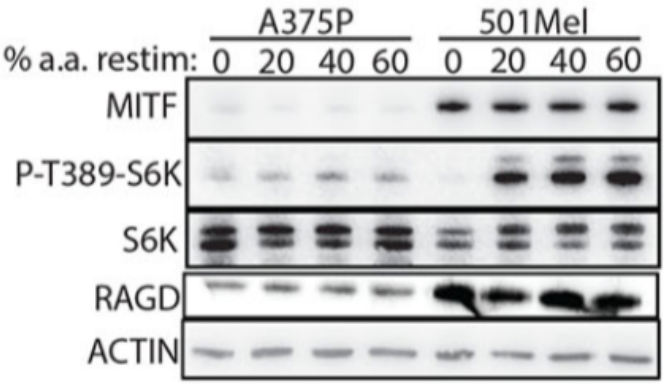

Fig.62. mTORC1 signaling and RagD protein levels are increased in 501Mel cells.

Representative immunoblotting analysis for the indicated proteins in control (A375P) and MITF-dependent melanoma (501Mel) cells stimulated with increased levels of amino acids.

Next, we depleted MITF in 501Mel cells and analyzed mTORC1 signaling after amino acids stimulation. We observed a decrease in the phosphorylation of S6K (Thr389) and also a reduction of RagD protein levels (Fig.63), supporting the

prominent role of the MITF-RagD-mTORC1 axis deregulation in this melanoma cells.

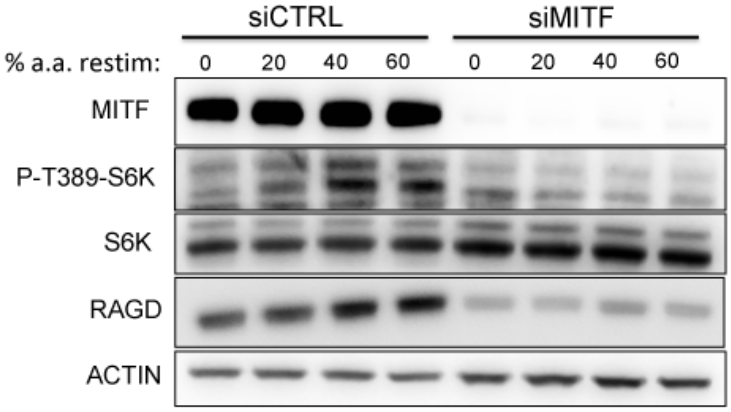

Fig.63. mTORC1 hyperactivation is reduced in 501Mel depleted for MITF.

501Mel cells were transfected with scramble (siCTRL) or MITF siRNA and then analyzed for the protein indicated upon stimulation with increasing % of amino acids.

Furthermore, the down-regulation of MITF or RagD rescued the hyperproliferative phenotype displayed by 501Mel cells (Fig.64), indicating that the overexpression of MITF is the driving element causing mTORC1 hyperactivity in these melanomas.

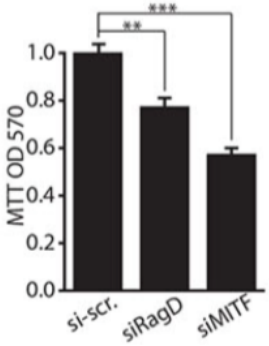

Fig.64. Hyperproliferation of 501Mel cells is reduce upon depletion of MITF or RagD.

Proliferation index of 501Mel cells transfected with SCR, RagD, or MITF siRNAs. Plot represents means of three independent experiments ± SEM; one-way ANOVA (**p < 0.01, ***p < 0.001,

Student's *t* test).

Human tumor xenograft are a valuable model to investigate the contribute of a specific molecular alteration to tumor growth. Thus, to assess the contribute of RagD upregulation in malignancies associated with MiT/TFE deregulation, in collaboration with Prof. Pellicci, at the European Institute of Oncology (IEO) in Milan, we performed xenografts experiments by using 501Mel cells silenced for RagD or with control shRNA against luciferase. We observed a drastic reduction in tumor mass development upon silencing of RagD compared to the tumor mass originated from control 501Mel cells (Fig.65). These data clearly support an important role for RagD in promoting tumor growth in tumors dependent on MiT/TFE hyperactivation.

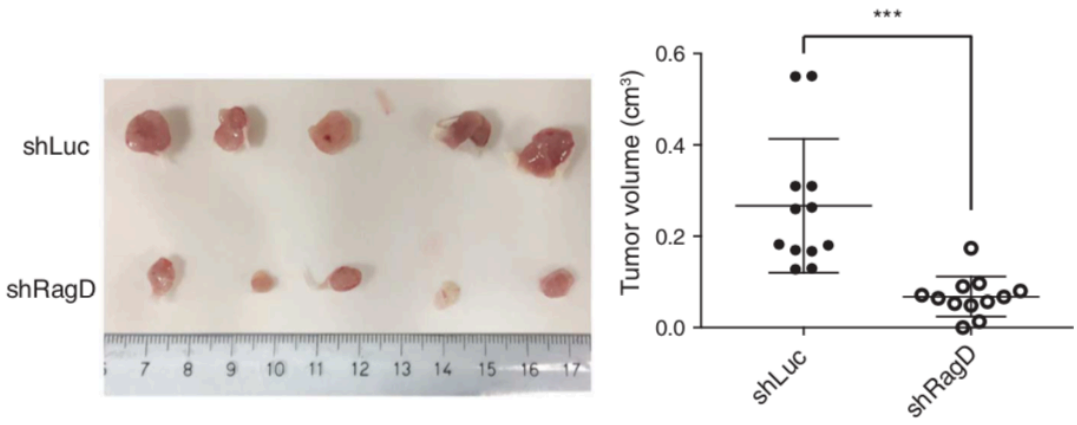

Fig.65. Xenograft tumor growth is reduced in melanoma cells silenced for RagD.

501Mel cells were infected with a lentivirus expressing a short hairpin RNA targeting the Luciferase (control, Sh-Luc) or RagD mRNAs and transplanted in NOD scid gamma (NSG) mice. **Left panel**: Representative picture of tumors isolated from both groups of mice. **Right panel**: Plot shows tumor volumes. Each dot represents a tumor. Twelve tumors (n = 12 mice) were analyzed per group; (***p < 0.001, Student's t test).

DISCUSSION

The lysosome was initially discovered as a digestive organelle, designated to the degradation and recycling of cellular waste (de Duve, 2005). However, over the years, its role has been better dissected and the lysosome has emerged as a key metabolic signaling center for the cell, thanks to its ability to transport nutrients, sense their availability, and communicate this information to growth-regulatory pathways (Perera and Zoncu, 2016). mTORC1 signaling is the main regulatory pathway involved in metabolic adaptation to nutrient availability in the cell and it exerts its activity on the lysosomal surface. In presence of nutrients, mTORC1 is active on the lysosome and promotes growth and energy storage, thus activating anabolic pathways; whereas, when nutrients are missing, mTORC1 is inactive and therefore catabolic pathways are activated to provide the required building blocks for sustain cell survival (Laplante and Sabatini, 2012; Saxton and Sabatini, 2017). In this way, mTORC1 regulates the balance between biosynthetic and catabolic states. The new view of the lysosome as signaling platform has been supported by the identification of TFEB as the "master regulator of lysosomes", controlling the expression of genes involved in lysosomal biogenesis, exocytosis, and autophagy (Sardiello *et al.*, 2009; Palmieri *et al.*, 2011). TFEB represents the crucial node of a lysosome-to nucleus signaling mechanism through which lysosomal functions can be coordinated to respond and to adapt to envinronmental cues.

TFEB, TFE3 and MITF subcellular localization is regulated by mTORC1-phosphorylation: when nutrients are available, the MiT/TFE factors are phosphorylated and retained inactive into the cytoplasm, whereas in starvation condition, mTORC1 is inactive and they can translocate into the nucleus, activating their target genes (Martina et *al.*, 2012, 2013, 2014; Roczniak-Ferguson *et al.*, 2012; Settembre *et al.*, 2011, 2012). mTORC1 inhibition of TFEB, and also

TFE3, activity is an additional way to block catabolic processes, triggering the transcriptional regulation of autophagic genes.

However, data from literature suggest that mTOR complexes may operate in the context of feedback loops, impliying that downstream effectors are also likely to be involved in upstream regulation, to maintain various aspects of cellular homeostasis (Eltschinger *et al.*, 2016). Thus, we reasoned that MiT/TFE members, as nutrient sensitive transcription factors, could in turn affect mTORC1 activity. Among the different inputs regulating mTORC1 signaling, amino acids levels are the most conserved ones, sensed through a complex machinery converging to the lysosome (Saxton and Sabatini, 2017). Upon amino acids stimulation, we observed that the levels of phosphorylation of mTORC1 substrates fluctuate together with TFEB expression levels. Moreover, TFEB overexpression is able to enhance common redouts of mTORC1 activity, such as cell proliferation and cell size. These were the first evidencies that supported the existence of a negative feedback loop mechanism by which TFEB is itself able to regulate its inhibitor. The following question was to elucidate the detailed mechanism of action and TFEB target gene/genes responsible for mTORC1 upregulation. We first hypothesized that autophagy was the link in between TFEB and mTORC1, since TFEB, as well as TFE3, are critical regulators of this process and, due to proteolysis events, autophagy is a source of amino acids in the lysosomal lumen. We thus evaluated whether these family of transcription factors regulate mTORC1 activity by modulating autophagy. However, we showed that TFEB-mediated activation of mTORC1 did not require the essential autophagy genes *Atg5* or *Atg7*, suggesting an autophagy-independent mechanism. We then decided to dissect the members of mTORC1 pathway, looking for putative TFEB target gene/genes. Starting from a bioinformatic analysis, looking for CLEAR elements in the promoters of mTORC1-

related genes, and subsequent validation experiments, *RagD* emerged as the putative target gene. RagD is one of the four RagGTPases present in mammals. The amino acid signaling centers around these proteins: in presence of amino acids, the active heterodimers RagA or B with RagC or D, promote mTORC1 recruitment on the lysosomal surface, which is necessary for its activation by Rheb (Kim *et al*., 2008; Sancak *et al*., 2008). The role of these GTPases has emerged during the last decade and this field is getting more and more complex over time. A recent paper by Lawrence *et al*. underlines their dynamic functions, claiming that the RagGTPases cycles beetween the lysosome and the cytoplasm in order to tightly regulate mTORC1 interaction with Rheb on the lysosome, thus its signaling. As for our work, we then analysed mTORC1 recruitment on the lysosome and how this could be affected by TFEB levels. Supporting the existence of a TFEB-RagD-mTORC1 axis, we observed that mTORC1 lysosomal localization is increased when TFEB is overexpressed. These data supported our hypothesis of this axis as a rapid way by which TFEB could rapidly switch off itself, increasing the amount of mTORC1 on the lysosome ready to be reactivated by nutrients. Indeed, we found a significant correlation between starvation-induced TFEB nuclear localization and RagD expression levels, at both mRNA and protein levels. Studies in mice confirmed RagD induction in fasting and TFEB upregulation of mTORC1 signaling, introducing the new mechanism identified in a physiological context. We then investigated more in detail the role of TFEB-RagD-mTORC1 axis in specific tissues that are remarkably influenced by mTORC1 activity. The liver is a metabolic organ particularly sensitive to nutrients, growth factors and energy, and thereby plays a central role in carbohydrate, protein, amino acids, and lipid metabolism. In Ballabio's group, we had available *Tcfeb*-liver specific conditional KO mice and we confirmed the impaired mTORC1 signaling in the livers of these

mice. The reduction in the protein synthesis rate in *Tcfeb*-LiKO mice is another evidence of the role of TFEB in cellular adaptation to nutrient availability. Moreover, up to date, it's widely known that mTORC1 promotes protein synthesis in muscles upon physical exercise to support muscle growth. This effect is well appreciated by bodybuilders, who know that eating a protein-rich meal after exercise is a good strategy to increase muscles. However the mechanisms underlying this process are still poorly understood. Interestingly, TFEB nuclear translocation is induced upon physical exercise as a consequence of its phosphatase activation (Medina *et al*., 2015). Therefore, we hypothesized that TFEB could regulate mTORC1 signaling in response to exercise. Indeed, we observed that exercised muscle-specific *Tcfeb* KO mice showed a reduced induction of mTORC1 activity and protein synthesis in response to leucine after exercise, indicating that mTORC1 activation upon physical exercise also requires MiT/TFE factors. Hence, our findings suggested the existence of a new molecular pathway, physiologically relevant, that collocated mTORC1 downstream of MiT/TFE factors.

How modulation of RagD levels alone can be sufficient to significantly impair mTORC1 signaling remains an open question. One would expect that RagC could compensate for RagD but our study suggest that these two Rags are less interchangeable than what was previously thought. Another critical point is that to be functionally active RagD needs to form heterodimers with either RagA or B. We noticed that RagD levels are lower compared to the other Rag GTPases and therefore, one possibility is that RagD represents a limiting factor for RagD/RagA and RagD/RagB heterodimer formation. In line with this hypothesis is the observation that perturbing MiT/TFE mediated transcriptional regulation of RagD only is sufficient to severely hampers mTORC1 lysosomal recruitment and hence

its activation. In summary, we defined a new regulation of mTORC1 activity in response to nutrients. Starvation inhibits mTORC1 thus allowing MiT/TFE nuclear translocation and hence activation of catabolism via the expression of autophagic and lysosomal genes. In the meantime, MiT/TFE factors induce the expression of RagD and this results in the assembly of inactive Rags heterodimers on the lysosomal surface. Feeding turn on Rags, which can now recruit mTORC1 to the lysosome and promote its activation. In this way, the cell gets ready to efficiently switch on anabolism and turn off catabolism when nutrients become available.

Once identified the TFEB-RagD-mTORC1 axis and its physiological relevance, we asked whether this axis could be implicated in pathological conditions. Due to the reported role in cancer of both the MiT/TFE factors, described as oncogenes in several type of cancers (Haq and Fisher, 2011; Kaufmann *et al.*, 2014; Perera *et al.*, 2015), and of mTORC1, highly implicated in cancer pathogenesis, mainly fueling tumor growth (Laplante and Sabatini, 2012), we investigated if the MiT/TFE-RagD-mTORC1 axis was deregulated in MiT/TFE-overexpressing tumors. The characterization of Renal Cell Carcinoma models, overexpressing TFEB or TFE3, and of patients-derived melanoma cells, overexpressing MITF, showed the increased activity of mTORC1, due to MiT/TFE overexpression, and upregulation of RagD. Xenografts experiments highlighted the role of the MiT/TFE-RagD-mTORC1 deregulated axis in tumorigenesis, confirming the involvement of this mechanism in tumor growth. These findings define a new oncogenic pathway in MiT/TFE dependent tumors with potential implications for therapy. Defining additional interacting partners and transcriptional targets of MiT/TFE proteins and further characterization of upstream signaling cascades that control MiT/TFE levels, stability, localization, and activity may contribute to find novel therapeutic strategies to switch off MiT/TFE in cancer cells.

BIBLIOGRAPHY

Aksan I and Goding CR, Targeting the microphthalmia basic helix-loop-helix-leucine zipper transcription factor to a subset of E-box elements in vitro and in vivo. Mol Cell Biol. 12, 6930-6938 (1998).

Anthony JC *et al.,* Leucine stimulates translation initiation in skeletal muscle of postabsorptive rats via a rapamycin-sensitive pathway. J. Nutr. 130, 2413–2419 (2000).

Argani P *et al*., Primary Renal Neoplasms with the ASPL-TFE3 Gene Fusion of Alveolar Soft Part Sarcoma. Am. J. Pathol. 159, 179–192 (2001).

Argani P *et al.*, A novel CLTC-TFE3 gene fusion in pediatric renal adenocarcinoma with t(X;17)(p11.2;q23). Oncogene. 22, 5374–5378 (2003).

Ballabio A, The awesome lysosome. EMBO Mol Med. 2, 73-76 (2016).

Bar-Peled L *et al.*, Ragulator is a GEF for the rag GTPases that signal amino acid levels to mTORC1. Cell. 150, 1196-1208 (2012).

Bar-Peled L *et al.,* A Tumor suppressor complex with GAP activity for the Rag GTPases that signal amino acid sufficiency to mTORC1. Science 340, 1100–1106 (2013).

Ben-Sahra I *et al.,* mTORC1 induces purine synthesis through control of the mitochondrial tetra- hydrofolate cycle. Science 351, 728–733 (2016).

Beckmann H *et al.*, TFE3: a helix-loop-helix protein that activates transcription

through the immunoglobulin enhancer muE3 motif. Genes & development 4, 167-179 (1990).

Bodine SC *et al*., Akt/mTOR pathway is a crucial regulator of skeletal muscle hypertrophy and can prevent muscle atrophy in vivo. Nat. Cell Biol. 3, 1014–1019 (2001).

Bothe GW *et al.*, Selective expression of Cre recombinase in skeletal muscle fibers. Genesis *26*, 165-166 (2000).

Brugarolas J *et al.*,mRegulation of mTOR function in response to hypoxia by REDD1 and the TSC1/TSC2 tumor suppressor complex. Genes Dev. *18*, 2893 2904 (2004).

Calcagnì A *et al.*, Modelling TFE renal cell carcinoma in mice reveals a critical role of WNT signaling. eLife 5, e17047 (2016).

Chantranupong L *et al*., The Sestrins interact with GATOR2 to negatively regulate the amino-acid- sensing pathway upstream of mTORC1. Cell Rep. 9, 1–8 (2014).

Chantranupong L *et al.*, The CASTOR Proteins Are Arginine Sensors for the mTORC1 Pathway. Cell *165*, 153–164 (2016).

Choo AY *et al*., Rapamycin differentially inhibits S6Ks and 4E-BP1 to mediate cell type-specific repression of mRNA translation. Proc. Natl. Acad. Sci. USA 105, 17414–17419 (2008).

Clark J *et al*., Fusion of splicing factor genes PSF and NonO (p54nrb) to the TFE3 gene in papillary renal cell carcinoma. Oncogene. 15, 2233–2239 (1997).

Crino PB *et al.*, The tuberous sclerosiscomplex. N. Engl. J. Med. 355, 1345–1356 (2006).

Cronin JC *et al.* , Frequent mutations in the MITF pathway in melanoma. Pigment Cell Melanoma Res, 22, 435–444 (2009).

Davies H *et al.,* Mutations of the BRAF gene in human cancer. Nature, 417, 949–954 (2002).

Davis IJ *et al.,* Cloning of an Alpha-TFEB fusion in renal tumors harboring the t(6;11)(p21;q13) chromosome translocation. Proc. Natl. Acad. Sci. U. S. A. 100, 6051–6056 (2003).

de Duve C. The lysosome turns fifty. Nat Cell Biol. 9, 847-849 (2005).

Dibble CC *et al*., TBC1D7 is a third subunit of the TSC1-TSC2 complex upstream of mTORC1. Mol. Cell 47, 535-546 (2012).

Dorrello NV *et al.,* S6K1- and betaTRCP-mediated degradation of PDCD4 promotes protein translation and cell growth. Science 314, 467–471 (2006).

Du¨vel K *et al*., Activation of a metabolic gene regulatory network downstream of mTOR complex 1. Mol. Cell *39*, 171–183 (2010).

Efeyan A *et al*., Regulation of mTORC1 by the Rag GTPases is necessary for neonatal autophagy and survival. Nature 493, 679–683 (2013).

Eltschinger S *et al*, TOR Complexes and the Maintenace of Cellular Homeostasis. Trends Cell Biol 26, 148-159 (2016).

Ennen M *et al*., Single-cell gene expression signatures reveal melanoma cell heterogeneity. Oncogene. 34, 3251–3263 (2015).

Ezaki J *et al*., Liver autophagy contributes to the maintenance of blood glucose and amino acid levels. Autophagy 7, 727–736 (2011).

Ferron M *et al*., A RANKL-PKCβ-TFEB signaling cascade is necessary for lysosomal biogenesis in osteoclasts. Genes Dev. 8, 955-969 (2013).

Frey JW *et al*., A role for Raptor phosphorylation in the mechanical activation of mTOR signaling. Cell. Signal. 26, 313–322. (2014).

Ganley IG *et al.,* ULK1.ATG13.FIP200 complex mediates mTOR signaling and is essential for autophagy. J. Biol. Chem. 284, 12297–12305 (2009).

Gingras AC *et al.*, Regulation of 4E-BP1 phosphorylation: A novel two-step mechanism. Genes Dev. *13*, 1422–1437 (1999).

Gossen M *et al.,* Transcriptional activation by tetracyclines in mammalian cells. Science 268, 1766-1769 (1995).

Grabiner BC *et al.*, A diverse array of cancer-associated MTOR mutations are hyperactivating and can predict rapamycin sensitivity. Cancer Discov. 4, 554–563 (2014).

Guertin DA and Sabatini DM. An expanding role for mTOR in cancer. Trends Mol Med. 11, 353-361 (2005).

Gwinn DM *et al.*, AMPK phosphorylation of raptor mediates a metabolic checkpoint. Mol. Cell 30, 214–226 (2008).

Halaban R *et al.*, Deregulated E2F transcriptional activity in autonomously growing melanoma cells. J. Exp. Med. 191, 1005–1016 (2000).

Hara K *et al.*, Aminoacid sufficiency and mTOR regulate p70S6 kinase and eIF-4E BP1 through a common effector mechanism. J. Biol. Chem. 273, 14484–14494 (1998).

Haq R , Fisher D. Biology and clinical relevance of the micropthalmia family of transcription factors in human cancer. J. Clin. Oncol. 29, 3474–3482 (2011).

He C, Klionsky DJ. Regulation Mechanisms and Signaling Pathways of Autophagy. Annu. Rev. Genet. 43, 67 (2009).

Hemesath TJ *et al.*, microphthalmia, A critical factor in melanocyte development, defines a discrete transcription factor family. Genes and Development 8**,** 2770-2780 (1994).

Hodgkinson CA *et al.,* Mutations at the mouse microphthalmia locus are associated with defects in a gene encoding a novel basic-helix-loop-helix-zipper protein. Cell 74, 395-404 (1993).

Hodis E *et al*., A landscape of driver mutations in melanoma. Cell, 150, 251–263 (2012).

Hoek KS *et al.,* In vivo switching of human melanoma cells between proliferative and invasive states. Cancer Res. 68, 650–656 (2008).

Holz MK *et al.*, mTOR and S6K1 mediate assembly of the translation preinitiation complex through dynamic protein interchange and ordered phosphorylation events. Cell 123, 569–580 (2005).

Hosokawa N *et al*. Nutrient-dependent mTORC1 association with the ULK1-Atg13-FIP200 complex required for autophagy. Mol. Biol. Cell *20*, 1981–1991 (2009).

Huan C *et al.* Transcription factors TFE3 and TFEB are critical for CD40 ligand expression and thymus-dependent humoral immunity. Nat Immunol. 10, 1082-

1091 (2006).

Ilagan E and Manning BD, Emerging role of mTOR in the response to cancer therapeutics. Trends Cancer. 2,241-251 (2016).

Inamura K *et al*., Diverse fusion patterns and heterogeneous clinicopathologic features of renal cell carcinoma with t (6; 11) translocation. Am. J. Surg. Pathol. 36, 35-42 (2012).

Inoki K *et al.,* TSC2 is phosphorylated and inhibited by Akt and suppresses mTOR signalling. Nat Cell Biol. 4, 648–657 (2002).

Inoki K *et al.*, Rheb GTPase is a direct target of TSC2 GAP activity and regulates mTOR signaling. Genes Dev. 17, 1829–1834 (2003).

Jacinto E *et al.,* Mammalian TOR complex 2 controls the actin cytoskeleton and is rapamycin insensitive. Nat. Cell Biol. 6, 1122–1128 (2004).

Jacinto E *et al.*, SIN1/MIP1 maintains rictor-mTOR complex integrity and regulates Akt phosphorylation and substrate specificity. Cell. 1, 125-137 (2006).

Jewell JL *et al.*, Metabolism. Differential regulation of mTORC1 by leucine and glutamine. Science 347, 194–198 (2015).

Kaizuka T *et al.*, Tti1 and Tel2 are critical factors in mammalian target of rapamycin complex assembly. J Biol Chem. 285, 20109-20116 (2010).

Kauffman E *et al*.. Molecular genetics and cellular features of TFE3 and TFEB fusion kidney cancers. Nat. Rev. Urol. 11, 465–475 (2014).

Kim DH *et al.*, mTOR interacts with raptor to form a nutrient-sensitive complex that signals to the cell growth machinery. Cell 2, 163-175 (2002).

Kim DH *et al.*, GbetaL, a positive regulator of the rapamycin-sensitive pathway required for the nutrient- sensitive interaction between raptor and mTOR. Mol. Cell 11, 895–904 (2003).

Kim E *et al*., Regulation of TORC1 by Rag GTPases in nutrient response.Nat. Cell Biol. 10, 935–945 (2008).

Kim J *et al*., AMPK and mTOR regulate autophagy through direct phosphorylation of Ulk1. Nat. Cell Biol. 13, 132–141 (2011).

Kuiper RP *et al.,* Upregulation of the transcription factor TFEB in t(6;11)(p21;q13)-positive renal cell carcinomas due to promoter substitution. Hum. Mol. Genet. 12, 1661–69 (2003).

Laplante M, Sabatini DM. mTOR Signaling in Growth Control and Disease. Cell 149, 274-293 (2012).

Lawrence RE *et al*., A nutrient-induced affinity switch controls mTORC1 activation by its Rag GTPase-Ragulator lysosomal scaffold. Nat Cell Biol. 9, 1052-1063 (2018).

Lee PL *et al.,* Raptor/mTORC1 loss in adipocytes causes progressive lipodystrophy and fatty liver disease. Mol. Metab. 5, 422–432 (2016).

Lim CY and Zoncu R. The lysosome as a command-and-control center for cellular metabolism. J Cell Biol 214, 653-664 (2016).

Linehan WM *et al.*, The genetic basis of kidney cancer: a metabolic disease. Nat. Rev. Urol. 7, 277–285 (2010).

Lipton JO and Sahin M, The neurology of mTOR. Neuron 84, 275-291 (2014).

Long X *et al*., Rheb binds and regulates the mTOR kinase. Curr. Biol. 15, 702–713 (2005).

Luzio JP *et al.* Lysosomes: fusion and function. Nat Rev Mol Cell Biol 8, 622-632 (2007).

Ma XM *et al*., SKAR links pre-mRNA splicing to mTOR/S6K1-mediated enhanced translation efficiency of spliced mRNAs. Cell *133*, 303–313 (2008).

Mahony CB *et al.* Tfec controls the hematopoietic stem cell vascular niche during zebrafish embryogenesis. Blood. 10, 1336-1345 (2016).

Malouf GG *et al.*, Next-generation sequencing of translocation renal cell carcinoma reveals novel RNA splicing partners and frequent mutations of chromatin-remodeling genes. Clin. Cancer Res. 20, 4129–4140 (2014).

Martina JA *et al.*, MTORC1 functions as a transcriptional regulator of autophagy by preventing nuclear transport of TFEB. Autophagy 8, 903-914 (2012).

Martina JA and Puertollano R., Rag GTPases mediate amino acid-dependent recruitment of TFEB and MITF to lysosomes. J Cell Biol. 200, 475-491(2013).

Martina JA *et al*. The Nutrient-Responsive Transcription Factor TFE3, Promotes Autophagy, Lysosomal Biogenesis, and Clearance of Cellular Debris. Sci Signal 7, ra9 (2014).

Medina DL *et al.*, Transcriptional activation of lysosomal exocytosis promotes cellular clearance. Dev Cell. 3, 421-430 (2011).

Medina D *et al*. Lysosomal calcium signalling regulates autophagy through calcineurin and TFEB. Nat Cell Biol. 3, 288-299 (2015).

Mori H *et al*., Critical roles for the TSC-mTOR pathway in b-cell function. Am. J. Physiol. Endocrinol. Metab. 297, E1013–E1022 (2009).

Nada S *et al.*, The novel lipid raft adaptor p18 controls endosome dynamics by anchoring the MEK-ERK pathway to late endosomes. EMBO J. 28, 477-489 (2009).

Nezich CL *et al.,* MiT/TFE transcription factors are activated during mitophagy downstream of Parkin and Atg5. J Cell Biol. 3, 435-50 (2015).

Nickerson ML *et al*., Mutations in a novel gene lead to kidney tumors, lung wall defects, and benign tumors of the hair follicle in patients with the Birt-Hogg-Dube´ syndrome. Cancer Cell 2, 157–164 (2002).

Okosun J *et al.,* Recurrent mTORC1-activating RRAGC mutations in follicular lymphoma. Nat. Genet. 48, 183–188 (2016).

Palmieri M *et al.*, Characterization of the CLEAR network reveals an integrated control of cellular clearance pathways. Hum Mol Genet. 19, 3852-3866 (2011).

Pastore N *et al.* TFE3 regulates whole-body energy metabolism in cooperation with TFEB. EMBO Mol Med. 5, 605-621. (2017)

Pearce LR *et al*., Identification of Protor as a novel Rictor-binding component of mTOR complex-2. Biochem J. 3, 513-522 (2007).

Perera RM *et al*.,Transcriptional control of autophagy-lysosome function drives pancreatic cancer metabolism. Nature 524, 361–365 (2015).

Perera RM and Zoncu R, The Lysosome as a Regulatory Hub. Annu Rev Cell Dev Biol. (2016) Epub 2016 Aug 3. Review.

Peterson TR *et al.*, DEPTOR is an mTOR inhibitor frequently overexpressed in multiple myeloma cells and required for their survival. Cell 137, 873-886 (2009).

Pogenberg V *et al.,* Restricted leucine zipper dimerization and specificity of DNA recognition of the melanocyte master regulator MITF. Genes & development 26, 2647–58 (2012).

Polak P *et al.*, Adipose-specific knockout of raptor results in lean mice with enhanced mitochondrial respiration. Cell Metab. 8, 399–410 (2008).

Powell JD *et al*., Regulation of immune responses by mTOR. Annu. Rev. Immunol. 30, 39–68 (2012).

Primot A *et al.*, ERK-regulated differential expression of the Mitf 6a/b splicing isoforms in melanoma. Pigment Cell Melanoma Res. 23, 93–102 (2010).

Rabinowitz JD and White E, Autophagy and Metabolism. Science 330, 1344–1348 (2010).

Reddy A *et al.,* Plasma membrane repair is mediated by Ca(2+)-regulated exocytosis of lysosomes. Cell 2, 157-169 (2001).

Rehli M *et al.,* TFEC is a macrophage-restricted member of the microphthalmia TFE subfamily of basic helix-loop-helix leucine zipper transcription factors. J Immunol. 3, 1559-1565 (1999).

Roczniak-Ferguson A *et al.,* The transcription factor TFEB links mTORC1 signaling to transcriptional control of lysosome homeostasis. Sci Signal. 228:ra42 (2012).

Rodríguez A *et al.*, Lysosomes behave as Ca2+-regulated exocytic vesicles in fibroblasts and epithelial cells. J Cell Biol. 1, 93-104 (1997).

Rodrik-Outmezguine VS *et al.*, mTOR kinase inhibition causes feedback-

dependent biphasic regulation of AKT signaling. Cancer Discov. 1, 248–259 (2011).

Rodrik-Outmezguine VS *et al.*, Overcoming mTOR resistance mutations with a new-generation mTOR inhibitor. Nature 534, 272-276 (2016).

Rommel C *et al*., Mediation of IGF-1-induced skel-etal myotube hypertrophy by PI(3)K/Akt/mTOR and PI(3)K/Akt/GSK3 pathways. Nat. Cell Biol. 3, 1009 1013 (2001).

Rousseau A and Bertolotti A, An evolutionarily conserved pathway controls proteasome homeostasis. Nature 536, 184–189 (2016).

Roux PP *et* al., Tumor-promoting phorbol esters and activated Ras inactivate the tuberous sclerosis tumor suppressor complex via p90 ribosomal S6 kinase. Proc Natl Acad Sci USA 101, 13489–13494 (2004).

Sabatini DM *et al.*, RAFT1: A mammalian protein that binds to FKBP12 in a rapamycin- dependent fashion and is homologous to yeast TORs. Cell *78*, 35–43 (1994).

Saftig P, Klumperman J, Lysosome biogenesis and lysosomal membrane proteins: trafficking meets function. Nat Rev Mol Cell Biol. 10, 623-635 (2009)

Sancak Y *et al.*, PRAS40 is an insulin-regulated inhibitor of the mTORC1 protein kinase. Mol Cell. 6, 903-915 (2007).

Sancak Y *et al*. The Rag GTPases bind raptor and mediate amino acid signaling to mTORC1. Science 320, 1496-1501 (2008).

Sancak Y *et al.*, Ragulator-Rag complex targets mTORC1 to the lysosomal surface and is necessary for its activation by amino acids. Cell. 141, 290-303

(2010).

Sarbassov DD *et al.,* Rictor, a novel binding partner of mTOR, defines a rapamycin-insensitive and raptor-independent pathway that regulates the cytoskeleton. Curr Biol. 14, 1296-1302 (2004).

Sarbassov DD *et* al., Prolonged rapamycin treatment inhibits mTORC2 assembly and Akt/PKB. Mol. Cell *22*, 159–168 (2006).

Sardiello M *et al*. A gene network regulating lysosomal biogenesis and function. Science 325, 473–477 (2009).

Sato S *et al.* CBP/p300 as a co-factor for the Microphthalmia transcription factor. Oncogene 25 ,3083-3092 (1997).

Saxton RA, Sabatini DM. mTOR Signaling in Growth, Metabolism, and Disease. Cell 168, 960-976 (2017).

Sengupta S *et al.*, mTORC1 controls fasting-induced ketogenesis and its modulation by ageing. Nature 468, 1100–1104 (2010).

Settembre C *et al.,* TFEB links autophagy to lysosomal biogenesis. Science 332, 1429–1433 (2011).

Settembre C *et al.*, A lysosome-to-nucleus signalling mechanism senses and regulates the lysosome via mTOR and TFEB: Self-regulation of the lysosome via mTOR and TFEB. EMBO J. 31, 1095–1108 (2012).

Settembre C *et al.*, TFEB controls cellular lipid metabolism through a starvation-induced autoregulatory loop. Nat Cell Biol. 6, 647-658 (2013a).

Settembre C *et al.,* Signals from the lysosome: a control centre for cellular clearance and energy metabolism. Nat Rev Mol Cell Biol 5, 283-296 (2013b).

Shen K and Sabatini DM, Ragulator and SLC38A9 activate the Rag GTPases through noncanonical GEF mechanisms. Proc Natl Acad Sci U S A 115, 9545-9550 (2018).

Spilman P *et al.*, Inhibition of mTOR by rapamycin abolishes cognitive deficits and reduces amyloid-beta levels in a mouse model of Alzheimer's disease. PLoS ONE *5*, e9979 (2010).

Steingrímsson E *et al.* ,The bHLH- Zip transcription factor Tfeb is essential for placental vascularization. Development 125, 4607–4616 (1998).

Steingrimsson E *et al.*, Mitf and Tfe3, two members of the Mitf-Tfe family of bHLH-Zip transcription factors, have important but functionally redundant roles in osteoclast development. Proc. Natl. Acad. Sci. U.S.A. 99, 4477–4482 (2002).

Steingrıḿsson E *et al.*, Melanocytes and the microphthalmia transcription factor network. Annu. Rev. Genet. 38, 365-411(2004).

Tabernero J *et al*., Dose- and schedule- dependent inhibition of the mammalian target of rapamycin pathway with everolimus: A phase I tumor pharmacodynamic study in patients with advanced solid tumors. J. Clin. Oncol. 26, 1603–1610 (2008).

Tanaka M *et al*., Perivascular epithelioid cell tumor with SFPQ/PSF-TFE3 gene fusion in a patient with advanced neuroblastoma. Am. J. Surg. Pathol. 33, 1416–1420 (2009).

Tang H *et al.*, Amino acid-induced translation of TOP mRNAs is fully dependent on phosphatidylinositol 3-kinase-mediated signaling, is partially inhibited by rapamycin, and is independent of S6K1 and rpS6 phosphorylation. Mol. Cell. Biol. 21, 8671–8683 (2001).

Tassabehji M *et al.,* Waardenburg syndrome type 2 caused by mutations in the human microphthalmia (MITF) gene. Nat Genet. 3, 251-255 (1994).

Tirosh I *et al*., Dissecting the multicellular ecosystem of metastatic melanoma by single-cell RNA-seq. Science. 352, 189–196 (2016).

Tsao H *et al.*, Melanoma: from mutations to medicine. Genes Dev. 26, 1131-1155 (2012).

Tsun ZY *et al*. The Folliculin tumor suppressor is a GAP for RagC/D GTPases that signal amino acid levels to mTORC1. Mol. Cell 52, 495–505 (2013).

Verhage M & Toonen RF. Regulated exocytosis: merging ideas on fusing membranes. *Curr. Opin. Cell Biol.* 19, 402–408 (2007).

Wang BT *et al.*, The mammalian target of rapamycin regulates cholesterol biosynthetic gene expression and exhibits a rapamycin-resistant transcriptional profile. Proc. Natl. Acad. Sci. USA 108, 15201–15206 (2011).

Wang S *et al.*, Metabolism. Lysosomal amino acid transporter SLC38A9 signals arginine suffi- ciency to mTORC1. Science 347, 188–194 (2015).

Watson K & Baar K. mTOR and the health benefits of exercise. Semin. Cell Dev. Biol. 36**,** 130–139 (2014).

Weterman MA *et al.*, Fusion of the transcription factor TFE3 gene to a novel gene, PRCC, in t(X;1)(p11;q21)-positive papillary renal cell carcinomas. Proc. Natl. Acad. Sci. U. S. A. 93, 15294–15298 (1996).

Weterman MJ *et al.*, Nuclear localization and transactivating capacities of the papillary renal cell carcinoma-associated TFE3 and PRCC (fusion) proteins. Oncogene. 19, 69–74 (2000).

Wolfson RL *et al.*, Sestrin2 is a leucine sensor for the mTORC1 pathway. Science 351, 43–48 (2016).

Xu H, Ren D. Lysosomal physiology. Annu Rev Physiol 77, 57-80 (2015).

Yang S *et al.*, Pancreatic cancers require autophagy for tumor growth. Genes Dev. 25(7):717–29 (2011).

Yang H *et al.,* mTOR kinase structure, mechanism and regulation. Nature 497, 217-223 (2013).

Zhang Y *et al.,* Coordinated regulation of protein synthesis and degradation by mTORC1. Nature 513, 440–443 (2014).

Zhao GQ *et al.* TFEC, a basic helix-loop-helix protein, forms heterodimers with TFE3 and inhibits TFE3-dependent transcription activation. Mol Cell Biol. 8, 4505-4512 (1993).

Zhao J *et al*., mTOR inhibition activates overall protein degradation by the ubiquitin proteasome system as well as by autophagy. Proc. Natl. Acad. Sci. USA 112, 15790–15797 (2015).

Zoncu R *et al.*, mTORC1 senses lysosomal amino acids through an inside-out mechanism that requires the vacuolar H(+)-ATPase. Science 334, 678–683 (2011).